UNIVERSITÀ DEGLI STUDI DI PADOVA

UNIVERSITA' DEGLI STUDI DI PADOVA

Dipartimento di Ingegneria Industriale DII

Corso di Laurea Magistrale in Ingegneria Energetica

A techno-economic analysis of a hybrid offshore wind-hydrogen plant

Relatrice: Prof.ssa Anna Stoppato

Correlatore: Prof. Paul Leahy

Lucia Magro 2013258

Anno Accademico 2021/2022

TABLE OF CONTENTS

Abstract

Le direttive europee prevedono di azzerare le emissioni di CO_2 entro il 2030 e per far fronte a questo obiettivo le fonti energetiche rinnovabili (RES) svolgeranno un ruolo fondamentale. In particolare, una nuova tecnologia ibrida, che prevede la produzione di idrogeno da RES, sta prendendo particolare importanza nei principali centri di ricerca. Questa tesi tratterà in particolare la configurazione ibrida con produzione di energia elettrica ed idrogeno accoppiata ad un sito eolico offshore. Verrà inizialmente svolta un'analisi tecnica spiegando passo passo come progettare e ottimizzare un sito eolico offshore tradizionale e come poterlo poi implementare a ibrido. Per l'ottimizzazione verranno definiti dei modelli di costo per calcolare CAPEX e OPEX dell'impianto. Il sito in esame è costituito da 16 turbine, di una potenza complessiva di 160 MW, con disposizione dei generatori quadrata 4 x 4 e un unico grande elettrolizzare AEL installato a terra. Il sito è installato nella costa orientale dell'Irlanda, di fronte alla costa di Bray nel mare Irlandese. Una volta completata l'ottimizzazione verranno analizzati diversi scenari. Nel primo scenario verrà fissato un valore di soglia per limitare la produzione massima di elettricità, mentre la produzione di idrogeno rimarrà variabile e verrà direttamente iniettata nel gasdotto nazionale. Successivamente il valore di soglia verrà variato per poter analizzare la sua influenza sui risultati ottenuti. Poi la produzione di idrogeno sarà fissata al 30% della produzione elettrica e verrà stabilito un opportuno accumulo. Infine, verrà analizzata un'ipotetica condizione futura dove il prezzo degli elettrolizzatori è ridotto rispetto al valore attuale.

The European polices predict a net zero emission scenario by 2030, in order to fulfil this goal the importance of the Renewable Energy Sources technologies is fundamental. In particular, a new hybrid technology that combines the hydrogen production with the exploitation of RES is having more importance in the research. This thesis will concern about the production of hydrogen from an offshore wind plant. At the beginning, a technical analysis will be done explaining step by step how to design and to optimize a traditional offshore wind farm and how to implement the hybrid part of the plant. For the optimisation some cost models will be defined in order to calculate the CAPEX and the OPEX of the plant. The site in exam presents 16 turbines with a total power of 160 MW; a 4 x 4 square layout and one big AEL electrolyser installed onshore. It is situated to Ireland's east side in front of Bray's shore, inside the Irish Sea. After the optimization, different scenarios will be analysed. In the first scenario a threshold on the maximum electricity production will be fixed while the hydrogen one will be variable and it will directly blended into the gas pipeline. Then, the threshold value will be modified for analysing the effects of this parameter on the results. On another scenario the hydrogen production will be fixed to the 30 % of the electricity one and a storage will be present. At the end, a hypothetic future scenario will be analysed where the price for the electrolysers is lower than present one.

Introduction

This thesis has the role to present how to develop a technical and economic analysis for a hybrid offshore wind-hydrogen farm situated in east offshore side of Ireland. First, a traditional offshore wind farm will be design leading a proper study on the geographic area of the Irish Sea, on the wind speed and direction and on the presence of natural reserves. After obtaining a realistic layout for the turbines arrangement, the study will be more focused on the electric interconnections between turbines.

The first part of the thesis will concern the state of art of the offshore wind technology and the production of hydrogen using the renewable sources. Then, a detailed description on the main technologies and electrical and piping arrangement used nowadays will be presented.

Then, the optimisation of the electrical interconnections will be presented. In this phase, the wind farm is simplified producing only electricity. Different cables arrangement will be studied, such as radial configuration, star configuration, mixed configuration and double ring configuration. The best solution for this study will be taken into consideration and it will be used in the following to design the hybrid wind-hydrogen farm. Then, the plant will be implemented to produce also hydrogen; the optimisation of the hydrogen pipelines and electrolysers will be done too. The optimisation will follow the economic aspect, therefore a study on the cost equations calculating CAPEX and OPEX of the plant will be reported.

At the end, different scenarios with different hydrogen production and solutions will be analysed in order to verify the feasibility of the plant's investment.

CHAPTER 1 – Energy policies

In this chapter the currently energy policies present in the worldwide and more in detail the one present for Ireland will be analysed. An observation about the onshore and offshore market and installations will be presented too.

1.1 - Renewable electricity target and policy perspective by 2030 and 2050

Nowadays the reduction of the greenhouse gases is a matter that is increasing of importance. Thus, to reduce emissions and achieve the scores imposed by the EU policies, RES play an important role and need to be increased in the following years. The EU has developed the European Green Deal, a roadmap for Europe in order to become a climate-neutral continent. From the European Parliament's website is possible to analyse all the directives present in the law. It imposes a reduction of 55% of the total emissions by 2030 and a net zero emissions of greenhouse gasses by 2050 [1]. This goal can be obtain increasing the installation of RES technologies and the efficiency of the systems. From a global emission study conducted by GWEC [2] the worst scenario is the one without any emissions plan action that will lead to a variation of 4.1 - 4.8 °C by 2100 whit an emission of 100 - 150 Gt/year of CO_2 equivalent. While for the scenario that considers the current polices the increase of temperature is lower than the previous one and will lead to an increase of temperature of 2.7 - 3.1 °C by 2100. There are also scenarios that present a global greenhouse emission lower than 50 Gt of CO_{2e} and the variation of temperature can be kept in the range of the Paris Agreement. In Figure 1.1 these results are summarized depending by the scenario taken into consideration.

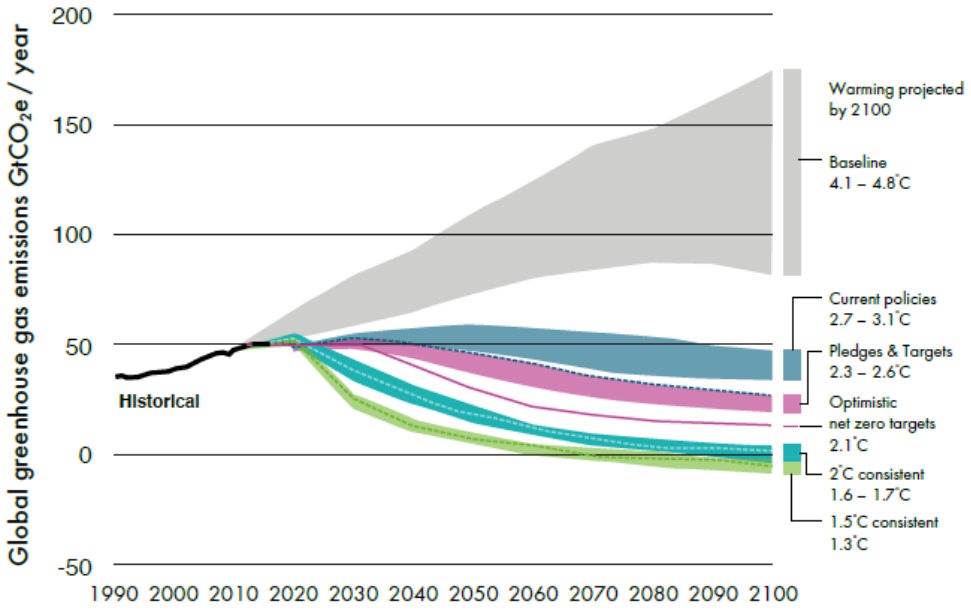

Figure 1.1 Expected global greenhouse emissions during the years depending by policies, source GWEC 2021 report

The Figure 1.1 shows the global greenhouse gas emissions expressed in Gt of CO_2 equivalent per year and the expected warming.

Wind and solar plants are the main technologies able to satisfy the energy demand reducing the emissions. In the current scenario, the wind energy plays an important role and it will see an increasing in the installed power in the next years. For that reason, the investments in the offshore wind farms will increase and new offshore power plant will be installed in the worldwide and in Ireland too and probably the possibility to export part of the energy produced from the country will be also considered. The worldwide total installed capacity for the onshore and offshore wind power plants in the past years is expressed in Figure 1.2.

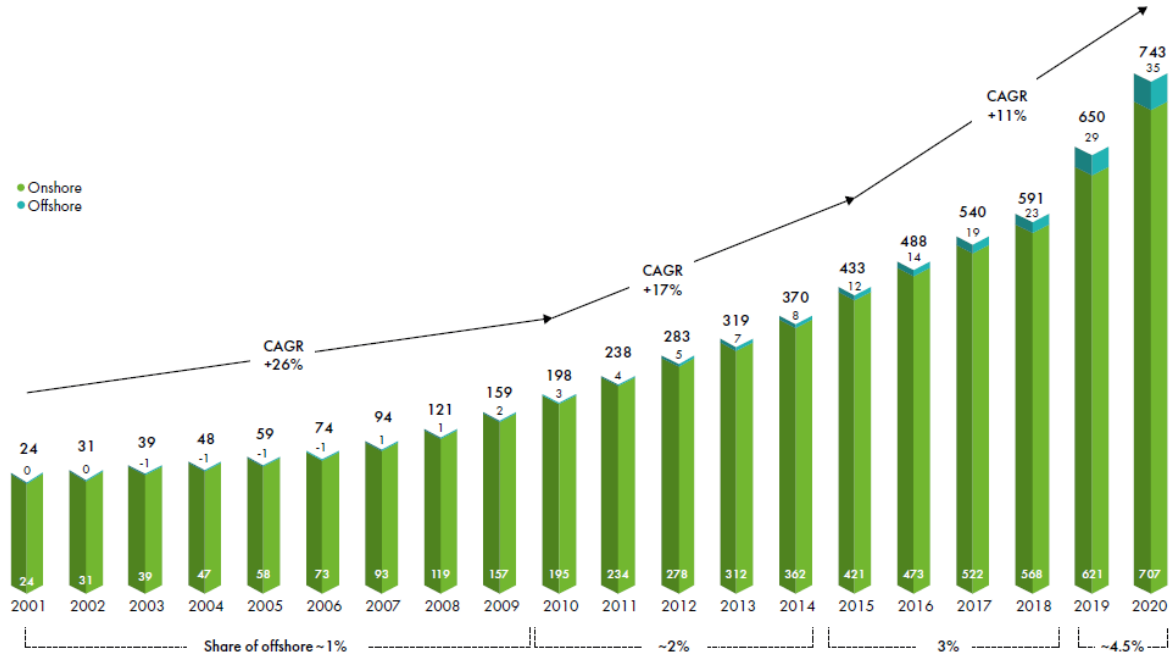

Figure 1.2 Worldwide wind farm installation during the years for offshore and onshore technologies in [GW], source GWEC

It can be seen in Figure 1.2 that the market for the onshore plants is more mature and it presents an installed capacity higher than the offshore plants, however in the last years the power capacity installed for the offshore plants is increased more, reaching 4.5% of the total onshore installed power capacity in 2020. It is also important to pay attention to the fact that even with a pandemic in action the investments for the wind sector are increased. Figure 1.3 presents the global trend for new installed capacity predicted for the wind sector, in this case it should be paid attention to the fact that for the future years this is only an estimation and the real future values can be different from the predicted ones.

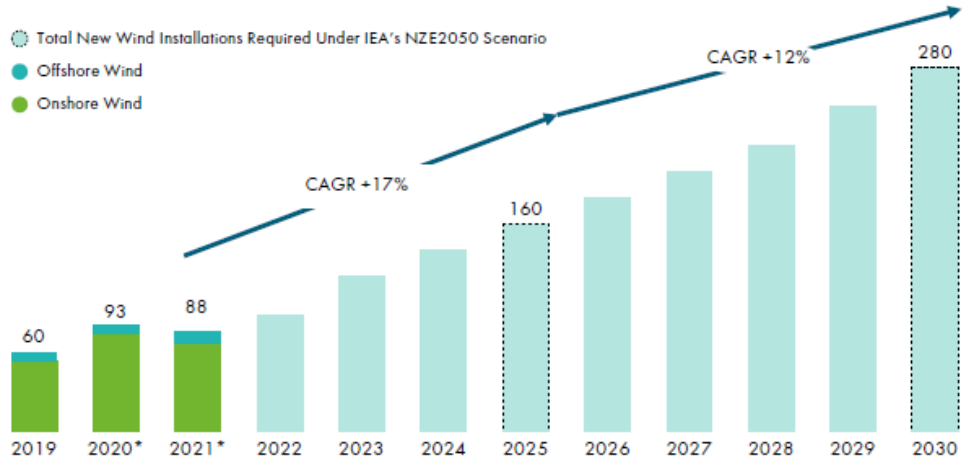

Figure 1.3 New global wind installation in [GW] for offshore and onshore technologies. All the volume in 2022-2024 and 2026 - 2029 are estimation, source GWEC

As it can be seen in Figure 1.3 the GWEC's report of 2021 predicts an increase in the total world installed wind capacity that will lead to 280 GW by 2030. It is interesting to notice that one year on from the beginning of the pandemic the installations are grown reaching a value of 93 GW. The major part of this contribute is largely due to China. Investment in offshore wind surpassed 2019, partly due to long project development timelines which are more resilient to the pandemic impacts. Before 2025, the industry will exceed 1 TW in global cumulative installations of onshore and offshore wind. In order to achieve the score of net zero greenhouse emissions by 2050, annual run rates for wind would need to be even steeper, reaching 160 GW by 2025 and then 280 GW by 2030 that it is 3 times the volume built in 2020.

2020 saw global new wind power installations surpass 90 GW, a 53% growth compared to 2019, bringing total installed capacity to 743 GW, a growth of 14% compared to 2019. New installations in 2020 in the onshore wind market reached 86.9 GW, while the offshore wind market reached 6.1 GW as it can be seen in Figure 1.4.

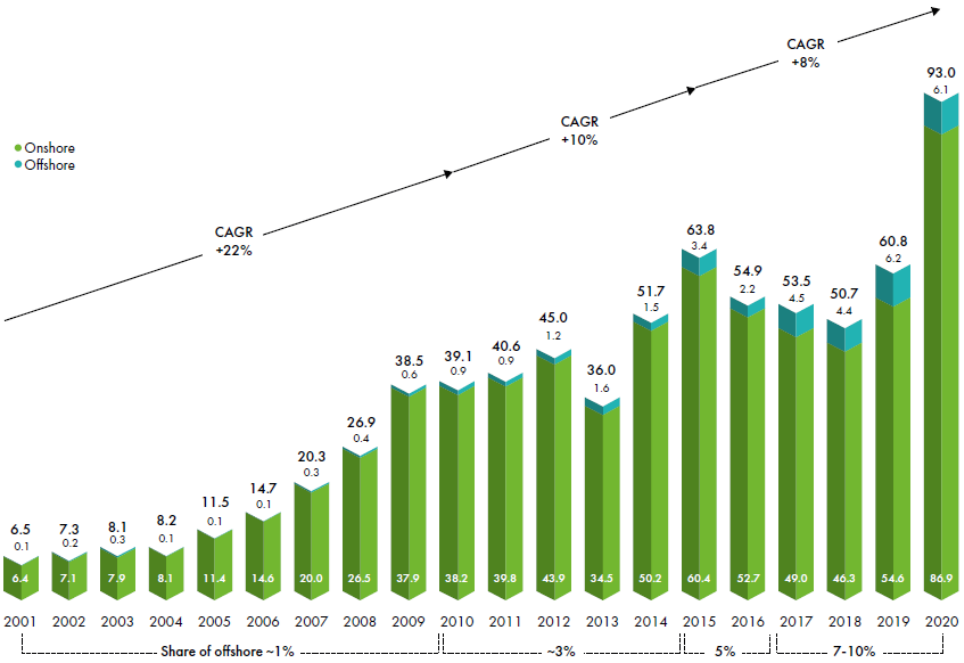

Figure 1.4 Historic development of new total installations in [GW] considering offshore and onshore technologies, source WEC

Despite the impact of COVID-19, the global offshore wind industry had its second-best year ever in 2020 installing over 6 GW of new capacity, keeping growth on track as it can be seen in the Figure 1.5.

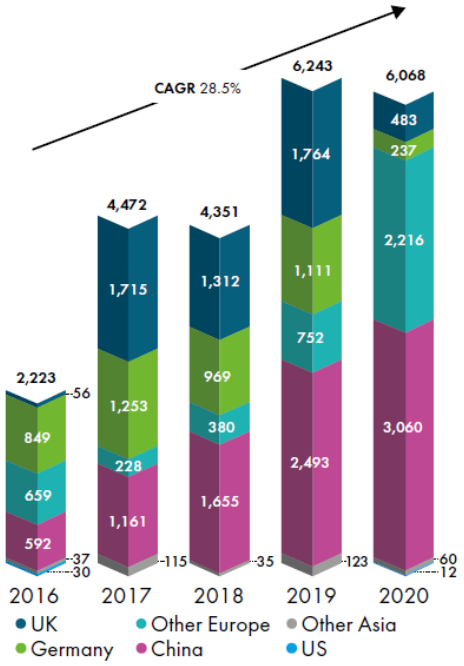

Figure 1.5 New offshore installation in [MW] divided by country, source GWEC

As it can be seen in Figure 1.5 China leads the world in the new annual offshore wind installations for the third year in a row with over 3 GW of new offshore wind capacity in 2020. While Europe is in a steady growth led by the Netherlands with 1.5 GW in 2020 and Belgium with 706 MW. These results can also be seen in the next graphs in Figure 1.6.

Figure 1.6 Currently status market of new and total installation by state for offshore and onshore technologies, source GWEC

As it can be seen in Figure 1.6 the major role in the new and total installation is played by China both for the onshore and offshore markets, followed by the US and the United Kingdom.

Besides even the IEA's report about the renewable power (2021) [3] attests that in order to meet the net zero emissions by 2050 renewable power should increase at an average rate of 12 % during 2021 – 2030. This value is twice of the value of 2011-2020. The percentage of power generation by RES is expressed in Figure 1.7.

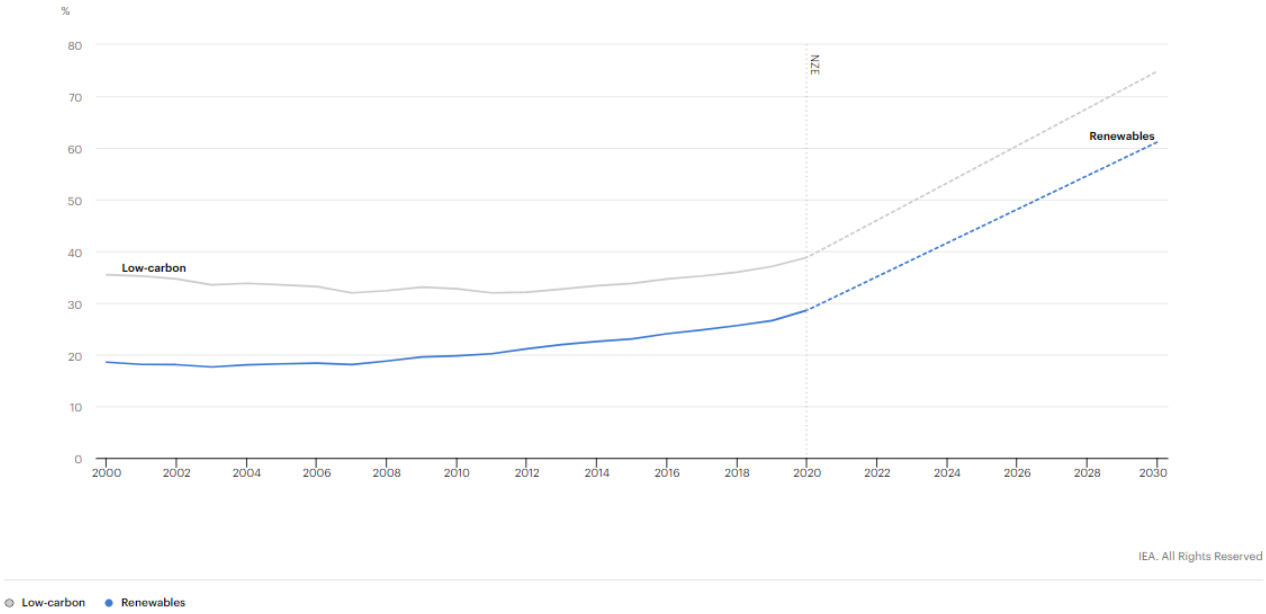

Figure 1.7 Renewables and low-carbon share in power generation in the Net Zero Scenario, 2000-2030, source IEA

As it can be seen from Figure 1.7 in 2020 the share of renewables in global electricity generation reached almost 29%. However, the drop in electricity demand caused by the pandemic in economic activity and mobility is a key reason for this important record.

Solar PV and wind technologies accounted for one-third of total 2020 renewable electricity generation growth as it can be seen in Figure 1.8.

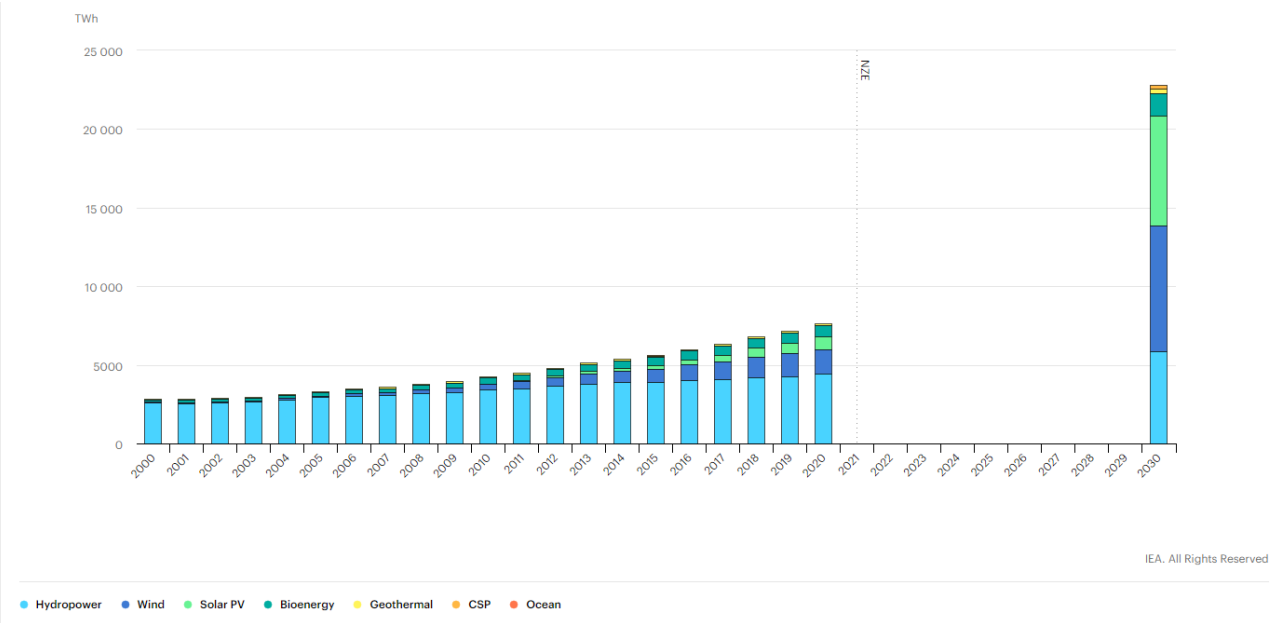

Figure 1.8 Renewable power generation by technology, historic and in the Net Zero Scenario, 2000-2030, source IEA

From the IEA wind power report (2021) [4] it is possible to know that in 2020 onshore wind electricity generation increased by 144 TWh (+ 11%). The capacity additions increased twice respect 2019 mainly owing to new installations from China and the US. While offshore wind generation growth to 25 TWh (+29%) in 2020, with a capacity addition of 6 GW from China, the EU and the UK. These results are confirmed in Figure 1.9

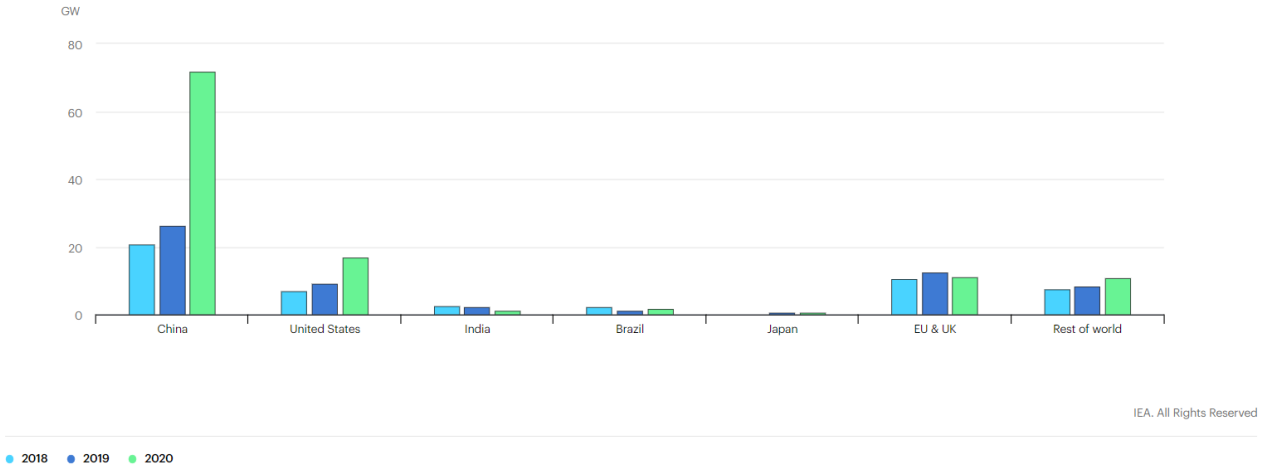

Figure 1.9 Net annual wind capacity additions, 2018-2020, source IEA

In order to reach the Net Zero Emissions by 2050 it is necessary to raise annual capacity additions to 310 GW for the onshore and 80 GW for the offshore. To reach this goal it is important to have a cost reduction and a technology improvement for the offshore wind.

1.2 - Actual situation in Ireland

Now on the situation will be more focused on the actual situation in Ireland, that was not mentioned in the previous paragraphs because it is not present in the list of the main investors for the offshore market. In fact, in the country the majority of wind installed capacity is dedicated to onshore technology rather than offshore one. In order to have an idea about the distribution and the density of the onshore wind farm the following Figure 1.10 shows how many onshore wind plants are present in around the island.

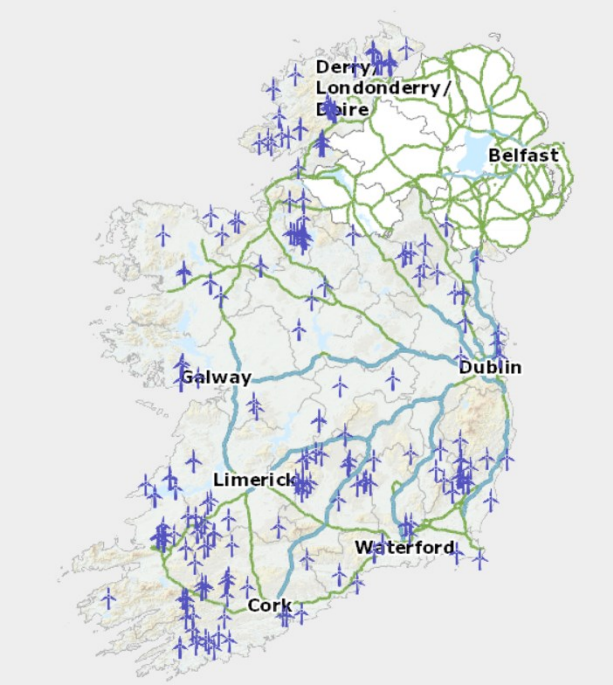

Figure 1.10 Onshore wind farm present in Ireland, source wind atlas (https://www.seai.ie/technologies/seai-maps/wind-atlas-map/)

In Ireland there are more onshore than offshore plants because it was easier to meet the renewable targets. In fact, lack of subsidies for offshore plants and inadequate planning and foreshore consenting process were present in the last years. Despite an abundant natural resource, Ireland's offshore wind sector is underdeveloped relative to its Northern European neighbours; but in these years a deep research has been started and more investments are present nowadays. The research synthesis document written by EirWind (2020) says that to satisfy the energy policies and export part of the produced energy Ireland's score will be to install 5 GW by 2030 in the offshore wind plants. The national target for offshore wind development moves to develop in the future 30 GW of floating wind in the Atlantic and intends to extend the Arklow Bank project, which has been consented for a minimum total installed capacity of 520 MW.

Ireland owes its wind energy resource to its geographic location at the eastern edge of the Atlantic Ocean, which provides abundant fetch for mid-latitude winds to deliver energy to Ireland's offshore areas. These wind energy resources permit to have advantageous abundance of wind energy, compared to other European nations, as it can be seen in Figure 1.11.

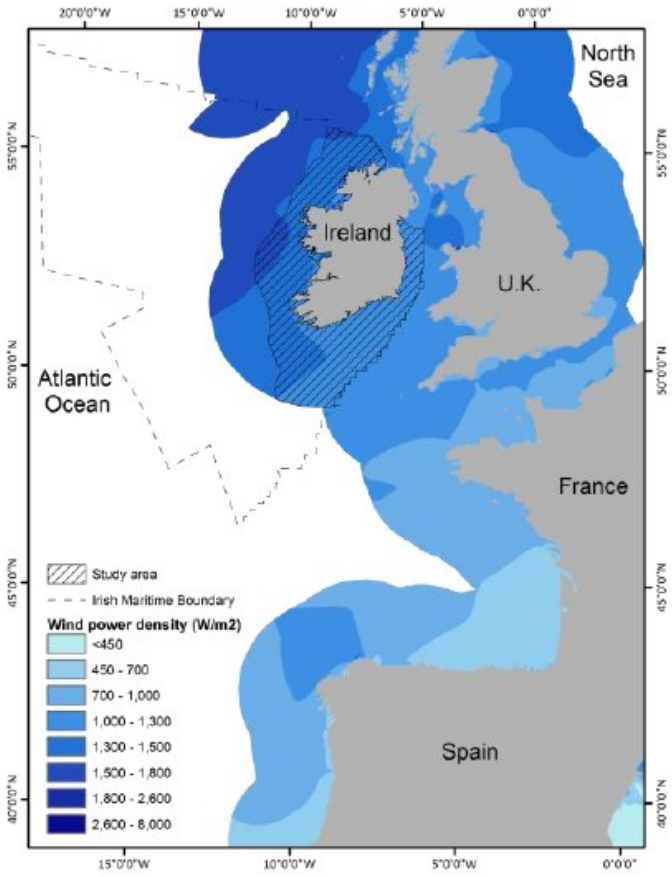

Figure 1.11 Wind power density in [W/m^2], source Global Wind Atlas

Ireland's sea area is equals to about 880000 km^2 and it is around ten times the size of its landmass. The country has one of the best offshore renewable energy resources in the world. This offers significant potential for offshore wind, wave and tidal energy. Ireland's Offshore Renewable Energy Development Plan indicates that the total amount of offshore wind farm development possible is 34.8 -39 GW without likely significant adverse effects on the environment. At present, there is only one operational offshore wind farm in the country, the 25.2 MW Arklow Bank Wind Park off the east coast. In order to understand where the farm is placed the operational site and the one that are in the phase of projection are presented in Figure 1.12.

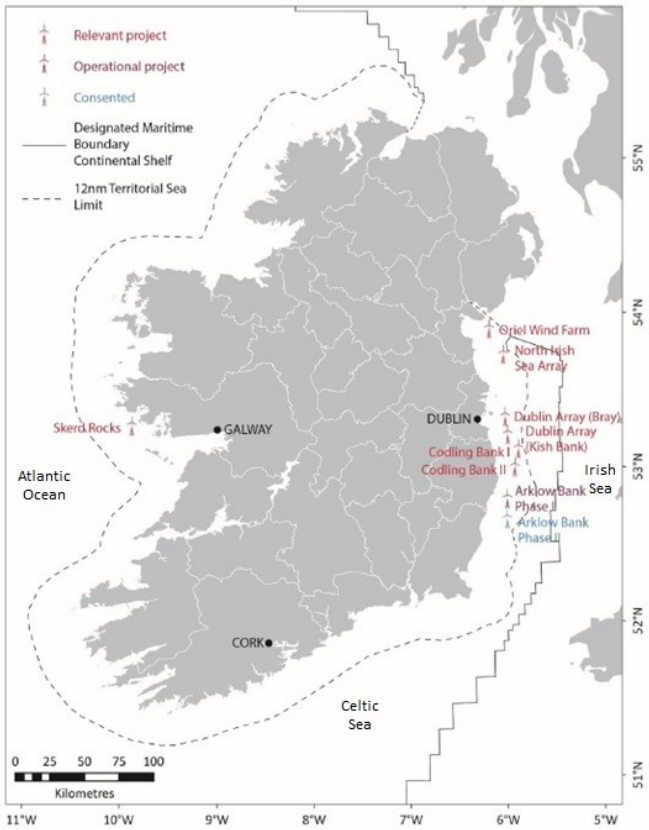

Figure 1.12 Operational, consented and relevant offshore projects in the Irish Sea and Atlantic Ocean

In order to reach the national targets, the main relevant projects identified by the government in May 2020 are expressed in Table 1.1.

Table 1.1 Main relevant projects in Ireland, identified by the government in May 2020.

Project	Location	Capacity [MW]
Oriel Wind Farm	East coast (Irish Sea)	330
Dublin Array (Bray and Kish Banks)	East coast (Irish Sea)	600
Codling Bank (Phase 1 and Phase 2)	East coast (Irish Sea)	2100
North Irish Sea Array	East coast (Irish Sea)	500
Skerd Rocks	West coast (Atlantic Ocean)	100

These wind farms in Ireland are at early exploratory and consultative stages and they include floating configuration proposals. The wind resources, depth of water and availability of space in the Celtic Sea and the Atlantic Ocean make these locations attractive for floating projects. The farm in the Atlantic Sea will be built after the others due to the complexity and the higher costs because the water depth is higher than the other solutions. The capacity of the Atlantic site will be small because it will be an experimental site because the water depth is huge and new technologies should be applied; probably in the future the knowledge acquired from this site will open the market for other offshore plant on the Atlantic Ocean.

CHAPTER 2 - State of art of the technology

In this chapter the currently state of art for the traditional offshore wind plants will be discussed. In particular, the attention will be reserved for the structure and foundation technologies. Then, it will be explained how the process for the production of hydrogen works and the principal aspects to take into consideration for a hybrid offshore wind hydrogen farm. At the end, the electric interconnection between turbines will be explain as well.

2.1 - Main configurations for the offshore turbines

The main technologies present nowadays for the offshore turbines can be mainly classify in:

- Fixed bottom structures
- Floating structures.

These two technologies present different configurations for the foundation of the turbine depending by the depth of the seabed. The main configurations present in the market are present in Figure 2.1.

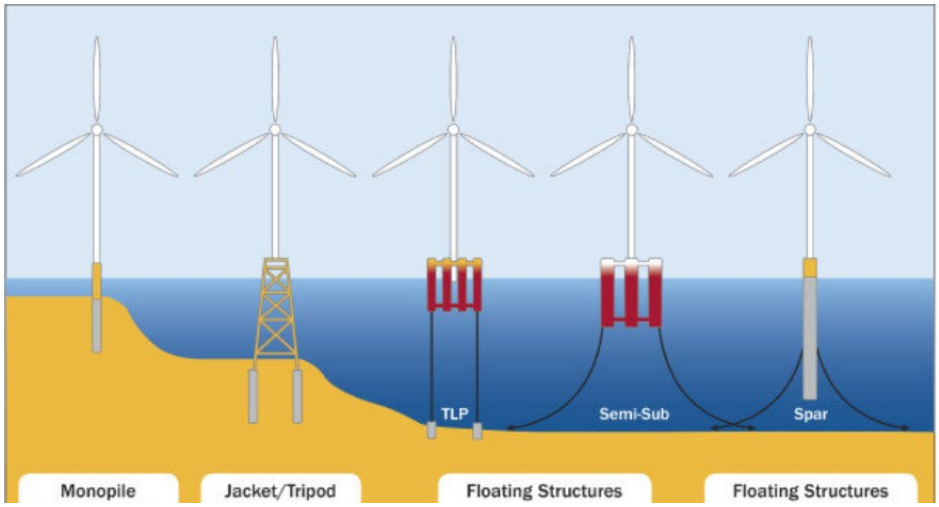

Figure 2.1 Main configuration present in the market for offshore wind turbines, source: https://www.researchgate.net/figure/Types-of-offshore-wind-turbine-foundations-reproduced-from-ref-102-source-Principle_fig4_266086383

2.1.1 - Fixed bottom foundations

For the fixed bottom technology, the wind turbines foundations can be in the form of a monopile or jacket/tripod, they are usually called BFOW (Bottom-Fixed Offshore Wind). The *monopile* is usually installed for seabed from 0 to 30 m while the *jacket/tripod* technology is installed for a depth of 30/50

m and usually the power of the turbine does not exceed 2.5 MW. Both the technologies can be seen in Figure 2.1. Nowadays the most common configuration in Europe is the steel monopile. The main advantage of this solution is that this sector is fully developed and the price is competitive. A lots of fixed substructure concepts have been developed to meet different site characteristics e.g. soil type, water depth, location manufacturing.

2.1.2 - Floating foundations

The floating foundation technology, which it is called FLOW (Floating Offshore Wind), presents three configurations:

- Semi-submersible platform or spar – submersible platform
- Tension Leg Platform (TLP)
- Spar-buoy.

Other configurations also exist, like for example more than one turbine can share a single floating foundation as it can be seen in Figure 2.2.

Figure 2.2 Main configuration present in the market for offshore wind turbines, source: https://www.researchgate.net/figure/Types-of-offshore-wind-turbine-foundations-reproduced-from-ref-102-source-Principle_fig4_266086383

The FLOW configurations can be deployed in 50 - 1000 m water depths and can have turbines until 10 MW of power each. The main drawback of this technology is that it is still in a pre-commercial phase, requiring development at volume and scale, to bring the cost down. In order to achieve this score, FLOW also requires treatment as an emerging technology with respect to government financial support mechanisms, which should differ from mature and established technologies. This will evolve rapidly over the coming decade. At the same time, there is still lots of capacity for bottom-fixed foundations in most markets around the world, in fact the main challenge for the floating technology is due to the commercial phase try to being investable and finding investors. Floating foundations

generally offer environmental benefits compared with fixed-bottom design due to less invasive activity on the seabed during installation. Floating offshore wind has the prospect of creating a much larger global market than fixed-bottom offshore wind turbines, due to the massive area of deep water with good wind resources. In addition, floating technology appears set for commercialisation just when offshore wind using convectional foundations reaches cost parity with other large-scale energy generation technologies.

The *spar buoy* configuration is made by a cylinder with low water plane area, ballasted to keep the centre of gravity below the centre of buoyancy, its representation can be seen in Figure 2.1. The foundations are kept in position by catenary or taut spread mooring lines with drag or suction anchors. The principal advantages of this configuration are that it presents a simple design, a lower installed mooring cost and tendency for lower critical wave-inducted motions. On the other hand, the main drawbacks are that it needs deeper water than other concepts (more than 100 m) and that the offshore operations require heavy-lift-vessels and currently can be done only in relatively sheltered, deep water. The first turbines were demonstrated in Norway in 2009 and Japan in 2013.

The *semi-submersible* configuration is composed by several large columns linked by connecting bracings / submerged pontoons, its representation can be seen in Figure 2.1. The columns provide the hydrostatic stability, and pontoons provide additional buoyancy. The foundation is kept in position by catenary or taut spread mooring lines and drag anchors. The main advantages of this configuration are that it can be constructed onshore or in a dry dock. It also presents a fully equipped platform (including turbines) that can float with drafts below 10 m during transport, thus the transport to site can be done using conventional tugs. Moreover, it can be used in water depths to about 40 m and the installed mooring cost are lower. While the main drawbacks are that it tends to use more material, larger structures and the fabrication is more complex in comparison to other concepts, especially spar buoys. This configuration was first demonstrated in Portugal in 2011 and then in Japan in 2013.

The *tension leg platform* is made with highly buoyant, with central column and arms connected to tensioned tendons, which secure the foundation to the suction / piled anchors and its representation can be seen in Figure 2.1. The main advantages are that it presents low mass, can be assembled onshore or in a dry dock and can be used in water depths to 50 - 60 m. The main disadvantages are that is harder to keep it stable during transport and installation, a special purpose vessel may be required, some uncertainty about impact of possible high – frequency dynamic effects on turbine and higher installed mooring cost. The first demonstration was done in Germany in 2016.

A number of pre commercial FLOW projects have been developed or announced at pilot and demonstration scale in Europe from UK, Norway, France, Portugal and Ireland.

2.2 - Power to hydrogen

Hydrogen is an energy carrier, a secondary source that is no present in nature and should be produced by human activity, it is suitable to be transported and converted. The main chemical and physical characteristics of hydrogen and other main fuels used nowadays are summarized in the Table 2.1.

Table 2.1 Energy carrier and fuel properties

Energy carrier / fuel	Molecular weight [u.m.a.]	Boiling point at 1 atm [°C]	Density at 15 °C, 1 atm [kg/m^3]	Lower Heating Value LHV at 25 °C [MJ/kg]	Flammability range in air at 20°C, 1 atm [vol %]
Hydrogen	2.016	-252.88	0.085 (g)	120	4 - 75
Methane	16.043	-161.52	0.677 (g)	50	5.3 - 15
Petrol	107.0	36 - 205	740 (l)	44	1 - 7.6

It is clear to see in Table 2.1 that hydrogen's main advantage is the high energy density per mass referred to the lower heating value that is equal to 120 MJ/kg, in particular this value is the highest one. This means that for the same amount of energy the weight is lower than the fossil fuels. While on the other hand the value for the density is really low, thus the volume for store the same quantity of energy is higher than the other fuels. Moreover, the boiling point is extremely low, this means that for maintaining the hydrogen liquid in ambient conditions it is needed to reach -252.88 °C compressing the gas and using a huge quantity of energy. For this aspect, the petrol is more convenient because it is easier to be transported and stored because it is present in the liquid phase at ambient pressure.

It is common to use the terms *Power To Hydrogen* (P2H) referring to the production of hydrogen from the surplus of energy production from RES, while *Hydrogen To Power* (H2P) is the conversion of hydrogen in electricity when the RES are not available.

Hydrogen can be produced in different ways, for that reason it can be classified with a different name depending by the type of production. The principal classification is:

- *Grey hydrogen*, it is formed using fossil fuels such as natural gas. Nowadays it accounts around 95% of the hydrogen used in the world. This option emits CO_2 in the atmosphere and it is not sustainable;
- *Blue hydrogen*, it is produced using fossil fuels but the carbon emissions are captured and stored with CCS processes;
- *Green hydrogen*, it is produced using water electrolysis to generate hydrogen and oxygen. The electricity that is used for the process is sustainable because it is produced by RES. The main renewable sources used are wind or solar energy, thereby producing only oxygen as a by-product guarantees that the production is emissions free and sustainable.

The production chains of the three types of hydrogen are schematised below in Figure 2.3.

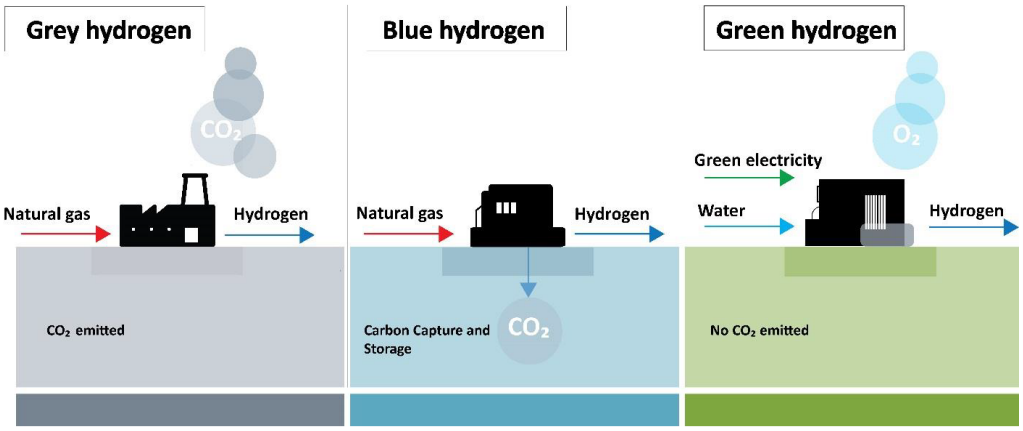

Figure 2.3 The chain production for grey, blue and green hydrogen, source: Eirwind

From now on it will be analysed only the green hydrogen produced by wind energy source. It can be produced directly with electrolysers on site on an offshore platform or on shore using the overproduction of electricity or a constant value of energy. This solution permits to satisfy the energy demand when the wind source is not present because the hydrogen is an energetic carrier that can be produced when the wind is present but there is not energy demand from the grid. Otherwise, it can be stored in tanks and used when needed. The energy vector can be applied in the mobility, industry and gas grid markets too.

Now the offshore hydrogen production process will be analysed. First, the chain production needs a pre-treatment of the seawater that consists in the desalination process in order to reduce the quantity of salt present in the compound. Then the real process to produce hydrogen is made using the electrolysis of water. Finally, hydrogen can be injected into the gas grid and it can be reconverted into electricity when it is needed or used for the mobility an industry markets. The total chain production is schematised in Figure 2.4.

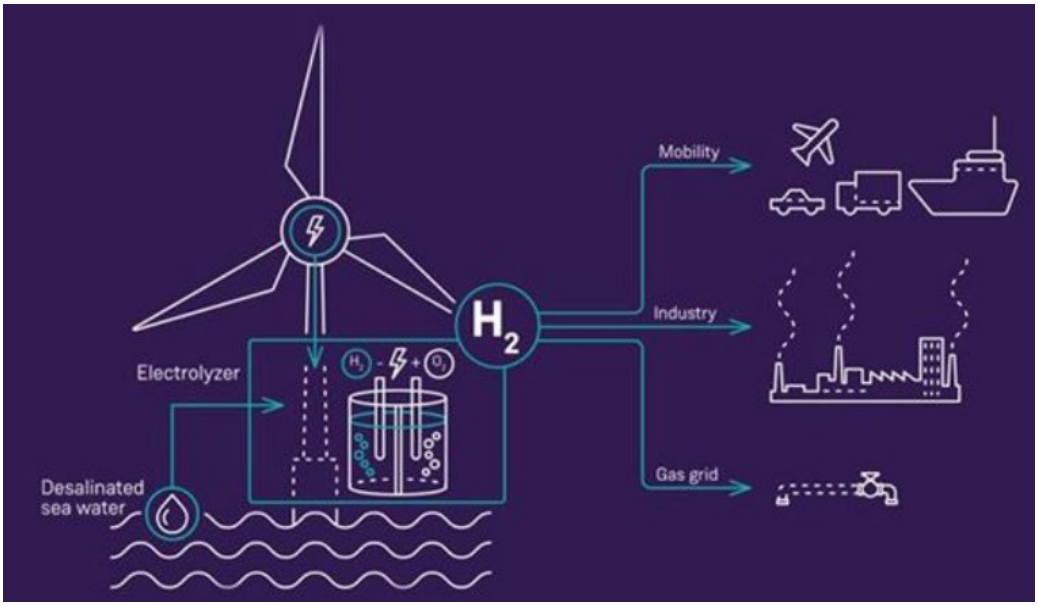

Figure 2.4 Offshore hydrogen production, source: Siemens gamesa

The electrolysis of water is an easy way to produce hydrogen and the presence of water is always available near an offshore wind plant, but it is sea water and it needs to be desalinated and purified.

In order to understand the process present in an electrolyser a simplified structure of it is present in Figure 2.5.

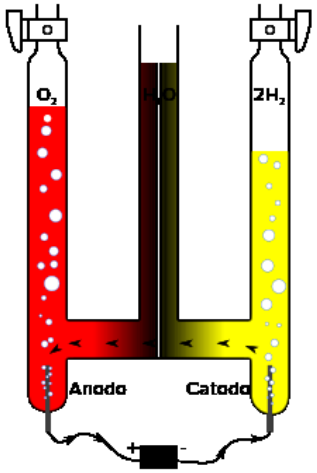

Figure 2.5 Simplified electrolyser

The electrolyser is composed by two electrodes, the anode (positive pole +) and the cathode (negative pole -), divided by a membrane where the water flows. At the ends of the electrodes a voltage difference is applied and the circuit is closed thanks to the conductivity of water in order to have a flux of current. The excess electric power of wind power generation is used to electrolyze water for hydrogen production. Thus, a current with low voltage runs inside the water and creates oxygen at the anode and hydrogen at the cathode following the reaction present in (2.1).

$$2H_2O_{(l)} \rightarrow 2H_{2(g)} + O_{2(g)} \quad (2.1)$$

Where $H_2O_{(l)}$ is the water in phase of liquid, $H_{2(g)}$ and $O_{2(g)}$ are hydrogen and oxygen respectively in the gas phase. Therefore, when the hydrogen is burnt the reaction is inverted respect (2.1), thus the combustion does not emit CO_2 but only water. Nevertheless, in reality it is more common to use air than oxygen to burn the hydrogen. In this case, air contains 78% of N_2 and with high temperature it can be recombined with oxygen producing NO_2 and N_2O emissions.

2.2.1 - Electrolyser technologies

In the market a huge variety of electrolyser configurations is present e.g. Alkaline Electrolysis (AEL), Polymer Electrolyte Membrane (PEM) and Solid Oxide Electrolysis Cells (SOEC).

The AELs is the cheapest technology in the market because this type of electrolyzer has been used on the industry for 100 years. On the other hand, this technology presents the disadvantage that it takes time to start the chemical reaction and the output pressure of the hydrogen produced is low and equal to 30 bar, which requires higher compression for transport and storage. From the studies of Calado et al. (2021) is possible to know that with this technology it is possible to produce 1 kg of hydrogen from 51 kWh of electricity.

The PEMs are more recent respect AEL technology and for this reason, they are more expensive too. They present main advantages like having faster start-up times and a smaller size of the electrolyser and higher output pressure. Calado et al. (2021) attest that with this technology is possible to obtain 1 kg of hydrogen from 58 kWh of electricity. During periods of shutdown, low amounts of energy are required to maintain the system in operation.

The SOEC is the newest technology and it is rarely used in commercial applications due to the high operating temperatures in the range of 700 – 900 °C. The main advantages of this technology are that it presents the best efficiency and it does not require any precious metals.

From the research of Gondal (2019) it is possible to know that PEM technology is one of the most promising water electrolysis technologies for direct coupling with renewable electrical sources because respect SOEC the consumption of auxiliary systems is lower and thus a higher amount of hydrogen can be produced. From this research it is also possible to know the average power consumption of an off-shore platform that houses an electrolyser. The study assumed that for a daily theoretical hydrogen production facility of 50 000 kg per day, the platform would need a power of 104 MW.

The installation of electrolysers is still a matter of study and the main solutions present in literature consider the possibility to install them on turbine platform, on shore or in an intermediate offshore platform. The company Siemens Gamensa is developing dedicated turbines in order to match properly

the hydrogen production. In general, all the offshore electrolysers are in a precommercial phase, and many aspects should be considered in detail such as the sizing of the systems, development of platforms and storage of the hydrogen generated. The main challenge is to match electrolysers with the offshore energy resources because the electric input is not constant due to the variability of the renewable wind source.

2.3 - System configurations

The location of the electrolyzer depends by the system configuration. In particular there are two possible options, it can be placed offshore near the wind farm or onshore near the existing grid coupling point.

2.3.1 – Onshore electrolyzers

When an electrolyzer is placed onshore it is also called hybrid system; the energy produced by the farm is transmitted to shore as electricity by cables and onshore it is used to produce hydrogen. In this way the hydrogen can be produced when the market price for the electricity is low. This solution is simpler and it has the advantage to install a competitive and mature technology for the turbines investing more money for the construction of the electrolyser plant. On the other side, the size for an electrolyser plant can be huge and the presence of space is not always available on shore. Figure 2.6 contains an overview of the onshore electrolyzer system.

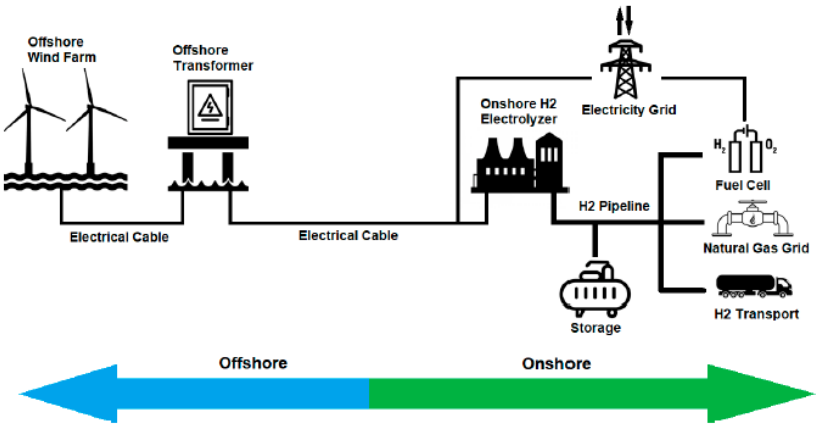

Figure 2.6 Onshore electrolyzer system

In this case it is also possible to place the electrolyzer and the other equipment inside a building in order to provide a better work environment for the operation and maintenance. For the onshore system both AEL and PEM technologies can be applied in the plant. Regarding the source of water there are

two possible options, use the freshwater grid or use the seawater installing a desalination unit next to the electrolyzer.

2.3.2 – Offshore electrolyzers

For the offshore electrolyzer technology the hydrogen is produced offshore and then it is transmitted to shore. In Figure 2.7 it is present an overview of the centralized offshore electrolyzer system.

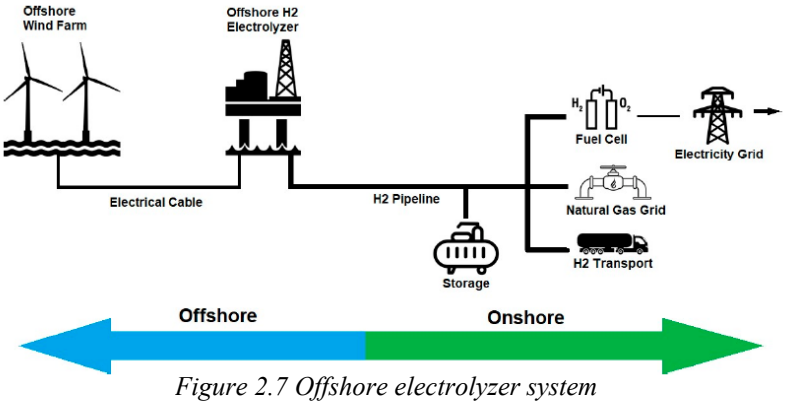

Figure 2.7 Offshore electrolyzer system

For this configuration the best choice is the PEM technology because it presents a smaller footprint, this permits to have a smaller platform. On the other hand, an additional compression is required because the output pressure is around 30 bar. Two electrolyzer configurations are possible: a unique centralized electrolyzer fed by the whole wind park or individual electrolyzers, which present one electrolyzer per wind turbine. The main components for both the configurations are:

- PEM and supporting electronics
- AC-DC rectifiers
- Desalination unit and reservoir for desalinated water
- Seawater pumps
- Export pipeline
- Backup power source
- Communication equipment.

The *centralized electrolyzer system* presents a typical installation for the offshore wind turbines. The power produced by each individual turbine is transmitted to a central platform through underwater cables. Once the electrical power reaches the central platform, most of it can be rectified to DC to produce hydrogen; the other part is used to power the seawater pumps and hydrogen compressor in AC. The produced hydrogen exits at 30 bar, thus it is compressed to the desired pipeline input pressure in order to be transmitted into export pipeline to the shore. In Figure 2.8 the arrangement of the system is depicted.

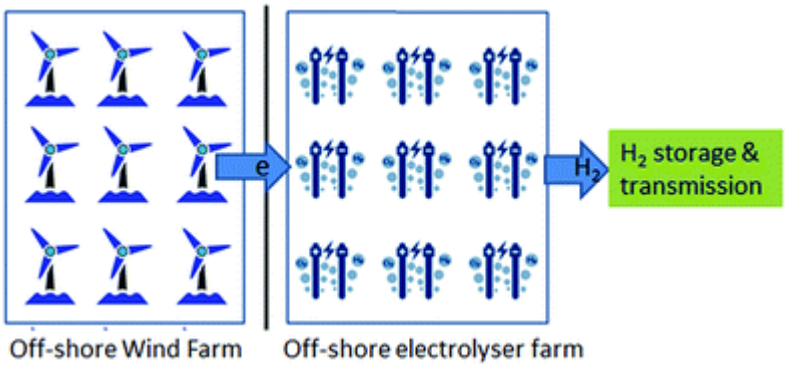

Figure 2.8 Centralized electrolyzer system

The *individual electrolyzer system* is usually installed when sufficient wind is present. In this case, most of the electricity is fed into the rectifiers to power the electrolyzer, while the remaining power is used to power the seawater pumps. The produced hydrogen exits the electrolyzer and is exported by a small dimension pipeline to a subsea collection manifold, which receives the hydrogen produced by each turbine-electrolyzer system and exports it to shore using a bigger diameter pipeline. In this case the compression process is done in a proper platform where the all the small pipeline are connected. An aspect to take into consideration is that the bottom fixed and floating technology require significant modifications to be able to support the extra infrastructure. In order to make the platform suitable for all the equipment, modifications need to take place. This configuration is depicted in Figure 2.9.

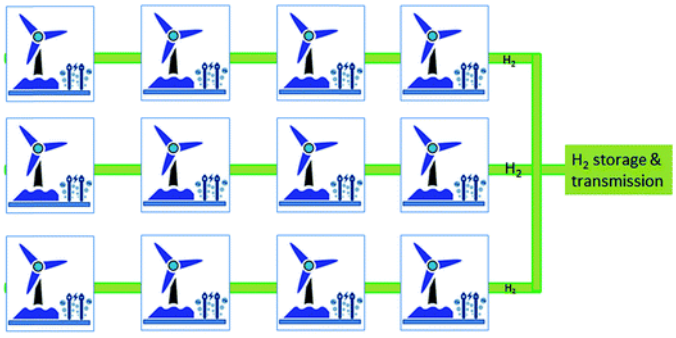

Figure 2.9 Individual electrolyze system

In the market number of commercial models of MW-scale industrial electrolysers are available. It is interesting also to notice the study conducted by Gondal (2019) in order to have an idea regarding technical data of the electrolysers. The study considers a PEM electrolyser Hylyzer-3000-30 manufactured by Hydrogenics. The salient features of the electrolyser are given in Table 2.2.

Table 2.2 Technical data of an offshore electrolyser

Parameter	Value
Output pressure	30 bar
Nominal hydrogen flow	3000 $Nm^3 h^{-1}$
Nominal input power	15 MW
AC power consumption	5-5.4 kW h Nm^{-3}
Footprint	600 m^2

Considering the output of an average 5 MW wind turbine, it can be seen that with the above mentioned electrolysers and a conversion factor of 11.1 Nm^3 hydrogen equivalent to 1 kg of hydrogen at ambient pressure and 20 °C; 240 metric tons of hydrogen is obtained from a single turbine over the course of a week. Thus, the farm output can be equivalent to approximately 7500 metric tons, assuming that the wind turbine and the electrolysers operate at the rated power and output (100% capacity factor). Considering a wind farm power equals to 300 MW as input for the above mentioned electrolyser (Hylyzer-3000-30) results in 20 electrolysers with a cumulative footprint of at least 12 000 m^2. This area is much larger than the main deck area of even large offshore oil platforms. It can be appreciated that these electrolysers will also have with them a network of electrical and gas fittings which further enhance the overall area requirement.

Hydrogen economy's greatest challenge still lies in large scale storage of hydrogen, the low energy density of hydrogen being the prime reason for lack of economical storage solutions. Table 2.3 gives the characteristics of hydrogen with respect to the storage methods.

Table 2.3 Hydrogen storage methods

Medium	Weight [kg]	Volume [L]	Density [% H_2 by weight]
Compressed gas at 35 MPa	45	145	6.7
Compressed gas at 70 MPa	50	100	6.0
Cryogenic H_2 liquid	40	90	7.5
H_2 solid in metal hydrides	215	55	1.4

Offshore renewable energies have the potential to generate large amounts of hydrogen, on the other hand the storage options available are not economically feasible to handle the amount of produced hydrogen from offshore renewable resources. Transition storage facilities have to be developed for hydrogen that is due to be shipped onshore. The main problems in gaseous storage are the low volumetric density and the high filling pressures of hydrogen. Liquefied hydrogen stored as a cryogenic medium has comparatively higher energy density; however, it is extremely susceptible to evaporation losses. Moreover, a lot of primary energy is required to keep hydrogen under cryogenic conditions (−253 °C). Hydrogen stored in solids (carbon nanotubes, metal hydrides and chemical hydrides) allows more hydrogen per volume unit to be stored than with liquid hydrogen. Practically offshore storage of hydrogen in large quantities in either the gaseous, liquid or solid form is infeasible in the current state of the art due to large scale infrastructural requirements in the form of compressors, liquefying equipment and the associated auxiliary apparatus. While the development of novel onshore

hydrogen storage technologies continues to progress, the focus on offshore storage of hydrogen has shifted to alternative options mainly concerned with transportation of the produced hydrogen. Transportation of gaseous and liquefied hydrogen in ship mounted tankers is already in operation and solutions for bulk carriage of hydrogen are in the developmental stage.

Hydrogen produced offshore can be liquefied and then transported like a fossil fuel or it can be directly sent to a pipeline. In particular, for this second option one possibility is to inject hydrogen in the existing gas network. Figure 2.10 depicts the currently pipeline network present in Ireland for the transportation of natural gas.

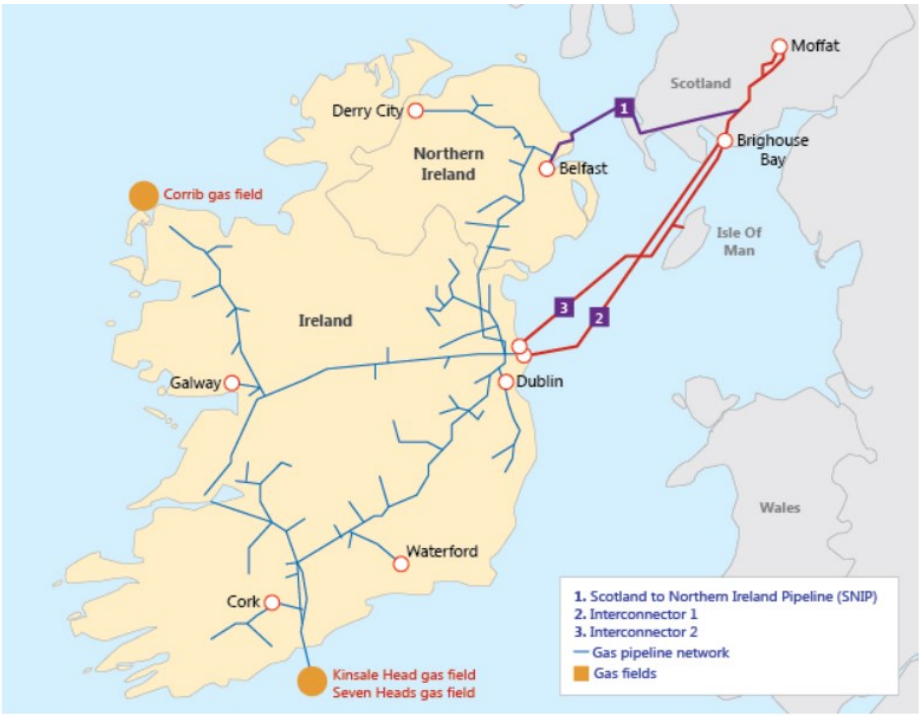

Figure 2.10 Ireland's natural gas pipeline, source https://consub.com/portfolio/gas-transmission-pipeline-eprs-study/

As it can be seen from Figure 2.10 the actual pipeline network is not able to satisfy the huge quantity of hydrogen that could be produced by RES and the cost for laying an equal-energy hydrogen pipeline is six times that for natural gas as Gondal (2019) attests. For that reason, a good option is to inject a low percentage (lower than 20%) of hydrogen into the gas pipeline. However, for delivering the output produced by offshore wind farms the pipelines require to be design with a larger diameter for transporting and deliver an equivalent amount of energy and an enhanced pressure. Hydrogen transported in a high-pressure transmission network means that hydrogen's volume transported has to be thrice that of natural gas. This results in an increase in compression capability as much as twice that of the conventional capacity for natural gas. Increased compression would require higher rotational velocities to achieve a mass flow rate. Nevertheless, increasing velocities are limited by the material strengths of the compressors; therefore, it may be concluded that the compressors installed

in the existing infrastructure are insufficient to handle hydrogen in the same quantity as that of natural gas. As the research of Gondal (2019) indicates a part from the infrastructural issues the cost for laying an equal-energy hydrogen pipeline is six times that for natural gas. Dedicated hydrogen pipelines and the layout of a new pipeline infrastructure for transport of offshore generated hydrogen for onshore demand centres are uneconomical as yet in comparison with the natural gas pipeline network. The cost of laying a hydrogen pipeline is as much as 40 - 50% higher than the conventional gas pipelines. Moreover, the cost of hydrogen transmission is substantially higher than the cost of oil and natural gas transportation. Figure 2.11 depicts a comparison in the total cost for different energy transportation options.

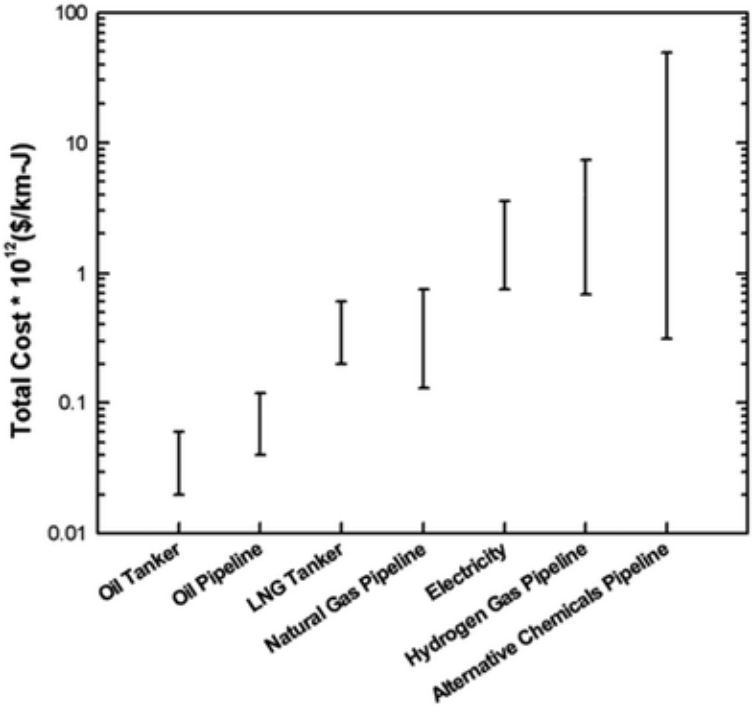

Figure 2.11 Total cost of different energy transportation options, source: Gondal (2019)

As it can be seen in Figure 2.11 hydrogen pipeline transport is one of the most expensive options. Resultantly, one of the options for transporting in existing gas pipeline infrastructure is to transport hydrogen as a mixture with natural gas. It has been found that hydrogen can be mixed with natural gas up to 17% by volume as Gondal (2019) attests. However, transmission of hydrogen as a mixture with natural gas would only be possible where offshore natural gas fields and infrastructure are already present. Furthermore, it cannot be considered as a long-term solution because offshore gas fields may have to be abandoned on depletion of the gas wells but there is the potential to reuse the infrastructure for 100% H_2 with upgrades. In order to use the natural gas infrastructure, it becomes important that any proposed offshore wind farm is situated near gas fields. This restriction may compromise the output of the wind turbine because of the possible reduced wind speed as compared to an appropriate offshore location with a higher wind speed. The issues concerning the transportation

of large quantities of hydrogen can be effectively addressed using Power-To-Gas technology (P2G). P2G technology has long been considered as a way to harvest RES where grid transmission of electricity is not available. Conversion of hydrogen into Synthetic Natural Gas (SNG) would enable the transportation of SNG using conventional ships or the existing natural gas pipeline infrastructures.

2.4 - Irish gas pipeline

The current gas pipeline is not well spread around the island and are present only two importing connections, they are named interconnection 1 and interconnection 2. The principal pipelines and nomenclature are present in Figure 2.12.

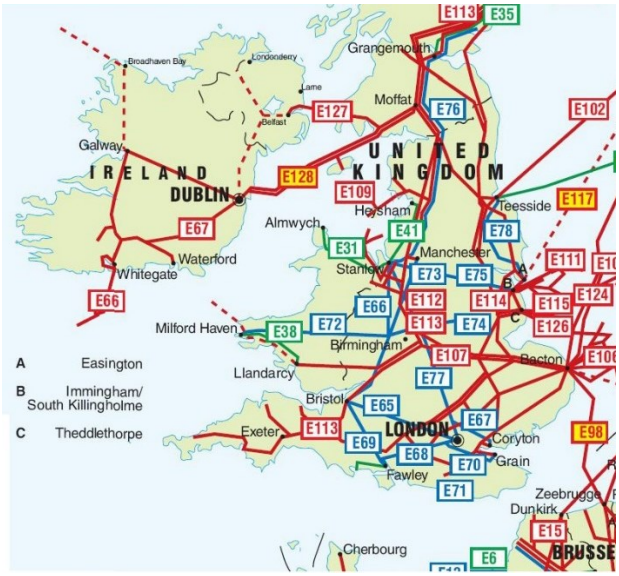

Figure 2.12 Ireland's gas pipelines, source: https://theodora.com/pipelines/united_kingdom_and_ireland_pipelines.html

Thanks to *Teodora*'s website [5] it is possible to have the main technical data regarding the principal Irish pipeline. The most important lines are:

- Connection 1 and connection 2 also named as E128. Both of them interconnect UK with Ireland with a tube diameter of 30 inches (610 mm and 762 mm) respectively and a pressure of 140 bar;
- E127 interconnects the Scotland with the North Ireland and it is also named as SNIP. It presents a diameter of 24 inches (610 mm);
- SNP connects the North Ireland with Gormanston with a tube diameter of 18 inches (450 mm) and a pressure of 75 bar.

Inside the Ireland's country the technology applied is equals to the SNP pipeline with a diameter of 18 inches (450 mm) with the only difference in the pressure that in this case is equal to 55 - 70 bar.

The commission for regulation of utilities attests that the transmission system in Ireland is settled to a potential maximum pressure of 85 bar, then the pressure is reduced to 19 - 40 bar and after it is supplied to the distribution system or to the customers. In the distribution system there are two pressure categories: the medium pressure that works with 1 - 4 bar and the low pressure that works at 18 -100 mbar. For the domestic, industrial or commercial users the final pressure is set at 20 mbar and 75 mbar respectively. Figure 2.13 presents all the cities that present the injections point present around the country.

Figure 2.13 Gas injection points to the internal Irish gas pipeline

2.5 - Electric connections

Regarding the electrical parts in an offshore wind farm the system is composed by the collector and transmission parts. In Figure 2.14 a typical arrangement is depicted.

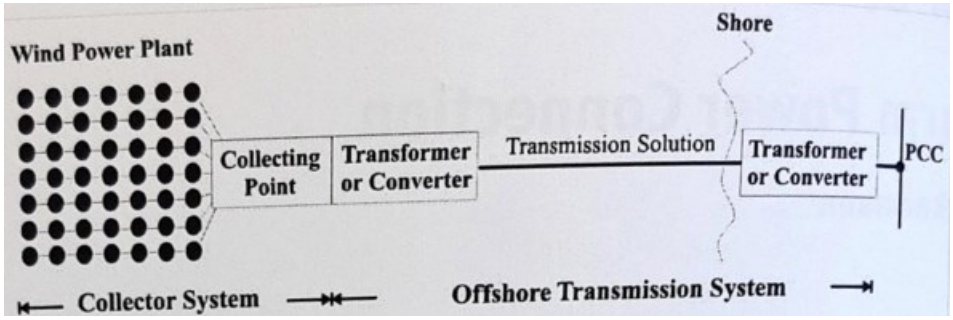

Figure 2.14 Offshore wind farm electric connections, source Twidell et al. (2009)

The inter-array cables among turbines in the *collector system* gather the energy from the turbines and transmit it to the collecting point. As described, present generators work in AC, thus the collector system is designed to function in AC and with a medium level of voltage. While the export cables are the one present in the *transmission system*, they transfer the energy from the collector point to the shore to the Point of Common Coupling (PCC). These lines can work in AC or DC depending by the configuration of the site and with a high level of voltage. Between the collector and transmission system an offshore substation is present where there is the transformer to increase the voltage.

The turbines used nowadays have a variable speed, thus they are able to sustain maximum efficiency over a wide range of speeds. Among variable speed wind turbines different solutions are present, e.g. limited variable speed generators, generator with partial scale frequency converter, variable speed generator with full-scale frequency. The *limited variable speed generators* use a variable rotor resistance known as OptiSlip developed by Vestas, which allows them to work at synchronous speed +0% to +10%. The *generators with partial scale frequency converter* are doubly fed induction generators with a partial scale frequency converter on the rotor circuit that can function at synchronous speed -40% to +30%. Finally, the *variable speed generators with full-scale frequency* converters with full variable speed. All these machines generate electricity in alternating current (AC) usually at low voltage (typically under 6 kV). As a result, the collector system will function in Medium Voltage Alternating Current (MVAC) and it usually works around 30 kV.

The collector system interconnects the wind turbines in the wind farm and connects them to the collecting point. For small wind power plants, without an offshore substation, the collecting point lies in the basement of a wind turbine. For larger wind power plants, the collecting point can be part of an offshore substation and very large offshore wind power plants might even have more than one collecting point/offshore substation. After the collecting point there is the offshore transmission

system composed by the transformer that raises the voltage level and the exporting cable that connects the transformer to the PPC to shore. For small wind farms and a short distance to shore, a transformer is not required because the voltage in the collector system (usually 30 kV) and to shore can be the same. In other cases, a transformer is usually necessary to increase the voltage in order to reduce the transmission losses. If the offshore transmission system uses high-voltage DC in the offshore substation will be also present the converter stations will be also present in order to convert the current in AC to DC. Onshore, either a transformer or a converter station is used to rise the voltage (usually to 400 kV) and to convert the current from DC in AC in order to inject the produced power to the onshore grid system. If the offshore transmission system operates at the same voltage as the onshore network, only switchgear is required at the point of common coupling. In Figure 2.15 an example of offshore wind farm connection is depicted.

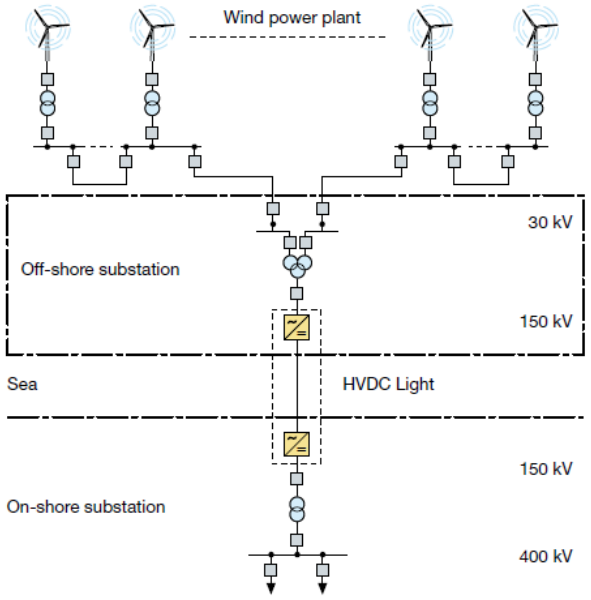

Figure 2.15 Possible electric interconnections of an offshore wind plant

The offshore collector system uses an AC network, which collects the power production from each wind turbine. The collector voltage used within onshore wind farms lies usually in the range of 33 – 36 kV. The collector system gathers the energy from the turbines so that it can be transmitted to shore. As described, present generators work in AC, and so the collector system is designed to function in AC too. In principle, the electrical collector system can be adapted to any wind farm layout although offshore wind farms tend to be larger in terms of total capacity and number of turbines, which increases the requirements on the design of the electrical collector system. However, installation costs and performance, e.g. losses, of the electrical collector system can vary substantially depending on the wind farm layout. The maximum number of turbines that can be connected to one feeder, for

instance, will depend on the maximum cable rating of the cable connecting each feeder to the collecting point.

The possible electrical system layouts following the studies Twidell et al. (2009) are:

- Single collector radial
- Single collector – single return
- Single collector – single sided ring
- Single collector – double sided ring
- Single collector - star clusters
- Multi - collector ring.

In Figure 2.16 all the electrical configurations are shown.

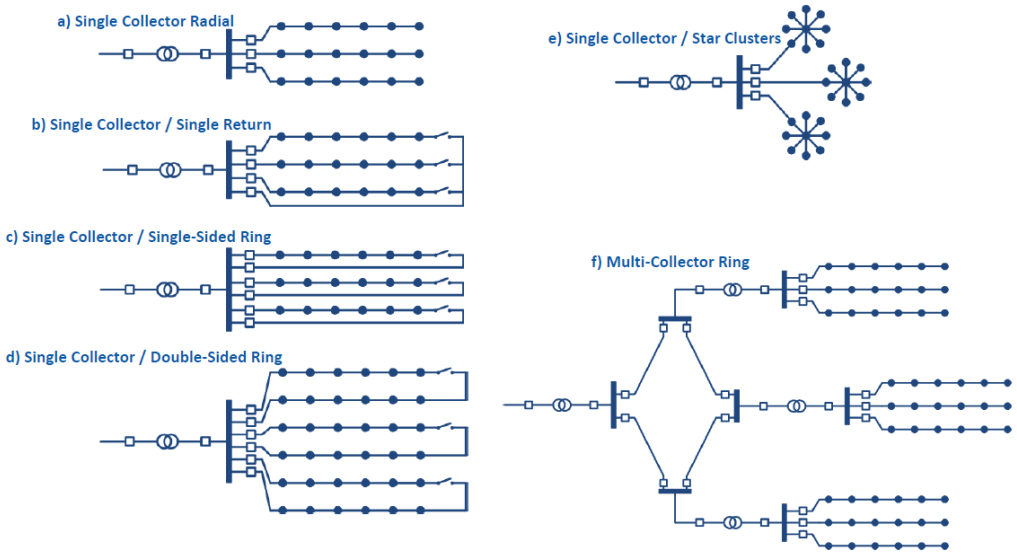

Figure 2.16 Possible configuration for the collector and turbines' layout, the dots are turbines and the line the cables

The *radial network* is the simplest arrangement for a large wind power plant; number of turbines are connected to the same feeder in a string arrangement. The main advantage of this configuration is the low cable costs. Lumbreras S. (2013) confirms that the average energy losses in the radial configured collector systems are about 2 % of the annual power production of the wind power plant, it is the design with the most losses. The major downside is the poor reliability of the system, since the cable or switchgear faults at the hub end of the radial cluster may prevent all downstream turbines exporting power from the duration of the fault. This configuration has been the most widely applied because of its lower cost and easy control. However, the lack of redundancy means that its reliability is poor, as any fault will potentially prevent upstream turbines from selling power.

With some additional cabling and switchgear, *ring layouts* can address the reliability of the simple radial layout by enabling alternative routes for exporting power during a cable fault. The additional security comes at the expense of increased cable costs for a given number of turbines. The ring configuration can be single-sided or double-sided. The *single-sided ring* is provided with an additional cable from the last turbine in a row back to the collection hub. This cable should be able to carry the total power generated by the string. It is the most expensive than the standard assortments, doubling the cost of a radial layout. However, it is also the most reliable and the one with the least losses. The *double-sided ring* tries to overcome the cost disadvantages of the single-sided ring by using the cable of the neighbour string as the redundant circuit. If a fault occurs, any string would needs to deliver the full power of two strings. Therefore, they should be rated at twice the power of a row. This option is thought to be around 60% more expensive than a radial design.

The *star layout* reduces cable ratings and provides high level of security for the wind power plant as a whole, since one cable outage in general only affects one wind turbine. The drawback is that this layout requires longer diagonal cables arrangement and some short sections of higher rated cabling. The star design was proposed as an attempt to reduce cable ratings because all the cables from its centre to the arms would just need to bear the power coming from one turbine. However, cables can be longer and the switchgear more complex, thus the cost advantage depends on the specific case under study. This configuration also offers a high level of security, with only failures of the cable that connects the centre to the collector hub affecting more than one turbine.

The *multi-ring* was conceived as a way of dividing the power generated in a faulted string among the rest of the rows, thus the capacity does not need to be upgraded as in the double-sided ring. This assortment has around 25% lower losses than a typical radial array. It is more reliable and its cost is only around 20% higher. Even though preliminary studies of standard designs are useful, both cost and reliability are so dependent on the particular geometry that the optimal solution is normally a hybrid of these architectures. What is more, in spite of symmetry in the geometry, the optimal layout can be asymmetric.

The *transmission system* takes the power generated and sends it to shore to the point of common coupling (PCC). The technology to be used is the most important decision. For the cabling to shore, either high voltage AC (HVAC) or high voltage DC (HVDC) connections can be used. For HVDC, there are two technical options:

- Line commutated converter (LCC) based HVDC
- Voltage source converter (VSC) based HVDC technology.

The study of Fernàndez-Guillamòn et al. (2019) reports that the choice mainly depends by the distance to the shore. All offshore wind power plants that are currently operating have adopted an AC alternative. This is because these wind power plants are comparatively small and/or at a short distance from the shore. The situation may change as future wind power plants are expected to be larger and to be situated further off the shore.

In particular, an HVAC transmission system consists of the following main components: AC based collector system within the wind farm, an optional offshore transformer station including offshore reactive power compensation, three-core cross-linked polythene (XLPE) HVAC cable(s) to shore; and onshore an optional Static VAR compensator. The main factor limiting the transmission distance of HVAC transmission systems is the reactive power generated by the cable system.

The HVDC transmission with thyristor based LCC technology can transmit large amounts of power at voltages as high as 800 kV. It is a mature technology that relies on large converter stations both onshore and offshore that include transformers, converters and filters, as well as an auxiliary power set. Their cost is only competitive at higher distances to shore. In addition, they decouple the OWF and the onshore grid so that failures are not propagated and operation can be done at frequencies non-synchronous. They also enable active and reactive power controls. However, this technology has the disadvantage of needing a voltage source in order to provide commutation for the thyristors, and the generally used control systems are unable to work when connected to a weak grid. The practical application of this technology has been limited for these reasons. A thyristor based LCC HVDC transmission system for an offshore wind power plant would consists in the following main components:

- AC based collector system within the wind farm
- an offshore substation with two three-phase two-winding converter transformers as well as filters
- a diesel generator which would supply the necessary short-circuit capacity
- DC cable(s)
- an onshore converter station with a single phase three-winding converter transformer as well as the relevant filters.

The VSC technology is based on self-commutated switches, mainly insulated gate bipolar transistors. Pulse width modulation was widely used until the development of more sophisticated strategies. VSC provides better and independent active and reactive power controls in each converter station, being able to operate in all the four quadrants of the PQ plane. This makes it possible to connect the OWF to a weak grid. In addition, there is no risk of commutation failure unlike with LCC. Furthermore, it is easier to implement multi-terminal schemes, and the system as a whole is more compact than the traditional HVDC. A VSC based HVDC transmission system presents the following main components:

- AC based collector system within the wind power plant
- an offshore substation with the relevant converter(s)
- DC cable pair(s)
- an onshore converter station.

The VSC HVDC is typically operated as a bipolar system and is usually not connected to ground, i.e. not earth-connected.

Lumbreras and Ramos (2013) compared the last three options and found that, in general circumstances, it is possible to determine which transmission system is more suitable for a given OWF just by taking into account its rated power and distance to shore. Table 2.4 summarizes this consideration.

Table 2.4 Preferred transmission technology

Distance [km]	Low power (<200 MW)	Medium power (200 MW<Power<300MW)	High power (>300 MW)
Short distance (<140 km)	HVAC	VSC HVDC	LCC HVDC
Long distance (>140 km)	VSC HVDC	VSC HVDC	LCC HVDC

According to their calculations, HVAC is only efficient for distances under 140 km and rated power under 200 MW. On the other side, VSC performs better for the rest of cases where power is below 300 MW. Whit a higher power, component limitations become relevant, and LCC HVDC is the preferred option.

2.6 - Cable technology

The cables used in the offshore wind farm are submarine cables, specifically designed to endure to salt water. One of the differences between land and subsea cables will be in the application of a longitudinal water barrier below the jacket of a single-core construction. Most commonly, a thin aluminium foil is used for that purpose. Additionally, submarine cables may have several layers composed of semi-conducting or non-conducting swelling tapes aimed to prevent water ingress into the insulation, see Figure 2.17.

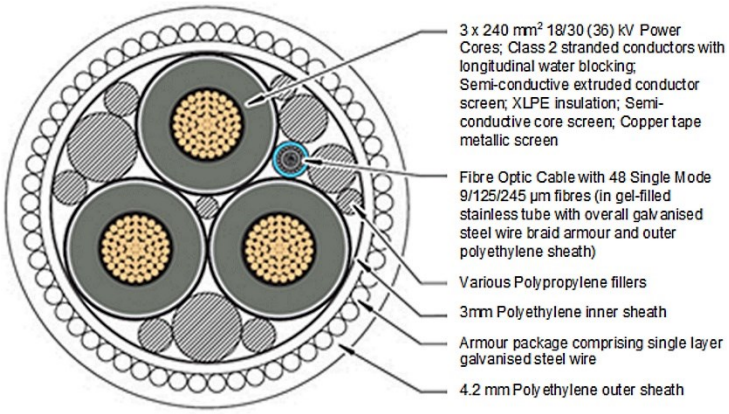

Figure 2.17 Cross section of an offshore submarine cable

Another important difference between land and submarine cables is the application of armour in the latter. Armour, most often built of steel wires in one or two opposite twisted layers, is applied with twisting in the same or an opposite direction with respect to the cores. It serves as a protective layer but also provides the required strength during the laying process and to achieve the required on-bottom stability to minimize the lateral movement of the cable on the seabed and to ensure that the integrity of the cable is not compromised.

Regarding the configuration of the cables in the offshore wind farm for the HVAC transmission the possible solutions are:

- Single core cable
- Three core cable.

The *three core* configuration permits to cancel the magnetic field leading to a reduction in power losses. Even the installation cost is lower respect the single core configuration. It is built by twisting three single-core cables and then applying armour reinforcement with several no conducting layers. On the other hand, the single core cable reacts better in the dissipation of heat and is easy to repair. The *single core* constructions currently most often use XLPE insulated cables, but paper-insulated cores are also quite common, especially in older installations. Usually the single-core design operates at higher voltages than the three core cables and it is usually used for a high voltage AC export cable and all DC cables.

In Figure 2.18 it is present the configuration of the two cable configurations.

Figure 2.18 Single core and three-core ABB cables

The most used configuration for inter-array and export cable is the three core submarine cables with copper wire for offshore wind plants.

Another classification of the cables depends by the type of foundations that the wind turbine presents in the farm. They can be classified as:

- Wet cable
- Dry cable or dynamic cable.

The main technical difference is that over the armour a layer of polypropylene strings is laid, and such structures are called wet structures, i.e., seawater can penetrate through the roving and armour into the inter-strand space in the cable or the dry structures which have a tight sheath made from high-density polyethylene under and above the armour. However, it should be mentioned that the cable could be covered with the extruded HDPE and still be classified as a wet design. The manufacturers sometimes drill a hole in the extruded outer sheath to make the cable wet design. The holes are made to eliminate the pressure inside the cable. As a consequence, they protect the joints and terminations against a possible damage. Due to the difficulties in execution and costs, wet cables constitute the vast majority of cables and are used for installations permanently laid on or under the seabed.

Dry cables or dynamic cables, usually with two or more layers of armour, are used for mobile applications; that is, for floating wind farms in which cables are suspended from a floating platform and hover in the sea thanks to special floats that keep them in the water. Technical solutions in wet cables are cheaper compared to dry dynamic cables, however, when designing a cable line, the material used for the production of conductors should also be considered.

The use of aluminium as the cheapest and lightest conductor may entail high service costs in the future directly resulting from its physicochemical properties. The most important are the high coefficient of thermal expansion and the high susceptibility to corrosion in the seawater environment. Cables in wind farms are subject to changes in the diameter of the working conductors. Current loads, wind force, and extreme weather conditions may cause thermal expansion of the conductor, which may result in the change of its diameter. The phenomenon of thermal expansion and contraction of the material harms the insulating layer. The result is micro cracks in the insulation system, which usually lead to partial discharges and, consequently, to a cable breakdown.

In the case of a breakdown and water intrusion into the cable, in which there are micro cracks, seawater may enter the micro pores causing aluminium oxidation. The effect of aluminium oxidation will be porous, large-volume aluminium oxides, which, due to their volume, will damage the insulation, making it impossible to perform local cable repairs and will force the replacement of the entire section. This phenomenon does not occur in cables with copper conductors. Therefore, at the design-stage of submarine cable lines, attention should not only be paid to investment costs, which will be lower for cables with aluminium conductors, but also to the costs of servicing such lines, which will be much higher compared to a cable line with aluminium conductors.

The main technological challenge in the production of submarine cables is to maintain the required long sections of up to 30 - 50 km in length. For technical reasons, it is often impossible to make the

factory section of insulated wires of such lengths. Because of the applied technological processes, it is not possible to use (land) joints, commonly used onshore, which significantly increase the diameter of the cable.

In order to have an idea about how many solutions are present in the market Figure 2.19 shows different technologies and application of submarine cables.

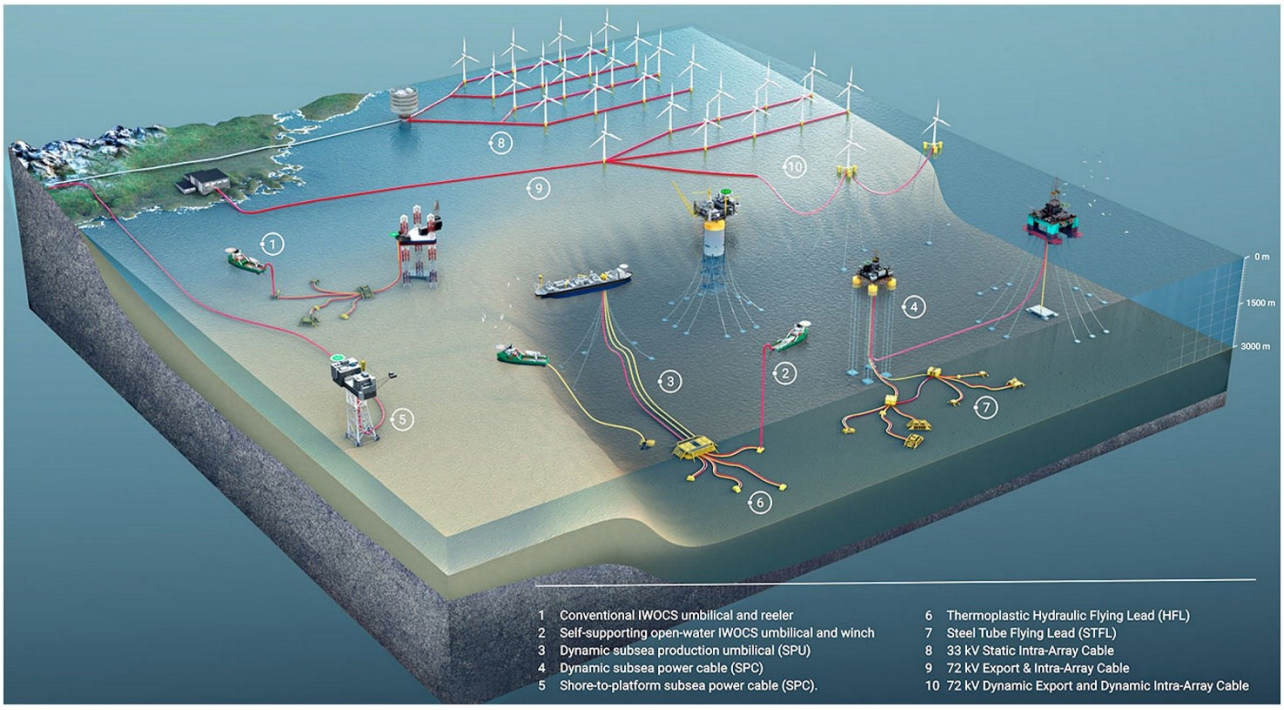

Figure 2.19 Different submarine cable configurations

In Figure 2.19 it can be seen all the available technology for submarine cables. The technology of dynamic cables for wind turbines is still in state of development and it is similar to the one used by boat application.

2.6.1 – The connectors

The connectors are an important part of the electric system, they are needed to connect two or more cables to a larger circuit. Depending on where they are mated they can be classify in dry-mate connectors or wet-mate connectors. The dry ones are mated in a dry environment and are deployed under water. While the wet ones are mated and deployed under water. The most suitable technology for the offshore wind turbine is the wet one.

All the information reported in this chapter will be used to correctly design the wind farm. In fact, an initial study on the state of art on the turbines, foundations, cables, piping, etc. is essential to understand which technologies are the most suitable for the plant because the site will be design starting from zero choosing the type of component to install.

CHAPTER 3 – Offshore wind farm

In this chapter it will be analysed the best location for the offshore wind farm that will be taken into examination. After the type of arrangement will be decided for the layout of the turbines considering the present literature and the data of the wind for the location. At the end, different types of electric connections will be taken into consideration.

3.1 – Design of the offshore wind farm

The design of an overall wind farm layout aims to maximizing the overall production, taking into account the distributions of wind speed and direction as well as the turbulence between turbines, site ownership and planning permissions. The layout of onshore wind farms can therefore vary considerably, e.g. accounting for particular site conditions and complex terrain. The layout of offshore wind farms has less topographical and site-ownership constraints, but may be influenced by water depth and seabed conditions across its area. However, often the entire offshore site has approximately equal water depth, and so minimizing wake and turbulence effects between turbines becomes the main design criteria. Consequently, the distance between individual offshore turbines is generally larger than for similarly sized machines onshore.

3.1.1 - Site analysis: natural restrictions and bathymetric chart

First, it will be decided which shore should be the best option. The west coast of Ireland presents a huge depth and thus in order to install an offshore wind farm an advanced and expensive technology should be applied such as the floating configuration. For this reason, it is preferable to install the plant in the east coast that presents a lower depth and a mature technology can be applied. This decision will lead to a more affordable site investment and the possibility to have a more detailed study thanks to a greater knowledge and literature in the sector. In particular, it is also important to consider a location where the point of injection to the gas pipeline is available and there is a developed city that it is also able to sell the hydrogen production to other countries. Considering all these reasons, it has been decided to place the offshore wind plant in Dublin that is the most developed city in terms of pipelines and export. Before defining the exact position where the farm should be placed it is important to make a study of the area. In fact, it is important to detect the existing restrictions.

At the begging, the environmental restrictions will be analysed; this can be done looking the nautical map presented in Figure 3.1.

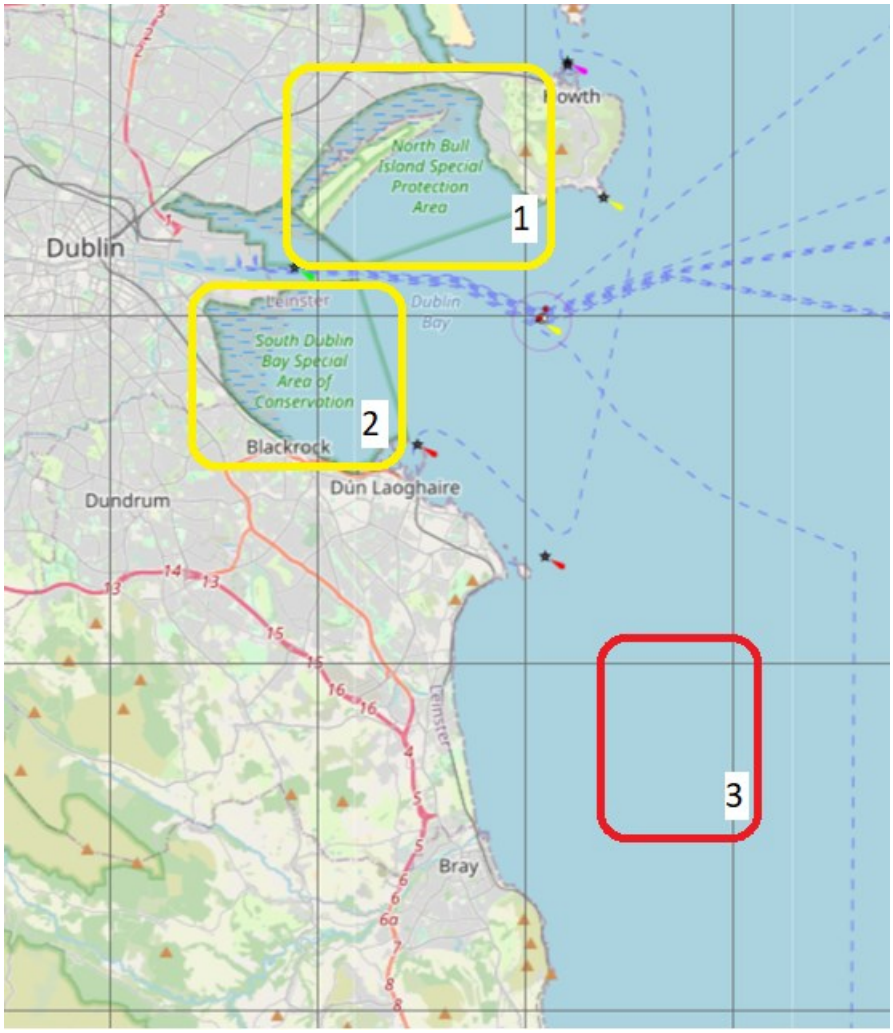

Figure 3.1 Dublin's nautical map. The yellow square 1 and 2 represent the natural resources and the red square 3 represents the place where the wind farm will be design, source https://map.openseamap.org/

It is possible to notice from Figure 3.1 that there are two conservation areas: the North Bull Island special protection area in the yellow rectangle 1 and the South Dublin bay special area of conservation in the yellow square 2. Moreover, the shipping lane presents in Dublin's bay is expressed by the dotted line and it cannot be interrupted. Thus, the Dublin's bay can be discarded because the wind farm cannot be placed in the natural reserve and the ship road cannot be interrupted. Due to the naval and natural reserves limitations it has been considered to place the plant to the south of Dalkey, precisely in front of Bray bay represented by the red rectangle 3. In this area there is only one naval course that could interfere with the project and it is the one that connects Dublin to Cherbourg. However, it is important to remember that the huge distance between the turbines permits to small ships to pass through the site, while the presence of huge ships is not allowed. Then it is also important to analyse the bathymetric chart in order to know the water depth of the seabed present in the area in order to install a proper foundation technology for the turbines. The chart of the interested area is present in Figure 3.2.

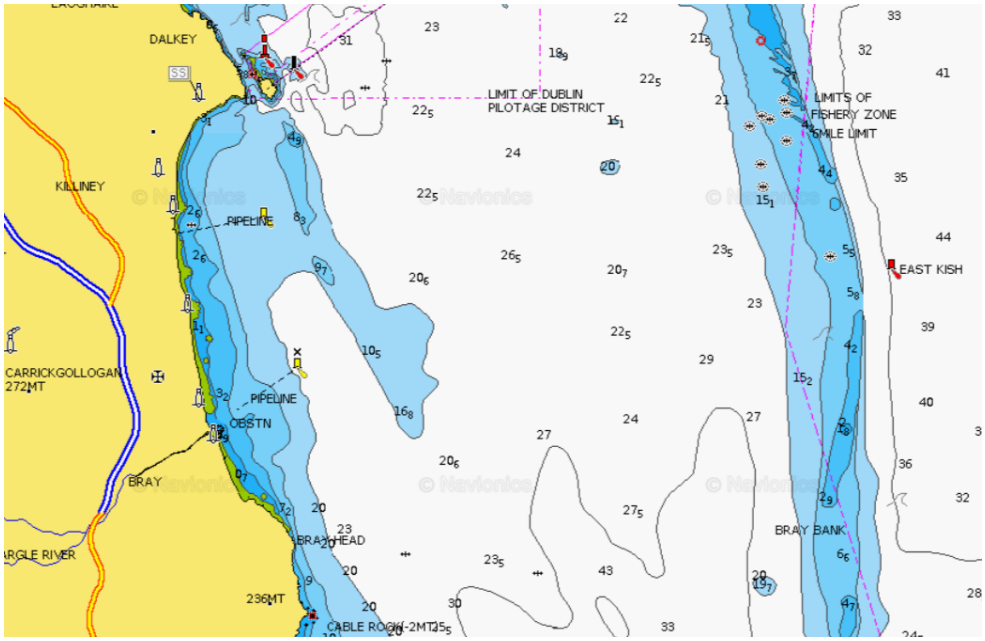

Figure 3.2 Bray's bathymetric chart in [m], source Navionics

As it can be seen in the bathymetric chart the depth of the seabed varies from 2 to 44 m depending by the location. The depth of the seabed is not too high and a traditional configuration can be considered for the installation of the wind turbine. This will permit to lower the installation cost and propose a plant with a lower investment cost. The best placement where install the turbines is into the white area in Fig 3.2 with a water depth between 20 and 26 m. This depth is suitable to install the wind farm and the gradient is not raised too much. The depth decreases getting closer to the shore, while it increases going to the open sea. In Figure 3.3 it is depicted where it has been decided to place the offshore wind farm.

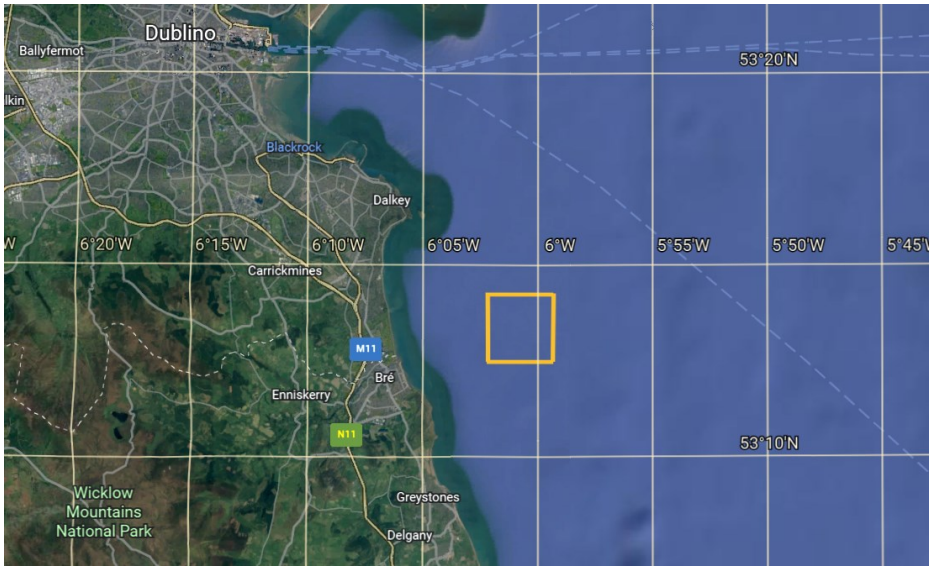

Figure 3.3 Location of the offshore wind farm

The yellow square in Figure 3.3 indicates where the plant will be installed.

The real constrains present in the location site indicated in Figure 3.1 have also been checked in the SEAI wind atlas site [6] ant it is verified that for the location selected in the yellow square in Figure 3.3 there are not any presence of navigation channels, danger areas, shore anchorages, thus the location is acceptable.

3.1.2 - Anemometric analysis

In the following, an analysis on the wind speed, its prevalent direction and frequency will be presented in order to understand in which direction to orient the generators.

The mean hourly data regarding the wind speed are obtained from the wind atlas of the SEAI (Sustainable Energy Authority of Ireland) for the location presented in Figure 3.3. The data in the atlas are referred to the year 2006 and an altitude of 50 m. It is important to remember that the proper altitude for the hub of a turbine is around 100 m, but the data are not present for this height. In fact, it is common that the data are acquired for an altitude that is lower than the hub turbine height because the anemometer tower is at maximum 50 m height due to cost reasons. The wind velocity changes with the altitude because the friction between air and ground slows down the wind near the soil; thus, it determines a velocity profile that is function of the height. The velocity trend changes with altitude and it depends by the roughness of the ground and obstacles as is depicted in Figure 3.4.

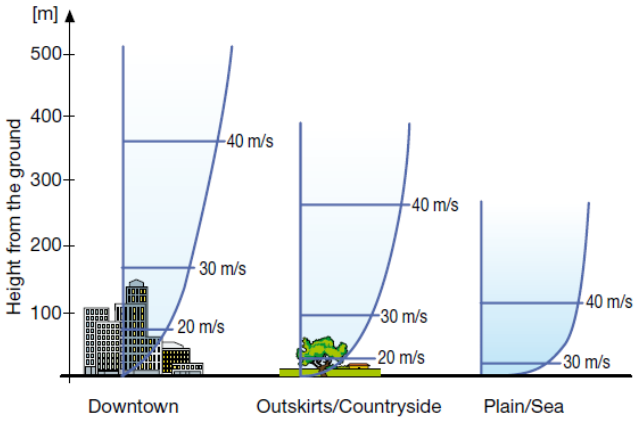

Figure 3.4 Vertical wind profile, source: technical application papers ABB

It can be seen in Figure 3.4 that in plain or in the sea the velocity trend changes less because it is less common to have obstacle at the surface. Moreover, at the typical height of the hub turbine it is present a slight variation in the velocity with respect to the measured velocity. The velocity change more in the range from 0 to 40 m/s but when the distance from the ground it is really huge (around 1500-2000

m) the ground effect becomes irrelevant and the wind velocity is function only by the weather conditions.

The data obtained from SEAI are elaborated because the hub height is different from the one of the anemometer. A vertical extrapolation of horizontal wind speeds has been applied using the Prandtl model because the hub of the turbine is 100 m height. This procedure follows the equations presented by Leahy (2021) and it is based on the general theory of the dynamic boundary layer and the Prandtl model.

The velocity at the hub can be extrapolated using equation (3.1).

$$\frac{v_2}{v_1} = \frac{\ln(\frac{z_2}{z_0})}{\ln(\frac{z_1}{z_0})} \tag{3.1}$$

Where v_2 is the velocity at the hub while v_1 is the velocity at the anemometer as it can be seen in Figure 3.5.

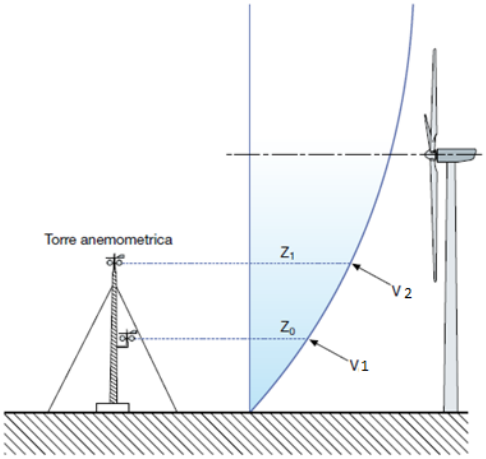

Figure 3.5 velocity profile

Moreover, z_0 is the surface roughness or roughness coefficient or roughness length depending on the ground configuration, and it is defined in (3.2).

$$z_0 = \frac{\alpha_c v_*^2}{g} \tag{3.2}$$

Where g is the gravity acceleration, α_c the constant Charnock parameter equals to 7 * 10^{-3} and v_* the frictional velocity dependent on the sea state, if is not available it can be considered as the product of 0.1 for the mean velocity. Usually for the offshore surface roughness is used 0.001 m and it is valid for calm sea. Some typical values for the roughness are reported in Table 3.1.

Table 3.1 Roughness length [m]

Class of ground	Roughness length [m]	Description
0	0.0002	Still water surface
0.5	0.0024	Open area with plane surface
1	0.03	Farming area without fence and sparse houses
1.5	0.055	Farming area with fence and some houses with an average distance of 1250 m
2	0.1	Farming area with fence and some houses with an average distance of 500 m
2.5	0.2	Farming areas with a lot of houses, plants and fences with an average distance of 250 m
3	0.4	Village, small town, farming areas with abundant forests.
3.5	2150.8	Big cities with height buildings
4	1.6	Metropolis with tall buildings and skyscrapers

As it can be seen from Table 3.1 the roughness length increases with the increase of the surface roughness. The class of the ground also affects the wind speed profile as it can be seen in Figure 3.6

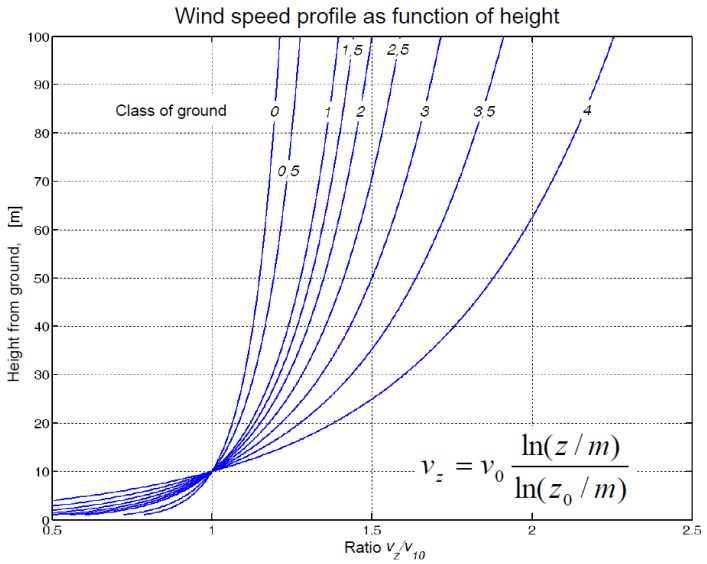

Figure 3.6 Wind speed profile as function of height, source: renewables course Padua

After the application of the vertical extrapolation of the wind speed data used for the location, the trend is depicted in Figure 3.7.

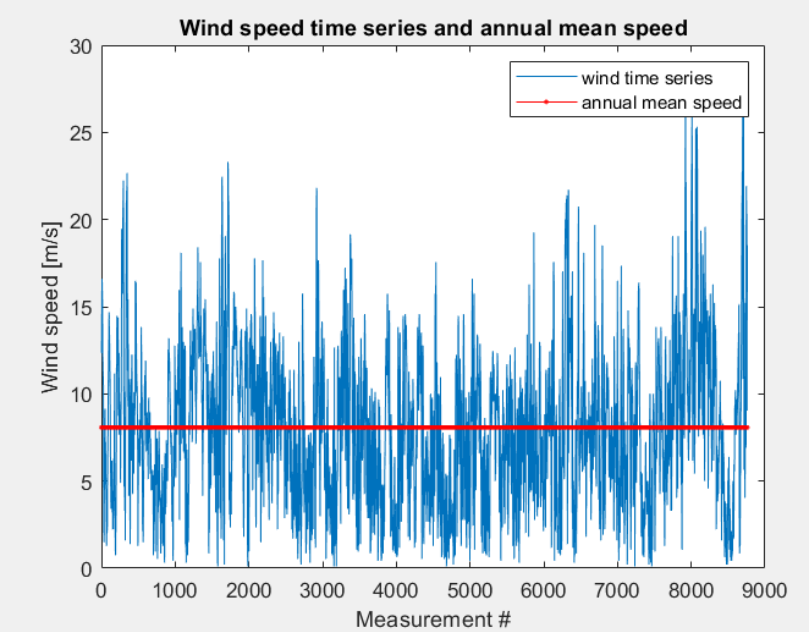

Figure 3.7 Hourly wind speed for one year at the proposed wind farm location

The wind speed time series is obtained for the offshore location, 4 km east of Bray and at the height of 100 m. As it can be seen from Figure 3.7, the wind speed varies a lot from 0 to 25 m/s during the year and the highest velocities are reached in December. In the chart it is also shown the annual average wind speed that in this case it is equal to 8.07 m/s.

Having the data regarding the direction and the wind speed and the annual mean wind speed, it is also interesting to create the Weibull function distribution and consider if the approximation curve well estimates the measurements. Moreover, having the wind data it is also possible to obtain the wind rose.

The Weibull distribution can be expressed using equations (3.3) and (3.4), the first is the probability density function $f(v)$ and it is equal to:

$$f(v) = \frac{k}{s}\left(\frac{v}{s}\right)^{k-1} \exp\left(-\left(\frac{v}{s}\right)^{k}\right) \tag{3.3}$$

While the cumulative distribution function $F(v)$ can be expressed as:

$$F(v) = 1 - e^{\left(-\left(\frac{v}{s}\right)^{k}\right)} \tag{3.4}$$

Where k is the shape factor, s is the scale factor and v is the wind velocity.

In order to obtain the Weibull distribution a simplified method has been used; it uses the information of the cumulative function. Two new auxiliary variables are defined in (3.5) and (3.6).

$$x = \log(v) \tag{3.5}$$

$$y = \log(-\log(1 - F)) \tag{3.6}$$

The chart that defines y function of x is described by the equation (3.7).

$$y = y_0 - mx \tag{3.7}$$

Where the angular coefficient m of the straight line is equal to the shape factor, while the y_0 value permits to evaluate the scale parameter using the equation (3.8).

$$s = e^{-(\frac{y_0}{m})} \tag{3.8}$$

The result of the distribution for the probability and cumulative Weibull density function are reported in Figure 3.8.

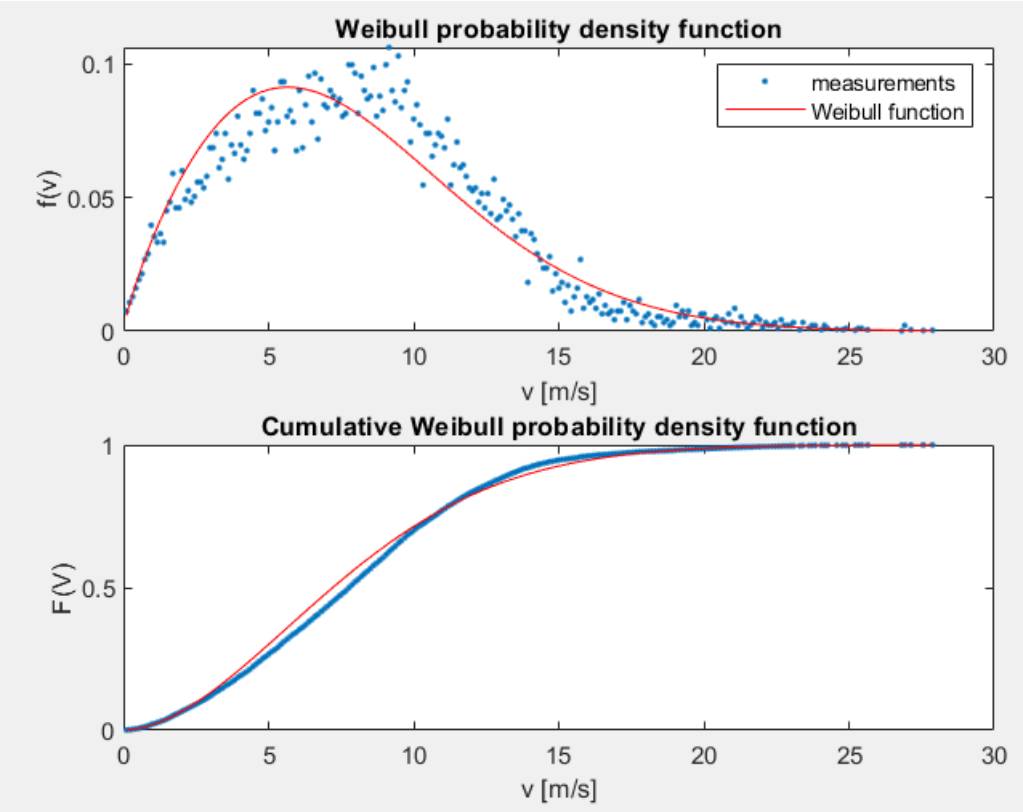

Figure 3.8 Probability and cumulative density function

As it can be seen from Figure 3.8, the Weibull distribution is able to well approximate the measurements on the windiness of the site. This means that the approximation curve created is

appropriate and if only the mean annual wind speed value for the location was known and it would be impossible to obtain the annual measurements the results would not change too deeply. This aspect is very important because it means that the characteristic parameters of the site are well estimated and that the Weibull distribution is a good method of approximation if the data of the wind speed for the site are not available. In particular, the main values obtained from the Weibull distribution for the plant are presented in the Table 3.2.

Table 3.2 Main value for the frequency for the site

Wind velocity [m/s]	Frequency [s/m]
0	0.001
1	0.0346
2	0.0576
3	0.0742
4	0.085
5	0.0904
6	0.0911
7	0.0879
8	0.0819
9	0.0738
10	0.0647
11	0.0552
12	0.046
13	0.0374
14	0.0298
15	0.0232
16	0.0177
17	0.0132
18	0.0097
19	0.007
20	0.005
21	0.0034
22	0.0023
23	0.0016
24	0.001
25	0.00067251

The parameter used to calculate the Weibull functions are expressed in Figure 3.9.

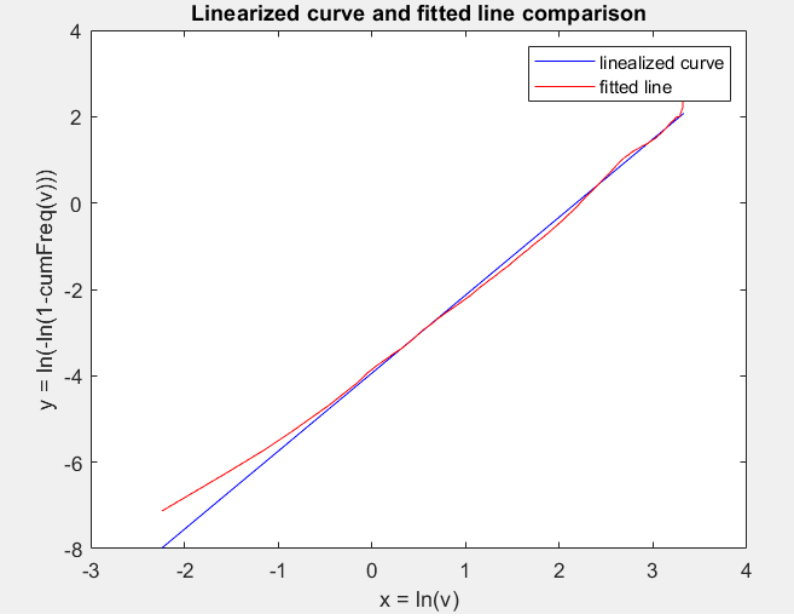

Figure 3.9 Linearized curve and fitted line

The simplified method leads to the equation (3.9) for the straight line and to (3.10) for the specific coefficients.

$$y = -1.8076\,x - 3.9376 \tag{3.9}$$

$$\begin{cases} k = 1.8076\ shape\ factor \\ s = 8.8319\ scale\ factor \end{cases} \tag{3.10}$$

The value of the shape factor is in line with the value present in the theory as reported in Table 3.3.

Table 3.3 Typical value for the shape factor (source: renewable course Unipd)

Shape factor k	Description
1.5	Mountain areas
2	Temperate climates and coastal areas
3	Wind – monsoon areas

The *shape factor* can vary between 0.5 and 4; the value depends on the irregularity of the wind, and it is homogeneous in similar climatic areas. It is indicative of the variability of the wind speed around the average value, high values (more than 3) indicate a site whit a low variation in the wind speed. While low values of k (around 1) indicate a site with high variability. When the shape factor is equals to 2 the Weibull distribution is referred to the Rayleigh distribution; this value is often used as reference to define a generic performance of a wind turbine without referring to a particular application site.

The *scale factor* is able to determine the average wind speed and it is an index of the windiness of the site.

Another way to calculate the Weibull distribution is using the Matlab to obtain the shape and scale factor from the measurements using the command "*wblfit*". After having obtain these two parameters it is possible to calculate the Weibull function using the command "*plot(x,wblpdf(x,s,k))*" where x is the vector with all the speed data, s is the scale factor and k is the shape factor. The result of this calculation is depicted in Figure 3.10.

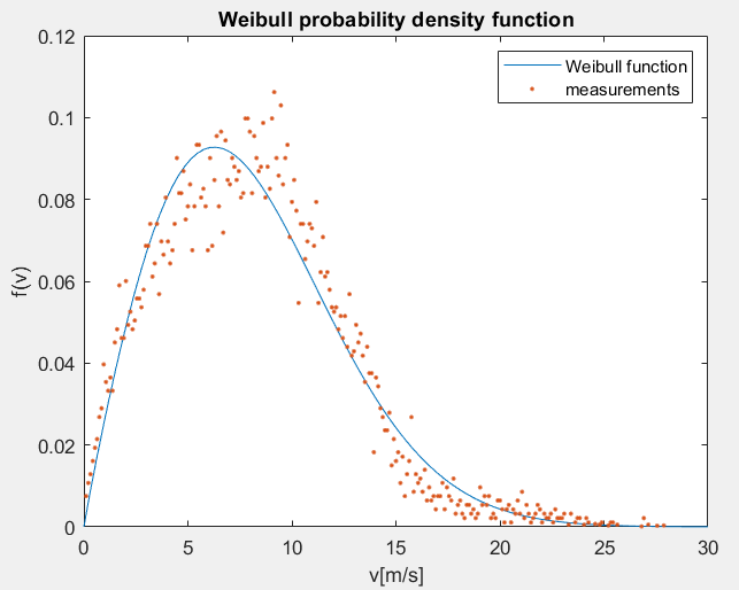

Figure 3.10 Weibull function with k=1.95 s=9.08

As it can be seen in Figure 3.10 the result almost similar to the one obtained in Figure 3.8. In this case, the values for the characteristic parameters are expressed in equation (3.11).

$$\begin{cases} k = 1.95\ shape\ factor \\ s = 9.08\ scale\ factor \end{cases} \tag{3.11}$$

The values for the shape and scale factor obtained with the two methods are similar. This means that they are valid for the site and in particular, the value of the shape factor is close to the value recommended in the SEAI wind atlas that for the same location and an altitude of 20 m results to be equal to 2.

Then the wind rose data has been created for the location of the plant and an altitude of 100 m. The result is expressed in Figure 3.11.

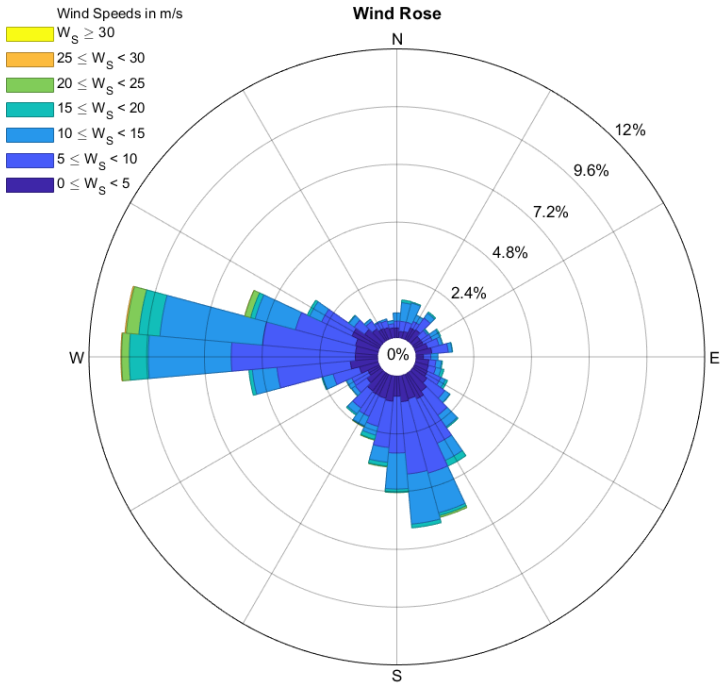

Figure 3.11 Wind rose with frequency

As it can be seen from Figure 3.10 the prevalent wind direction is west with a maximum frequency around 10 % and a wind speed between 25 and 15 m/s. This value is important because it determines the orientation of the turbines in the site.

3.1.3 - Offshore wind farm's technical data

After having done all the previous analyses all the technical data have been decided for the offshore wind power plant. It will be placed offshore of Bray bay with 16 wind generators of 10 MW each and a total capacity of 160 MW. The wind farm site as a 4 x 4 square grid layout, where the centres of the 16 squares are the positions of the turbines.

The site presents the same type of model and size for the turbines with an average hub high of 100 m and the water depth change between 22 and 26 m. This depth permits to use a monopile configuration for the turbines foundations, as expressed in chapter §2.1. The model of turbine used is a Vestas turbine named V164 - 10.0 MW, the main technical data are presented in Table 3.4 and obtained from the data sheet present in Vestas' website [7].

Table 3.4 Main characteristics of the V164 - 10.0 MW turbine

Parameter	Value
Power regulation	Pitch regulated with variable speed
Rated power	10 MW
Cut – in wind speed	3 m/s
Cut – out wind speed	25 m/s
Wind class	IECS or S,T
Standard operating temperature range	From – 15 °C to + 25 °C with a de-rating interval from +25 °C to +35 °C
Rotor diameter	164 m
Swept area	21124 m^2
Frequency	50/60 Hz
Converter	Full scale
Gearbox type	Medium speed
Generator voltage	6.6 kV
Operating current	104 A
Foundations	Monopile
Hub heights	Site - specific

Considering all the assumptions in chapter §3.1.2 the turbines will be arranged using an equal distance between the turbines of the same row and the distance between the rows. In order to avoid having high wake losses an appropriate distance between rotors has been decided following the theory of Samorani (2013). Then, the value of the distance between turbines is equal to 5 diameters of the rotor that in this case corresponds to 820 m. An advantage of this decision is also that this distance permits the transit of small ships but the transit of big ships is avoided except the one for maintenance of the plant. The distance between the wind farm to the shore is equals to around 4 km.

Regarding the electrical part it will be consider an MVAC interconnection between the turbines and an HVAC type for the cable that connects the transfer station to shore. These assumptions are acceptable and in line with the theory reported in chapter §2.3. In fact, the distance from the shore is less than 140 km and the value of the total capacity is lower than 200 MW. In particular, for the cables a three-core cable with copper configuration has been considered in order to reduce the cost and optimize the losses as it was recommended by literature in chapter §2.4. The installation for the cables is underground and the cables are placed 1 or 2 meters under the seabed in the space between turbines.

It was assumed that the collection point and the offshore transformer will be installed in the same offshore platform. Moreover, it was also considered that the onshore transformer will be installed in the same place of PCC.

In Figure 3.12 it is possible to see the layout configuration of the turbines in the farm.

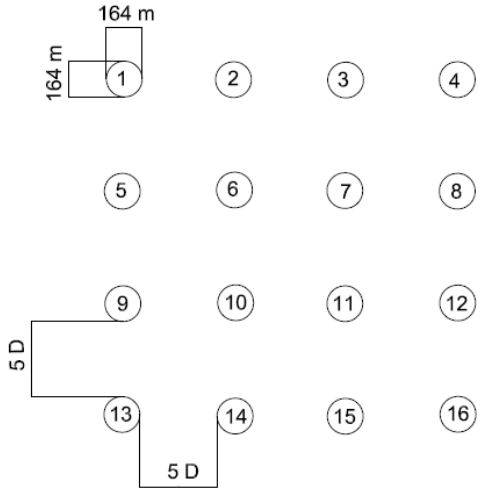

Figure 3.12 Offshore wind farm layout

As it can be seen in Figure 3.12 the site presents a square configuration and the circles correspond to the wind turbines.

In the following tables is presented a summary of the most important data of the offshore wind farm. In particular, in Table 3.5 there are all the information regarding the structure of the site.

Table 3.5 General information about the 66 kV wind farm

Parameter	Value
Total wind power plant capacity	160 MW
Total number of turbines	16
Size of wind turbines	10 MW
Number of substation transformer	1
Size of substation transformer	160 MVA
Size of wind turbine transformer	10 MVA
Length of interarray cables	0.82 – 3.16 km
Distance from offshore substation to PCC	4 km
Voltage level at PCC	132 kV
Nominal operating frequency	50 Hz

While in Table 3.6 are reported the main information regarding the wind turbine transformer.

Table 3.6 Specification of the wind turbine transformers of the 66 kV wind farm

Parameter	Value
Rated power	10 MVA
Rated voltage HV side	66 kV
Rated voltage LV side	0.69 kV
Configuration	DYN11 * 30 deg

In Table 3.7 the main information regarding the offshore transformer that it is install in a proper offshore substation are reported.

Table 3.7 Specification of the offshore substation transformer of the 66 kV wind farm

Parameter	Value
Rated power	160 MW
Rated voltage HV side	132 kV
Rated voltage LV side	33 kV
Configuration	YNd1

3.2 - Energy yield of the site

At the beginning the energy yield for one turbine will be calculated, then in the following the total energy of the wind farm will the calculated.

The energy yield of a single turbine in one year can be calculated using equation (3.12).

$$E = 8760 \cdot \int_{v_{cut-in}}^{v_{cut-off}} P(v) \cdot f(v) \cdot dv \ \left[\frac{MWh}{year}\right] \tag{3.12}$$

In particular:

- 8760 is the number of hours in one year
- $P(v)$ is the power expressed in [MW] produced by one turbine, function of the wind velocity v expressed in [m/s], this value can be obtained from the power curve given by the turbine manufacturer
- $f(v)$ is the Weibull statistic distribution function of occurrence frequency of wind speeds at the installation site expressed in [s/m]
- v_{cut-in} is the value of velocity where the blades start to turn and the turbine starts to produce energy
- $v_{cut-off}$ is the value of velocity where the blades are stopped from the control system in order to guarantee the safety for the turbine. In fact, high wind speeds can damage the turbine.

As expressed previously the power curve of the turbine V164-10.0 is given by the manufacturer and is depicted Figure 3.13.

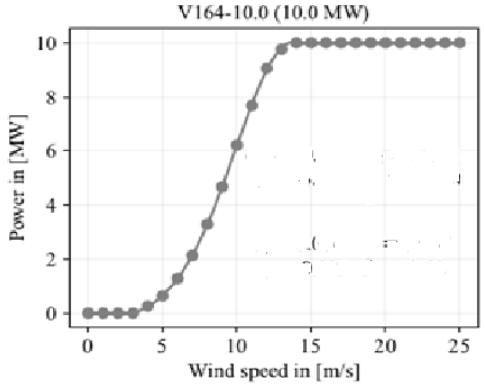

Figure 3.13 Manufacturer's power curve of wind turbine V164-10.0

As it can be seen from Figure 3.13 the cut in velocity at 3 m/s, after this value the blades of the turbine start to rotate and it produces power. While the cut off velocity is 25 m/s and after this point the control system blocks the blades and power production of the turbine is interrupted. It is also interesting to notice that the power trend increases with the wind speed until it reaches the value of 14 m/s. In this point the rated power equals to 10 MW is reached by the turbine and even with higher velocities the power production is constant, and it remains equal to the rated value.

The manufacturer's power curve has been interpolated in order to have all the values of power for the wind speed range from the cut-in to the cut-off velocity. The interpolated curve is presented in Figure 3.14.

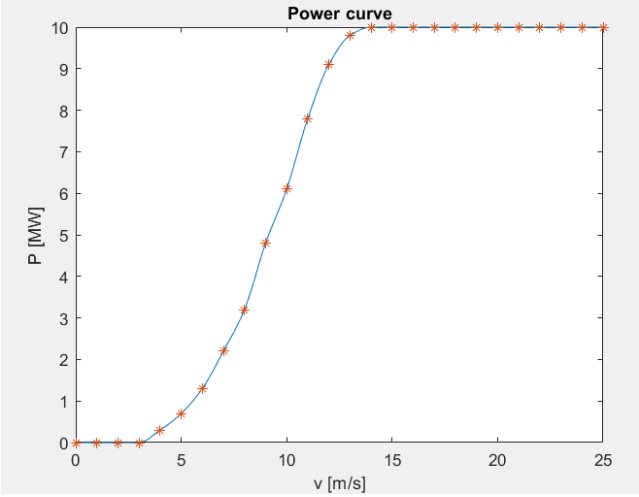

Figure 3.14 Interpolated power curve of wind turbine V164-10.0

As it can be seen from Figure 3.14 the interpolation curve matches well the real data and can be used for the next calculations. At the end, the energy yield produced by one turbine is equal to 33045 MWh/year. The annual production of a turbine can often be expressed as equivalent hours per year h_{eq} and its value can be calculate using the equation (3.13).

$$h_{eq} = \frac{E}{P_n} \left[\frac{h}{year}\right] \quad (3.13)$$

Where:

- E is the annual production of a turbine
- P_n is the rated power of the turbine.

In this case one turbine works for 3304.5 hours per year. This means that the turbine run for 3304.5 fictitious hours at its rated power and stands still in the remaining 5455.5 hours in order to produce the estimated power over a year period.

It is important to notice that the previous values of the annual production and the equivalent hours per year are related to only one turbine and not to the whole site. In fact, the total energy yield of the wind power plant can be obtained by summing the real production of the single turbines because not all the turbines present the same value of production. Another solution can be calculated knowing the production of one turbine, and obtaining the value for the site multiplying it for a suitable correction factor. This factor considers any possible aerodynamic interference between the turbines and the losses in the connection among the different units and between the plant and the grid are kept into consideration. Otherwise, it can be calculated knowing the average behaviour of a turbine and multiplying this value for the number of generators installed. In fact, the total energy generated by a wind power plant is lower than the sum of the energy produced by the single turbines installed separately and also the total power curve of a wind power plant is different from that of a turbine consider separately.

In this case is not possible to recreate the power curve of the single turbine and the one of the site in detail because is not possible to acquire the real data of the energy production. In fact, in this study case is not possible to acquire the real values for the energy production of the farm because it is not already placed. Nevertheless, in the following it will be explained the procedure applied to obtain a proper corrective factor that can well estimate the real situation.

First, it will be calculated the annual energy produced considering an ideal site without any wake effect or losses, considering that every turbine has the same energy production. In this case, the total annual energy is obtained as the product of the energy of a single turbine for the number of turbines present in the site. Thus, the value of the ideal total energy production is equal to 529 GWh/year.

This assumption is not acceptable because in every real plant depending by the installation layout every turbine produces a different value of energy. In this case, it will be considered the production of the worst scenario for the turbine and an average will be done between the best and worst scenarios in order to have an average behaviour that can be applied to each turbine. In this way, it will be possible to estimate the average production for the real average turbine and to obtain the real energy production of the plant. The main aspect that will be considered in the real case is the presence of the

wake effect that the first row of turbines creates with the prevalent wind direction. This phenomenon slows down the inlet velocity to the next row of turbines and this will lead to a lower power because it is proportional to the cubic inlet wind velocity, in fact the equation of the electric power generated P_e it is equal to equation (3.14).

$$P_e = \eta_{el}\, \eta_{mec}\, C_p \frac{1}{2}\, \rho\, A\, v^3\, [W] \tag{3.14}$$

Where:

- η_{el} is the efficiency of the electrical generator
- η_{mec} is the overall mechanical efficiency of the drivetrain
- C_p is the power coefficient
- ρ is the air density
- A is the swept area by the blades of the wind turbine
- v is the wind velocity in the inlet section of the rotor.

The efficiency of a wind turbine decreases when it is installed with other turbines in a wind farm. This is caused by changes in wind speed and the turbulence that arises behind each wind turbine due to the movement of the rotor blades. The weakening of the wind speed and thus the efficiency of a wind turbine is called the wake effect. In particular, a wind turbine placed behind another one is strongly influenced if the distance in the wind direction between the two turbines is insufficient. The wake effect in downstream wind turbines is stronger than upstream. The wind speed regains its strength after some distance behind the wind turbine and for that reason the turbines should have enough distance one to the other.

The wake losses can be estimated using a corrective factor C_f that consider the configuration of the offshore wind farm array. The coefficient has been extrapolated from the research done by Argyle et al. (2017) considering a uniform wind rose. In this case, for a row and column separation equals to 5D x 5D and an average yearly wind speed close to 8 m/s the coefficient is equals to 0.93. In this way, the real total energy yield of the farm can be calculated with equation (3.15).

$$E_{real} = C_f \cdot E_{1wt} \cdot n = 0.93 \cdot\ 33045 \cdot 16 = 491709.6\ \frac{MWh}{year} \tag{3.15}$$

Where E_{1wt} is the energy production of one turbine and n is the total number of turbines present in the array. The final result is that the site produces 492 GWh/year; thus, the total energy production sees a decrease of 7%.

Finally, the wind farm efficiency $\eta_{windfarm}$ can be calculated with the following equation (3.16).

$$\eta_{windfarm} = \frac{E_{real}}{E_{ideal}} = \frac{492}{529} = 0.93 \tag{3.16}$$

This parameter considers the performance of the wind farm, at the numerator appears the real total energy production of the site and in the denominator the ideal energy production appears considering that every turbine operates as a single turbine. In this case the wind farm efficiency is equal to 93%, this means that the distance between the turbines is appropriated and the optimization of the layout is satisfied. Therefore, it is also important to remember that only the wake effect has been considered in this calculation but in reality, there are other effects that can decrease this efficiency. The real final value can only be calculated acquiring the data of production for the installed site.

The annual energy production is also used to calculate the Capacity Factor (CF). The capacity factor can be used to assess how efficient a site is. It is defined as the produced power in relation to the nominal power of the wind farm as expressed by equation (3.17).

$$C_F = \frac{E_{real}}{\Delta t_{year} \cdot P_{nom}} = \frac{491709.6}{8760 \cdot 160} = 0.35 \tag{3.17}$$

Where E_{real} is expressed in MWh, Δt_{year} is equal to the hours in a year (8760h) and P_{nom} is the nominal power of the wind farm expressed in MW.
This value is in line with the one presented in literature and the IEA confirms the CF range depending by the technology in the 2019 report [8], the results are expressed in Figure 3.15.

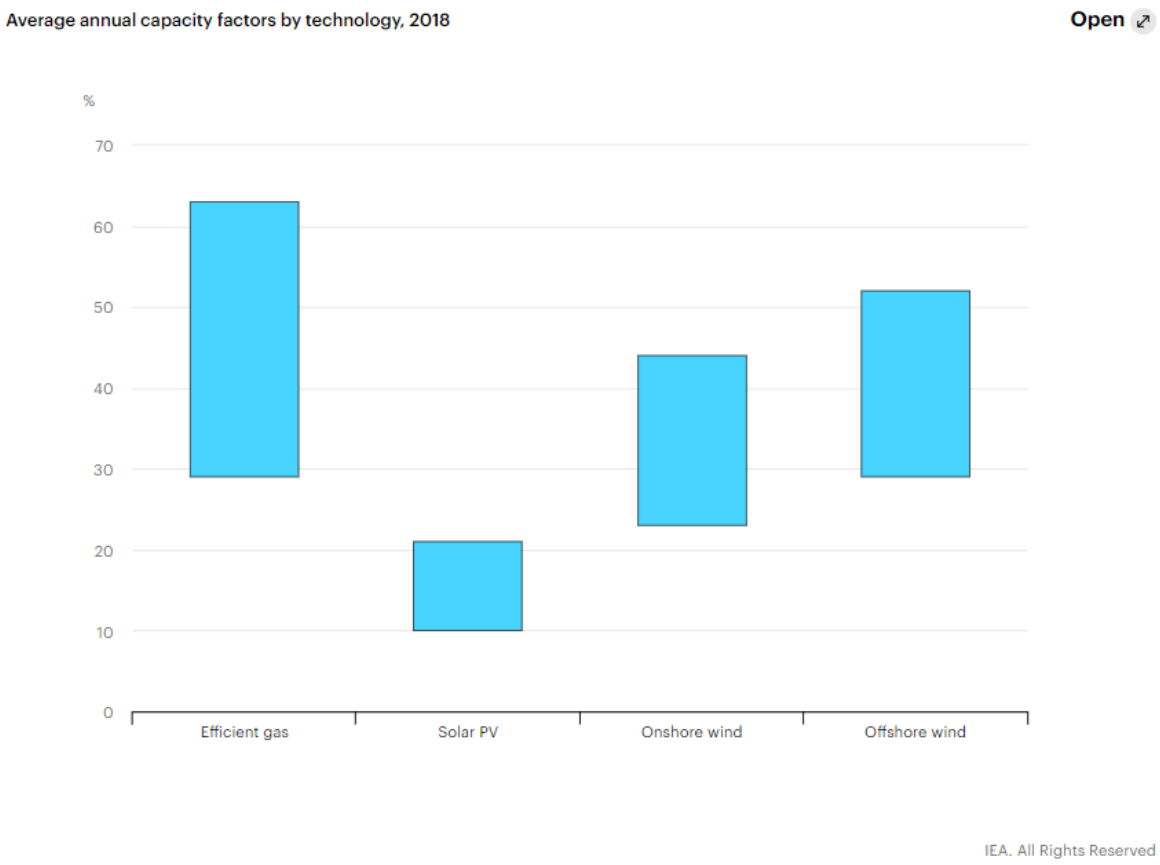

Figure 3.15 Capacity Factor of different technologies, source IEA https://www.iea.org/reports/offshore-wind-outlook-2019

As it can be seen from Figure 3.15 the offshore wind CF is about in the range of 30% - 50% and the designed plan is inside the suggested range.

In this chapter the main technical aspects related to the wind speed and the energy yield of the site are calculated in order to verify if the site is in line with the theoretical and realistic values present in literature. All the contributions calculated are verified, thus this means that the site is well design and it does not need any important variation.

CHAPTER 4 – Design and optimization of the electric connections

In this chapter the design and optimization of the connections of the site will be developed. It will consider different arrangements presented in literature considering the economic aspects and the losses too.

4.1 - Design of different electric interconnections

The main electric arrangements that will be taken into exam follow the most popular layouts present nowadays for the offshore wind power plant as expressed in chapter §2.3. They are: radial, star, mixed and double ring configuration; all of them are depicted in Figure 4.1.

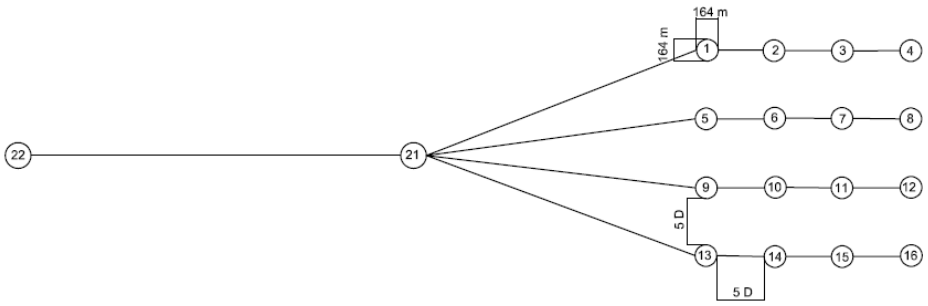

(a)

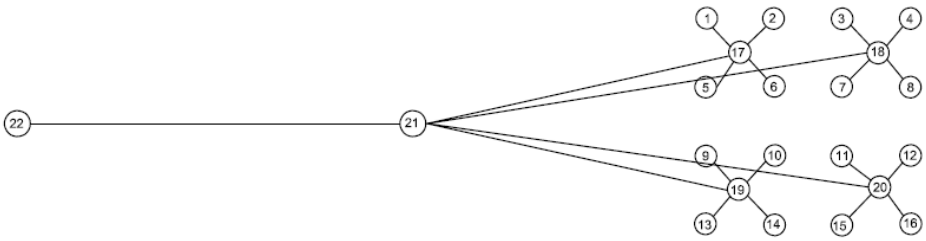

(b)

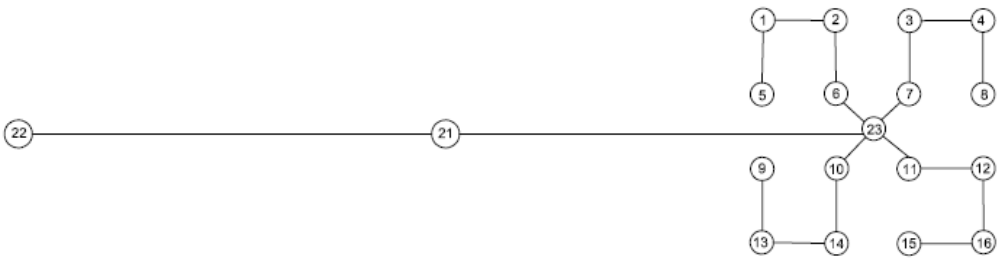

(c)

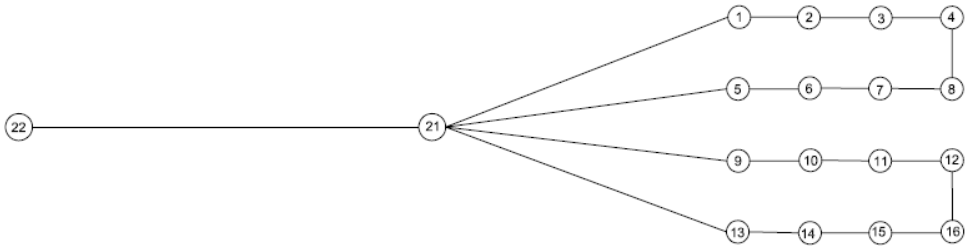

(d)

Figure 4.1 Electric arrangement consider for the plant. (a) Radial configuration, (b) star configuration, (c) mixed configuration, (d) double ring configuration.

In Figure 4.1 it is possible to see the layouts of the electrical connections taken into exam. The nodes from 1 to 16 are the wind turbines, while node 21 is the offshore transfer station installed in a proper offshore substation; here the voltage is raised from 66 kV to 132 kV. While the node 22 is the PCC onshore. At the end, the lines represent the electrical connections between the nodes. For the configuration (d) two different scenarios will be analysed, one with a cable capacity able to transmit all the power in case of a fault and another one able to transfer only half of it. In particular, all the different arrangements that will be analysed are presented with all the technical data in Table 4.1, Table 4.2, Table 4.3, Table 4.4 and Table 4.5.

Table 4.1 Technical information about the radial configuration or arrangement A

Cable line	Length [m]	Capacity [MW]	Cable type
21-22	4000	160	Z
21-1, 21-13	1585.21	40	Y
21-5, 21-9	1080.79	40	Y
1-2, 5-6, 9-10, 13-14	820	30	X
2-3, 6-7, 10-11, 14-15	820	20	X
3-4, 7-8, 11-12, 15-16	820	10	X

Table 4.2 Technical information about the star configuration or arrangement B

Cable line	Length [m]	Capacity [MW]	Cable type
21-22	4000	160	Z
21-17, 21-19	1631.10	40	Y
21-18, 21-20	3158.31	40	Y
1-17, 2-17, 5-17, 6-17, 3-18, 4-18, 7-18, 8-18, 9-19, 10-19, 13-19, 14-19, 11-20, 12-20, 15-20, 16-20	1159.66	10	X

Table 4.3 Technical information about the mixed configuration or arrangement C

Cable line	Length [m]	Capacity [MW]	Cable type
21-22	4000	160	Z
21-23	2230	160	2*W
			Y
5-1, 8-4, 9-13, 15-16	820	10	X
1-2, 3-4, 13-14, 16-12	820	20	X
2-6, 3-7, 10-14, 11-12	820	30	X

Table 4.4 Technical information about the double ring configuration with full cable capacity or arrangement D

Cable line	Length [m]	Capacity [MW]	Cable type
21-22	4000	160	Z
21-1, 21-13	1585.21	70	J
21-5, 21-9	1080.79	70	J
1-2, 5-6, 9-10, 13-14	820	60	X
2-3, 6-7, 10-11, 14-15	820	50	Y
3-4, 7-8, 11-12, 15-16	820	40	P
4-8, 12-16	820	30	K

Table 4.5 Technical information about the ring configuration with half cable capacity or arrangement E

Cable line	Length [m]	Capacity [MW]	Cable type
21-22	4000	160	Z
21-1, 21-13	1585.21	55	J
21-5, 21-9	1080.79	55	J
1-2, 5-6, 9-10, 13-14	820	45	X
2-3, 6-7, 10-11, 14-15	820	35	Y
3-4, 7-8, 11-12, 15-16	820	25	P
4-8, 12-16	820	15	K

All the cables used are ABB three core cables with copper for submarine purpose, this choice follows all the suggestions presented in chapter §2.6. The technical information for the different type of cables are presented in Table 4.6.

Table 4.6 Technical data of the ABB's cables present in the different arrangements

Cable type	Cross section [mm^2]	Rating current [A]	Voltage [kV]	Resistance [ohm/km]
X	95	300	66	0.247
P	120	340	66	0.196
Y	150	375	66	0.160
K	240	480	66	0.100
C	300	530	66	0.080
J	500	655	66	0.0536
W	630	715	66	0.044
Z	630	715	132	0.044

The choice of the cables for every connection is done calculating the rating current per every interconnection using the equation (4.1) as Thyssen (2015) suggests.

$$I = \frac{S}{\sqrt{3}\,V} \qquad [A] \tag{4.1}$$

Where S is the apparent power of the cable and V is the voltage present in the interconnection.

Then the rating power is used to obtain the cross section of the cable using ABB's datasheet for submarine cables with copper [9]. The results of the applied cables with the relative cross sections are present in Table 4.6.

4.2 – Transmission power losses, CAPEX and OPEX of the arrangements

For analysing the transmission losses of the configurations, the power losses of the lines are calculated using the equation (4.2).

$$P_{loss} = 3 \cdot r_{90°} \sum l_k I_k^2 \qquad [W] \tag{4.2}$$

Where:

- $r_{90°}$ is the specific cable resistance at 90 °C expressed in Ω/km
- l_k is the length of the cable expressed in km
- I_k is the current passing through the cable expressed in A.

The values for the resistances are obtained from specific tables from Benato (2018). In these tables, the resistance is function of the cable's cross section. The main values for the resistances at 90 °C are summarised in Table 4.6.

It should also be considered that all the losses have been calculated considering that all the configurations work at nominal conditions, thus in reality the values will be lower.

Then, the cost model is defined and the costs that are included in the CAPEX (Capital Expenditure) are summarize in the equation (4.3).

$$CAPEX = CAPEX_{WT} + CAPEX_{transf} + CAPEX_{foundations} + CAPEX_{cables} + CAPEX_{con} \tag{4.3}$$

Where $CAPEX_{WT}$ is referred to the cost for the turbines, $CAPEX_{transf}$ for the transformer, $CAPEX_{foundations}$ for the foundations of the wind turbines, $CAPEX_{cables}$ for the electric cables and $CAPEX_{con}$ for the connectors.

The equation for calculating the wind turbine cost for one single turbine is expressed in (4.4) as Timmers et al. (2022) suggest.

$$C_{WT} = 1.051 \left(1.374 \frac{P_T^{0.87}}{N_{WT}} + 0.363\, P_{WT}^{1.06}\right) [M€/turbine] \quad (4.4)$$

P_T is the total active power of the wind farm, P_{WT} is the rated power of an individual wind turbine both expressed in MW and N_{WT} is the number of wind turbines present in the site. The result is multiplied for the numbers of turbines present in the wind farm for having the total cost.

The cost for the cable is calculated with different equations depending by the type of cable applied in the interconnection. In this case only MVAC cables for the inter-array connections are used and a HVAC cable for the export line. The equations are all presented in (4.5), (4.6) and (4.7) as Timmers et al. (2022) suggest and for more completeness the equation for MVDC is reported too even if it is not used in this model.

$$C_{cableMVAC} = 0.1437 \cdot \left(A_p + B_p \cdot \exp\left(\frac{C_p S_n}{100}\right) + 2.4\right) \quad [M€/km] \quad (4.5)$$

$$C_{cableMVDC} = 0.1437 \left(A_p + B_p \cdot P_{cable} + 2.4\right) \quad [M€/km] \quad (4.6)$$

$$C_{cableHV} = 1.452 \cdot (A\, P_{cable}^2 + B\ \cdot P_{Cable} + C + D) \quad [M€/km] \quad (4.7)$$

Where P_{Cable} is the rated power of the cable expressed in MW, S_n is the rated power of the cable expressed in MVA, while the other factors are constants depending on the type of the cable and they can be obtain from Table 4.7, 4.8 and 4.9.

Table 4.7 Parameters for MVAC cables

Voltage [kV]	Ap	Bp	Cp
33	0.411	0.596	4.1
66	0.688	0.625	2.05
132	1.971	0.209	1.66
220	3.181	0.11	1.16

Table 4.8 Parameters for MVDC cables

Voltage [kV]	Ap	Bp
40	-0.314	0.0618
160	-0.100	0.0164
230	0.079	0.0120
300	0.286	0.0097

Table 4.9 Parameters for HVAC and HVMC cables

Parameter	HVAC	HVDC
A	$5.05 * 10^{-6}$	$1.31 * 10^{-7}$
B	$- 1.32 * 10^{-3}$	$1.47 * 10^{-4}$
C	0.43	0.29
D	0.79	0.85

For the transformer the cost has been obtained using the equation (4.8) as Timmers et al. (2022) suggest.

$$CAPEX_{transf} = 1.1495 \cdot (0.0427 \cdot (P_{TR})^{0.7513}) \quad [M€] \tag{4.8}$$

Where P_{TR} is the rated power of the transformer expressed in MVA.

For the specific foundations cost the equation (4.9) for a monopole technology is used as Bosch et al. (2019) suggest.

$$CAPEX_{foundations} = 0.97 \cdot (201\, x^2 + 612.93\, x + 411.464) \quad \left[\frac{€}{MW}\right] \tag{4.9}$$

Where x is the water depth of the seabed expressed in [m].

The connectors cost is calculated using the equation (4.10). The value of the cost is equal to 150 k€ per each as Collin et al. (2017) estimate.

$$CAPEX_{con} = 0.15 \cdot N_C \quad [M€] \tag{4.10}$$

Where N_C is the number of connectors present in the arrangement.

The OPEX (Operative Expenditure) of an offshore wind farm covers the operational and maintenance costs (O&M costs) of the plant, including other cost components such as administrative costs, insurance premiums and royalties. It is calculated using the equation (4.11) as Bosch et al. (2019) suggest.

$$OPEX = 61 \cdot 0.97 \cdot P \quad [k€] \tag{4.11}$$

Where P is the total capacity installed in the plant expressed in MW.

The cost results and the discounted payback time for all the electrical configurations are summarized in Table 4.9. For calculating the discounted payback time three different electricity selling prices are used, for a more detailed explanation on how to calculate the payback time see the appendix §A.2. The values of the selling prices permit to have a view with different market scenario and see how the result can change. These selling prices are for business and they are obtained from the SEAI's (Sustainable Energy Authority of Ireland) electricity prices trend without taxation of the Irish market along the years [10]. In particular it is selected the value of 2021 for a price of 188.6 €/(MWh) and the one of 2018 with a price of 137.1 €/(MWh) for avoiding considering special events that are happening in this year such as the pandemic and the war that affect the selling price. These two values are present in SEAI's website [10]. For analysing a scenario with a lower selling price it is also considered the strike price proposed by 2022 Eirgrid's report equals to 97.87 €/(MWh). For all the solution it is supposed that the selling price remain constant along the day and the year. The results are expressed in Table 4.9.

Table 4.9 Costs and discounted payback DPB with different electricity selling prices

	Conf A	**Conf B**	**Conf C**	**Conf D**	**Conf E**
CAPEX [M€]	289.92	298.08	292.54	291.56	291.12
OPEX [M€]	9.47	9.47	9.47	9.47	9.47
DPB [years] with el price 97.87 €/(MWh)	10	10	10	10	10
DPB [years] with el price 188.6 €/(MWh)	4	4	4	4	4
DPB [years] with el price 137.1 €/(MWh)	6	6	6	6	6

In Table 4.10 it is also possible to analyse the main characteristics of the configurations taken into exam.

Table 4.10 Main characteristics of the configurations

Configuration	**CAPEX [M€]**	**Total length of cable [km]**	**No. interconnections**	**No. connectors**	**Reliability**	**Transmissions Losses [kW]**
A (radial)	289.92	19.17	17	1	Low	1286.07
B (star)	298.08	32.13	21	5	High	2153.90
C (mixed)	292.54	20.71	18	1	Medium	1540.23
D (double ring)	291.56	20.81	19	1	Very high	1416.38
E (double ring)	291.12	20.81	19	1	Very high	1178.90

From Table 4.9 and 4.10 it can be seen that from an economical point of view the configurations present a similar CAPEX among them. The most convenient arrangement in terms of money is the radial configuration (conf. A) because it is the simplest one and the one with the lower number of connections and total length. As disadvantage, the reliability of the electric system is law because if the first turbine of the row that connects the turbines to the transformer is subjected to a fault all the turbines present in the row are not able to inject the produced power to the grid. While the most

expensive solution is the star configuration (Conf B.), this result is due to the fact that it is present a lot of diagonal interconnections between the nodes and this leads to a higher length and cost. The number of interconnections is also increased respect the previous configuration and the reliability too. For the other configurations (Conf C, D, E), they present a low difference of the CAPEX between them because the number of interconnections and total length is similar. The mixed configuration (Conf. C) is one of the most common in reality and it is composed by radial and star arrangements. It permits to have a medium level of reliability and a reduction in the number of the interconnections. Then for the double ring configurations (Conf. D, E) they present a similar value even if the capacity of the cable in the configuration E has been reduced. In this case, the reliability of the system is maximized and the system is able to work even if a fault will happened in the first turbine that connects the row to the transfer station. In the case of the arrangement D, the interconnections are design for transmit all the power while in the arrangement E the capacity is halved. In particular, in this case to choose the configuration D instead of the configuration E is preferable because the CAPEX difference is really low but the reliability is higher in case of fault.

In terms of OPEX the value is equals for all the solutions because it is proportional to the installed power that in this case is the same for the arrangements.

For the losses the value changes a lot between the different solutions and is pretty high for the radial solution (conf. B) due to the higher value of the total length of the cables. The cheapest solution in this case is the double ring configuration (Conf. E) because the average value of the resistances is lower respect the other solutions.

It is important to consider that an absolute perfect arrangement does not exist. It can be different plant by plant because the objective can vary. In fact, not all the geographical configurations are the same and the objective of the investors can be different and the presence or not of incentives given by the country can affect the decision too.

Regarding the DPB, the contribution of the selling price highly affects the result of the return of the invested capital. In fact higher is the selling price and less time is needed for the return of capital. If the price will stay constant along the year to the one that is currently present the return of the investment will return back in 4 years otherwise if the price is fixed to the strike price the return of the investment will be 10 years. The more realistic scenario is the one with the strike price equals to 97.87 €/(kWh) because the other scenarios use a price that is higher due to the unusual events along the past years that affects the balance of the market. It is important to use a price that will be constant around the year or that is more precautionary for avoiding to have a profitable investment to the first years but that is not after a while when the selling price halves its value.

In the plant considered for the study it is decided to reduce as much as possible the costs and this is possible only choosing the radial arrangement, the aim is to reduce at maximum the cost to return faster the investment and use part of the return investment for the hybrid part of the plant. Now on it will only consider the radial solution for the electrical configuration.

A sensitivity analysis on the selling price of electricity it done considering three different scenarios where in all of them it is supposed to sell the whole produced electricity. The NPV (Net Present Value) is expressed graphically in Figure 4.2 considering a lifetime of the whole site equals to 20 years. For knowing how the NPV is calculated see the Appendix §A.3.

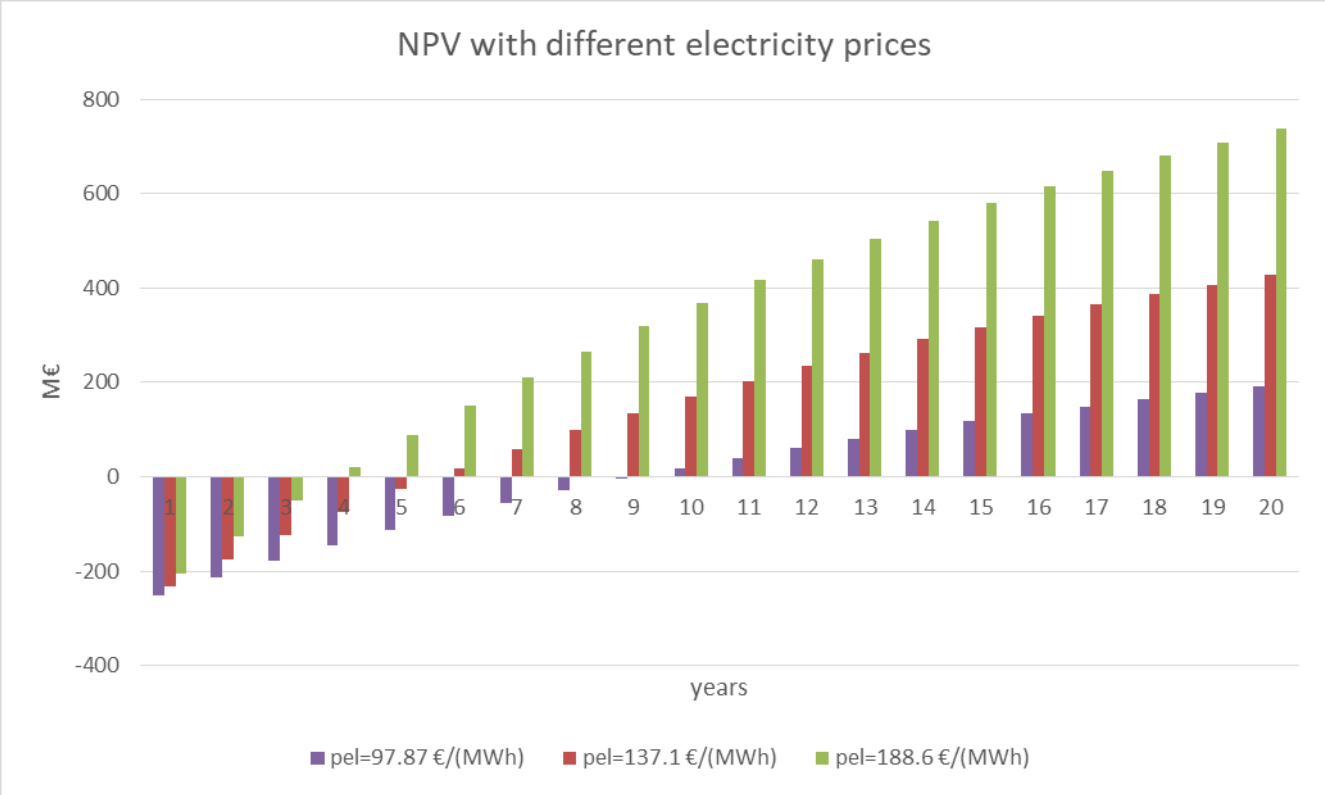

Figure 4.2 NPV with different electricity prices for the radial arrangement

As it can be seen in Figure 4.2 the most profitable solution is the one with the highest selling price. The contribution of the price is very important and usually it is a variable that cannot be fixed by the investors but it is chosen by the market. It is important to notice that the calculation is done without considering the presence of incentives that can improve the solution.

CHAPTER 5 - Design and optimization of the hybrid plant

In this chapter it will be analysed the feasibility of having a hybrid wind farm. In particular several configurations will be analysed in order to select the most profitable one.

5.1 - Electrical average daily production along the year

Before designing the hybrid plant it is important to estimate the quantity of hydrogen produced in the site along the year for sizing correctly the site. The production of hydrogen is connected with the electricity one, therefore it is needed to analyse the trend of the electricity production during the year. For this calculation it is used the data of the wind speed along the year, the power production curve of the turbine and the efficiency of the plant presented in Chapter §3.1.2 and §3.2 respectively. In Figure 5.1 are present the average daily trends month per month for the electricity production of the whole site.

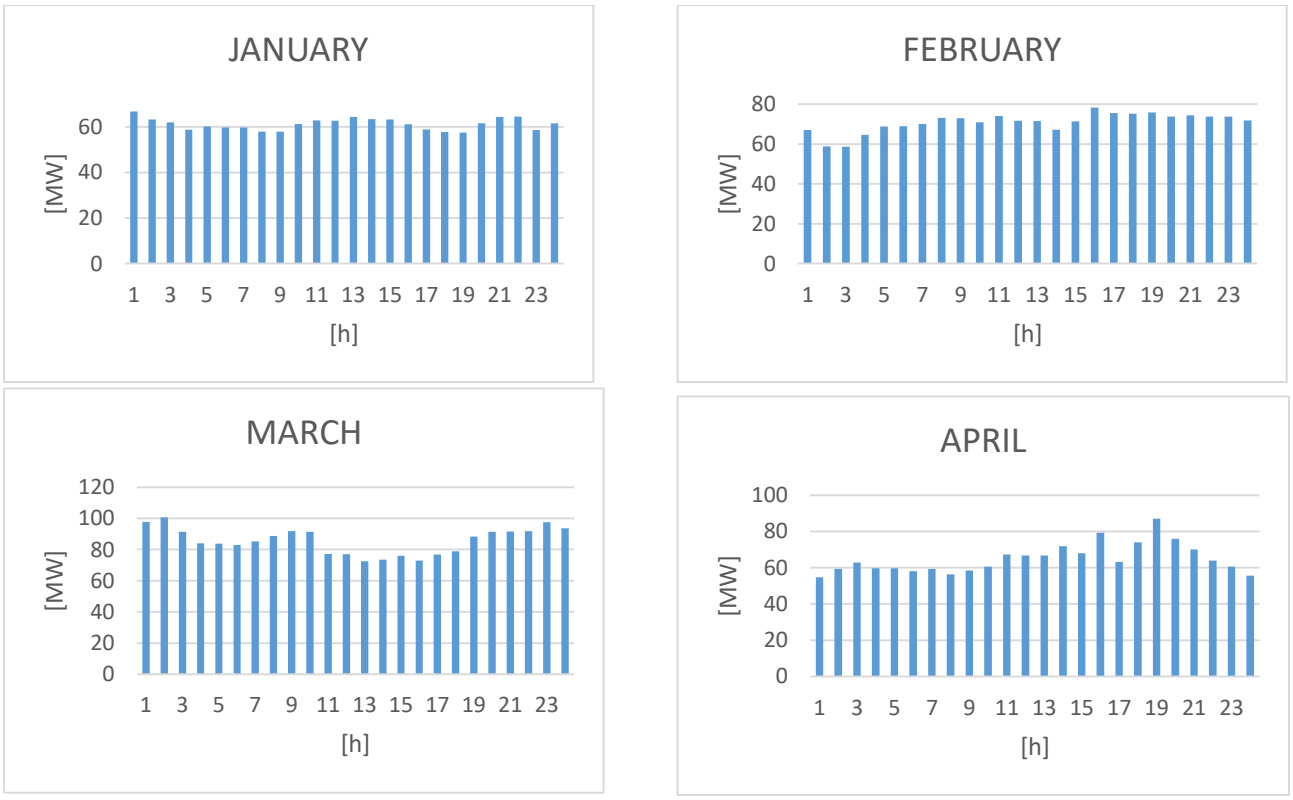

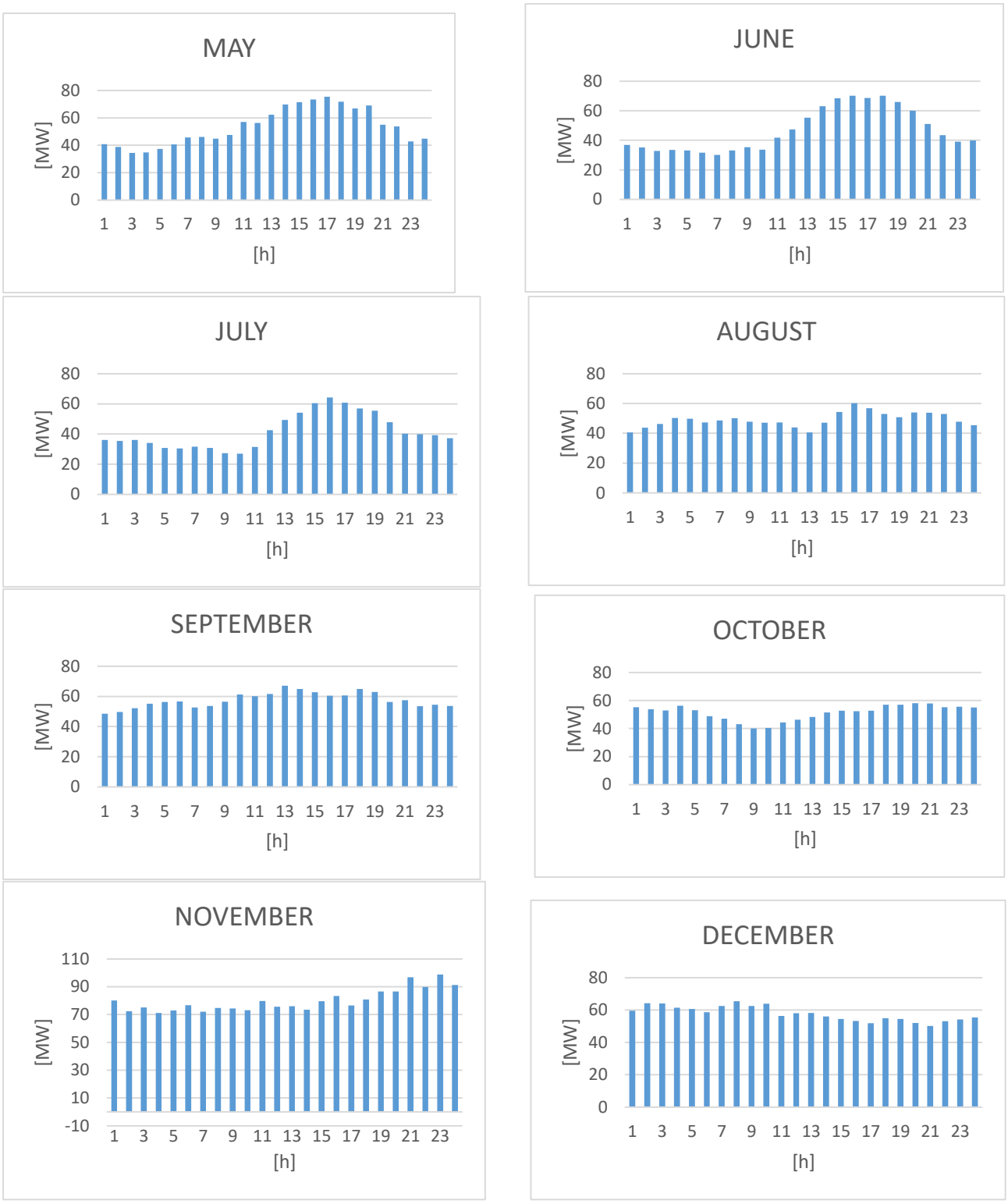

Figure 5.1 Daily electricity energy production along the year

The sum of the whole columns below the curves in Figure 5.1 represents the energy production during an average day along the months. The variability along the months is really high and this is justified by the fact that the wind energy source is variable along the year with an energy variation in the range of 27 - 98 MWh. A huge variation is present along the winter and summer months, this is justified by

the fact that during the summer period the intensity of the wind speed is lower and this leads to a lower value of the energy production.

In order to have a better idea of how much is important the variability in the wind sector Figure 5.2 depicts how the power production changes along the months.

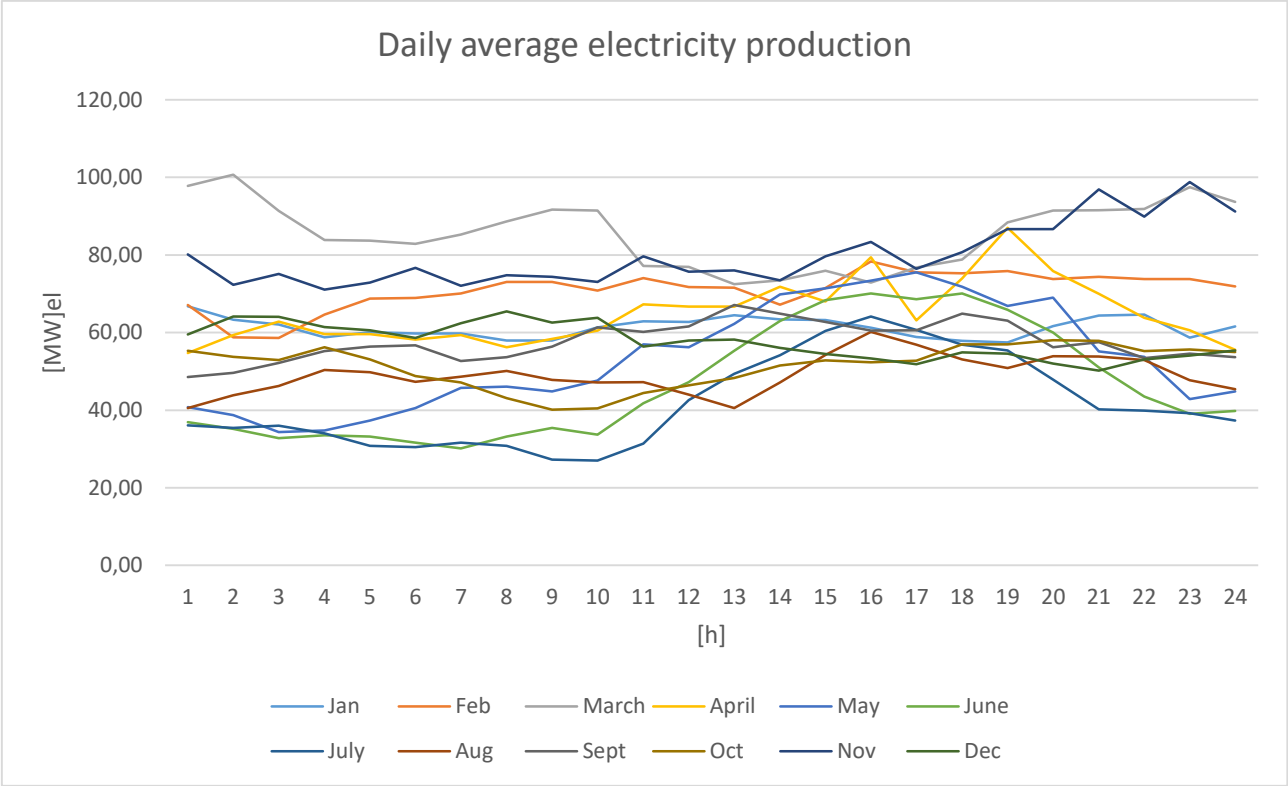

Figure 5.2 Variability of the energy production along the year

The months with the highest production are March and November while the ones with the lowest production are July and June. The variability is not only present between months but also during the average day. The wind is in fact stronger during the second part of the day and the production is higher too. It is important to remember that the graphs represent an average trend for the month but the variability between the days in the same month could be really high; an example is expressed in Figure 5.3 for three different days during September.

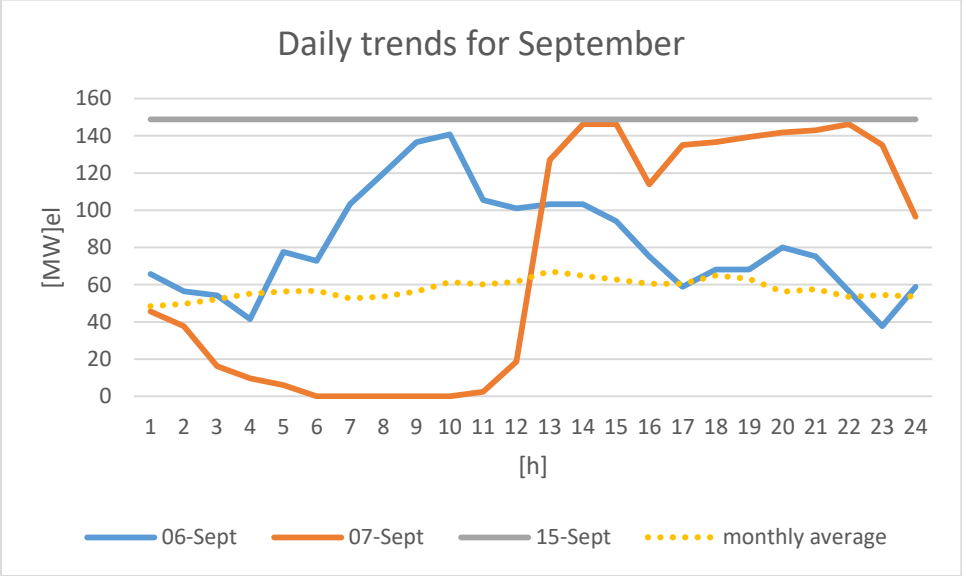

Figure 5.3 Daily electricity production curves for different days in September

In this case from Figure 5.3 is possible to notice how the variability is important in the wind production. For two consecutive days the electricity production changes a lot and especially for the 7th September; the production is not constant during the day and it changes sharply from 0 MW to a production over 140 MW. While the 15th the production is high and constant along the whole day. Therefore, the average monthly trend takes into consideration about all these aspects however in the one specific day can be really different from the average curve.

5.2 – Design and optimization of the hybrid connections

In this part it will be analysed which hydrogen technology is the best in the market. The electric solution that it is decided to use is the radial arrangement in order to reduce as much as possible the investment costs. The plant will be considered hybrid, therefore the plant produces both hydrogen and electricity. The hybrid system is composed by radial electrical array and the electrolyser is placed offshore or onshore depending by the scenario.

5.2.1 – Design of the hybrid site

In particular, three different solutions for the hybrid plant will be analysed:

- Scenario A: with 4 offshore PEM electrolyzers installed in each row of the wind farm and an hydrogen pipeline to transport the hydrogen

- Scenario B: with 1 offshore PEM electrolyzer installed in the transformer station and a unique pipe that connects the electrolyser to the shore
- Scenario C: with 1 onshore AEL electrolyser installed onshore without the instalment of the hydrogen pipe.

After the electrolyser station the hydrogen is produced and it can be sent into a pipeline to the injection station or stored in a tank and then it can be re-electrify. The hydrogen produced is blended to the national gas pipeline following the main suggestions present in literature and without avoiding exceeding the 20% of the total mixture.

For all the scenarios the PEM electrolyser used in the calculation is the Sylizer 300 of Siemens and for the AEL is the thyssenkrupp's electrolyzer. Both technologies present a life time of 20 – 30 years as the RSE's document (2021) attests. For the offshore electrolyser it is preferable to use a PEM technology while for the onshore one it is better to use the AEL one as explained in Chapter § 2.4.2. The main technical characteristics of both the electrolysers are reported in Table 5.1 and Table 5.2 using the information reported by the technical datasheets [11] [12].

Table 5.1 Main characteristics of the Silyzer 300 electrolyser

Characteristics	Value
Type	PEM
Power demand [MW]	17.5
No. of modules per array	24
Hydrogen production [kg/h]	330
Efficiency	75.5% on HHV
Dimension array [m]	15 x 7.5 x 3.7

Table 5.2 Main characteristics of the Thyssenkrupp electrolyser

Characteristics	Value
Type	AEL
Power demand [MW]	20
Hydrogen production [kg/h]	360
Efficiency	82% on HHV

5.2.2 – CAPEX and OPEX calculation

For obtaining the best solution in terms of money the calculation of CAPEX and OPEX for the different scenarios is followed.

The CAPEX related to the hybrid part of the plant $CAPEX_{hybrid}$ is calculated considering the equation (5.1) for all different scenarios.

$$CAPEX_{hybrid} = CAPEX_{electrolyzer} + CAPEX_{pipe} + CAPEX_{injection} + CAPEX_{comp} \quad (5.1)$$

The main contributions are the one for the electrolyzer $CAPEX_{electrolyzer}$, the pipes $CAPEX_{pipe}$, the injection to the gas grid $CAPEX_{injection}$ and the compressor $CAPEX_{comp}$. These contributions are calculated using Christensen (2020)'s equations that are expressed in equation (5.2) and equation (5.3).

$$CAPEX_{PEM} = 1182 \cdot Pel \quad [€] \tag{5.2}$$

$$CAPEX_{AEL} = 988 \cdot Pel \quad [€] \tag{5.3}$$

Where Pel is the electrolyser's power expressed in kW.

The OPEX of the electrolyzer $OPEX_{electro}$ is calculated using the Christensen (2020)'s suggestion equals to 2% of the CAPEX as expressed in equation (5.4).

$$OPEX_{electro} = 2\%\ CAPEX_{electrolyzer} \tag{5.4}$$

While the CAPEX and OPEX of the hydrogen pipe $CAPEX_{pipe}$ is calculated using Todesco et al. (2021) equations expressed in (5.5) and (5.6).

$$CAPEX_{pipe} = 16\,000\,000 \cdot \frac{E_{cap} \cdot P_{rate}}{\rho\ v\ \pi} + 1\,197\,200 \sqrt{\frac{E_{cap} \cdot P_{rate}}{\rho\ v\ \pi}} + 329\,000 \quad [€/km] \tag{5.5}$$

$$OPEX_{pipe} = 2\%\ CAPEX_{pipe} \tag{5.6}$$

Where E_{cap} is the electrolyser capacity and P_{rate} is the electrolyser production rate respectively expressed in MW and kg H_2/(s MW).While ρ is density and v the velocity inside the tube.
The density is calculated using the equation of the ideal gas expressed in (5.7). It results to be equal to 6.26 kg/m^3 at 15°C and 75 bar.

$$\rho = \frac{MM\ p}{RT} \left[\frac{kg}{m^3}\right] \tag{5.7}$$

Where MM is the molecular weight of hydrogen in [g/mol], p is the pressure expressed in [Pa], R is the gas constant equals to 8.314 J/(mol*K) and T is the temperature in [K].

The recommended velocity inside the tube it is equal to 20 m/s. This value is usually used to design the pipelines and it is suggested from *PetroWiki's* and *Process Instrumentation's* websites [13] [14].

This velocity value permits to avoid high levels of erosion and to contain the losses that are proportional to the square of the velocity.

At the end the CAPEX and OPEX for the injection $CAPEX_{injection}$ and $OPEX_{injection}$ respectively are calculated using the equations proposed by FCH (Fuel Cells and Hydrogen) (2017). The equations are expressed in (5.8) and (5.9).

$$CAPEX_{injection} = 56000\ € \tag{5.8}$$
$$OPEX_{injection} = 8\%\ CAPEX_{injection} \tag{5.9}$$

While for the compressor the CAPEX is calculated using the equation proposed by Christensen (2020) expressed in (5.10).

$$CAPEX_{comp} = 2545 \cdot \frac{Q}{3600} \cdot \frac{Z \cdot T \cdot R \cdot N \cdot 1.4}{M_{H_2} \cdot \eta \cdot 0.4} \cdot \left(\left(\frac{P_{out}}{P_{in}} \right)^{\frac{0.4}{N \cdot 1.4}} - 1 \right) \tag{5.10}$$

Where Q is the flow rate expressed in [kg/h], P_{out} is the outlet pressure of the compressor, P_{in} the inlet pressure of the compressor, Z is the hydrogen compressibility factor equal to 1.03198, N is the number of compressor stages assumed to be 2 for this work, T is the inlet temperature of the compressor equal to 310.95 K, M_{H_2} is the molecular mass of hydrogen equal to 2.15 g/mol, η is the compressor efficiency ratio taken as 75% and R is the universal constant of ideal gas equal to 8.314 J/(mol K).

Now that the cost equations are settled it will be analysed a configuration where the hybrid plants are design to use 80 MWel to produce H_2 with an outlet pressure of the electrolyser equals to 75 bar for all the scenarios. The length of the pipes is equals to 4 km for the Scenario A while it is 9.33 km for the Scenario B while the junction station is supposed to be in Bray in the PCC point. All the hydrogen pipelines are settled to 75 bar taking in consideration the state of art of the gas pipeline in the country presented in Chapter §2.5 and the data present on Wikipedia to the voice "*United Kingdom–Ireland natural gas interconnectors*" [15].

The results of the hybrid costs are expressed in Table 5.3.

Table 5.3 CAPEX and OPEX in euro for a hybrid plant with 80 MWel in input

Configuration	Total length [km]	CAPEX pipe [€]	CAPEX electrolyser [€]	CAPEX injection [€]	CAPEX compressor [€]	CAPEX hybrid[€]	OPEX hybrid [€]
Scenario A: 4 PEM offshore	9.33	3 274 881	94 560 000	560 000	12 103 625	110 498 506	2 001 498
Scenario B: 1 PEM offshore	4	1 521 875	94 560 000	560 000	12 103 625	108 745 500	1 966 437
Scenario C: 1 AEL onshore	0	0	79 040 000	560 000	10 559 116	90 159 116	1 625 600

As it can be seen from Table 5.3 the most convenient solution is to install an onshore AEL electrolyser. In this way the cost for the pipe and for the electrolyser can be reduced and a profitable solution can be obtained from the investment. The presence of less components leads the Scenario C to be the most profitable one. The low price of the AEL technology is due to the fact that it is a more mature technology than PEM electrolysers as expressed in Chapter §2.4.1 and §2.4.2. It also appears as Scenario B is slightly more convenient respect Scenario A. This is due to the fact that the pipe's CAPEX is proportional to the total length and in Scenario A it is higher respect the other option. It is also important to consider that in reality the scales economy effect is present for large scale products. In the pipe CAPEX equation this contribution is not present but in reality it should be considered and it will guide even to a lower cost for Scenario B.

Considering only the radial arrangement for the electric part, the global CAPEX for every scenario for the hybrid plant is presented in Table 5.4. The result is obtained summing the hybrid CAPEX calculating using equation (5.1) with the one calculated for the electric part with equation (4.3).

Table 5.4 Global CAPEX and OPEX for the hybrid plant in different scenarios

Configuration	CAPEX electric [€]	OPEX electric [€]	CAPEX hybrid[€]	OPEX hybrid [€]	TOT CAPEX hybrid [€]	TOT OPEX hybrid [€]
Scenario A: 4 PEM offshore	289 920 000	9 470 000	110 498 506	2 001 498	400 409 506	11 471 489
Scenario B: 1 PEM offshore	289 920 000	9 470 000	108 745 500	1 966 437	398 665 500	11 436 437
Scenario C: 1 AEL onshore	289 920 000	9 470 000	90 159 116	1 625 600	380 079 116	11 095 600

As it can be seen in Table 5.4 the main difference is present in the CAPEX, while the OPEX is really similar between the different scenarios. The cheapest solution is the Scenario C because it presents less components, while the most expensive one is the Scenario A that present the highest length of the hydrogen pipe.

CHAPTER 6 – Analysis of possible hybrid scenarios

In the following some possible applications will be analyse in order to verify the feasibility of the investment. For this chapter it is decided to consider only the most profitable hybrid solution that is the Scenario C with only one AEL installed onshore and the radial electrical configuration for the electrical part in order to minimize the cost of the investment. All the economic analysis present in the following use the total hybrid CAPEX calculated in Table 5.4 in Chapter §5.2 for the Scenario C. Initially the system is design considering different quantities of hydrogen that will be produced using different thresholds of electricity considering the power production curves presented in Figure 5.1; then a scenario with a storage will be analysed and at the end a future prospective will be taken into consideration using a lower price for the electrolyser.

6.1 – Scenario 1: High H_2 production with direct blending to the gas piping

In this scenario the hybrid site uses a maximum of 20 MWel for the production and direct reselling of electricity in the grid. The electricity prices used for this chapter are equal to 137.1 €/(MWh) and 97.87 €/(MWh), these prices were also used in chapter §4.2. While the remaining variable part produces electricity which is sent to the AEL electrolyser. The hydrogen produced is directly blended to the gas pipeline and it is sold to the natural gas price equals to 53.7 €/(MWh). This value is obtained from the gas price trend present in the SEAI's website; it is the net price without taxation to business for the year 2021 [9]. For being precautionary the chosen price for the natural gas is the value of the last year in the semester before the Ukraine conflict happens. This event leads to a higher selling price on the market. For long time investment it is better to use a price that can be acceptable for more years and do not use one that is due to a strong variation on the market due to political reason. In this way the price is supposed to be stable and constant during the lifetime of the plant.
In this scenario the production of hydrogen is variable, and the production of electricity is maintained as much constant as possible. The variability of the energy produced by RES is the main problem and this configuration can help to level the production of electricity injected to the electric grid by RES.

The results of the NPV with different electricity prices are reported in Figure 6.1 and Figure 6.2.

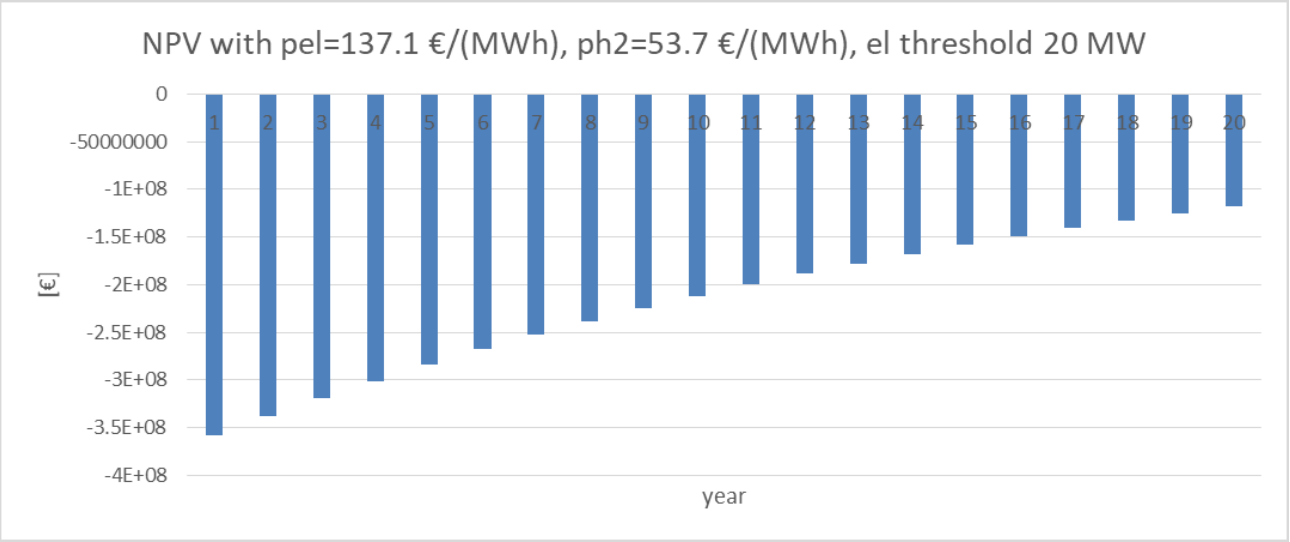

Figure 6.1 Electric threshold 20 MW and direct blending to the gas piping to a hydrogen price of 53.7 €/(MWh) and an electricity price of 137.1 €/(MWh).

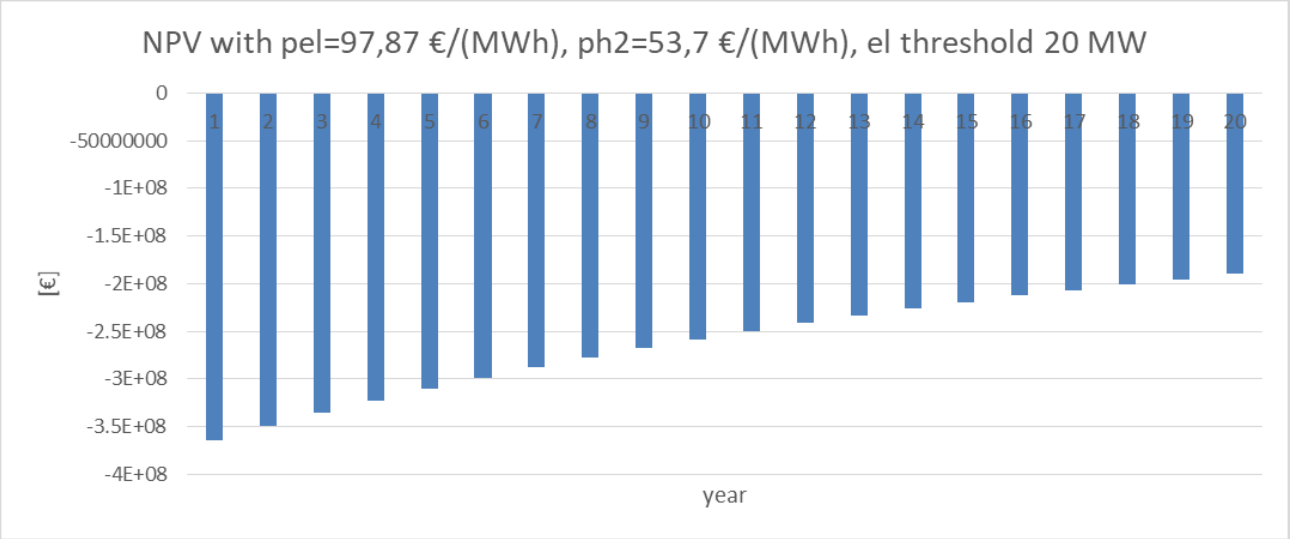

Figure 6.2 Electric threshold 20 MW and direct blending to the gas piping to a hydrogen price of 53.7 €/(MWh) and an electricity price of 97.87 €/(MWh).

As it can be seen in Figure 6.1 and 6.2 the investment is not profitable because the price for the hydrogen is not enough high to recover the investment, furthermore the quantity of sold electricity is not enough to cover both the investment for the hybrid plant. The more realistic solution is represented in Figure 6.2 and as expected the trend of the NPV is more negative than the one with the higher electricity price.

6.2 – Scenario 2: Low H_2 production with direct blending to the gas piping

A possibility to improve the solution is to reduce the quantity of produced hydrogen. In this scenario the threshold for the electricity production is higher than in Scenario 1 and equals to 40 MWel. In this case the size for the electrolyser is reduced and this permits to have a lower investment cost that can be refunded sooner. For this part the selling prices for electricity and the hydrogen are the same of Scenario 1. The electricity prices are equals to 137.1 €/(MWh) and 97.87 €/(MWh), while the hydrogen is sold to the natural gas price equals to 53.7 €/(MWh). The results on the NPV are presented in Figure 6.3 and Figure 6.4.

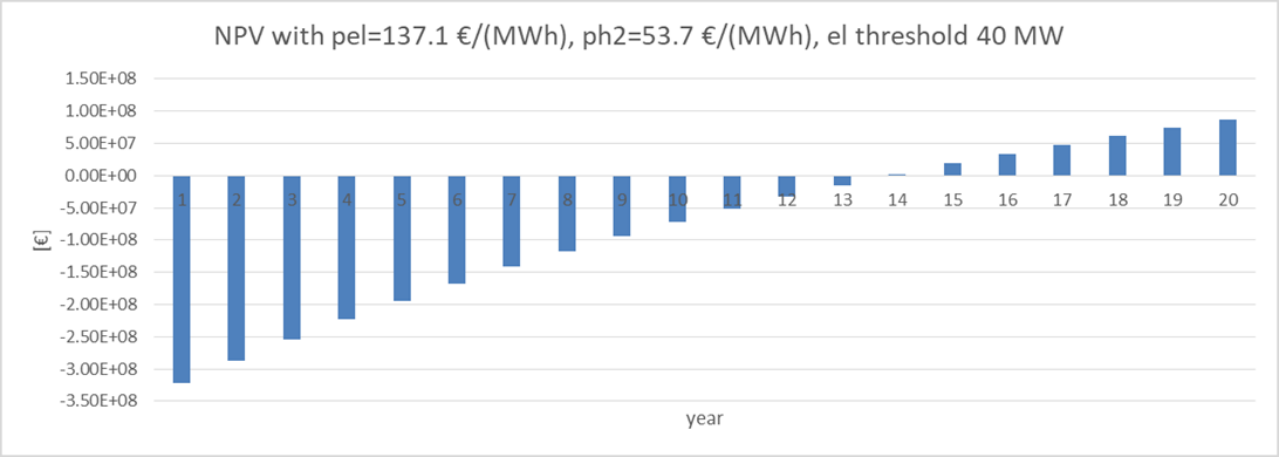

Figure 6.3 Electric threshold 40 MW and direct blending to the gas piping to a hydrogen price of 53.7 €/(MWh) and an electricity price of 137.1 €/(MWh).

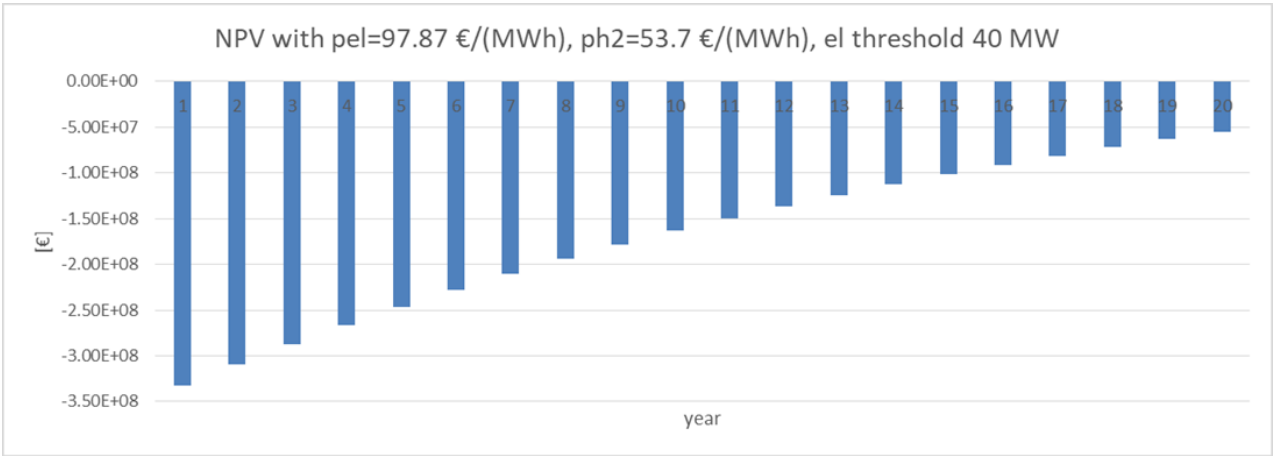

Figure 6.4 Electric threshold 40 MW and direct blending to the gas piping to a hydrogen price of 53.7 €/(MWh) and an electricity price of 97.87 €/(MWh).

As it can be seen in Figure 6.3 and 6.4 in this case the investment is more profitable because the quantity of sold electricity is higher respect the Scenario 1. Until the price for the MWh for the hydrogen is lower respect the one for electricity it is more convenient to sell electricity instead of the

hydrogen. But it is important to remember that one hypothesis of these two scenarios is that all the production of electricity and hydrogen is sold to the market. Nowadays the renewable sources have a priority in the dispatchment, while in the future when the presence of RES will be very high the priority of injection of this energy to the grid will be a problem and probably a maximum quantity of this energy could be directly sold. In this case the selling of hydrogen instead of electricity will be more convenient even if the selling price is lower instead of throwing away the exceeding part of electricity.

6.3 – Scenario 3: H_2 daily storage and reconversion in electricity

In this scenario the production of hydrogen is always set to 30% of the daily electric production. The hydrogen produced is stored in a daily tank storage and it is reconverted into electricity the day after in order to be resold it and cover the peak of demand with a higher selling price. In this case are present two time bands: the off peak and the peak one with different prices. The *off peak band* is the electricity directly produced from the site and the prices considered are 137.1 €/(MWh) and 97.87 €/(MWh). While the *peak band* is the electricity reconverted from hydrogen in order to satisfy the peak of demand with a price 30 % higher than the off peak one.

In this case the calculation for the CAPEX includes different elements respect the previous two scenarios, thus it has been calculated using the equation (6.1).

$$CAPEX = CAPEX_{electricity} + CAPEX_{AEL} + CAPEX_{storage} + CAPEX_{comp} + CAPEX_{fc} \qquad (6.1)$$

Where $CAPEX_{electricity}$ is the electricity contribution calculated in equation (4.3), $CAPEX_{storage}$ is the storage cost that it is calculated using the technical data present in FCH (2017), $CAPEX_{comp}$ is the cost for the compressor that it is needed for the storage and it has been obtained from technical data present in FCH (2017) and $CAPEX_{fc}$ is the cost for the fuel cell that re-converts hydrogen into electricity and it has been obtained from technical data present in FCH (2017).

The cost contribution for the storage is calculated using the equation (6.2).

$$CAPEX_{storage} = 470 \cdot k \text{ [€]} \qquad (6.2)$$

Where k is the total amount of H_2 to store expressed in [kg]. For the storage is needed a pressure higher than 400 bar as expressed in FCH (2017)'s document. For the storage it has been used an appropriated tank with a daily storage. The storage efficiency is equal to 37%, this value is also proposed by the IEA's report (2020).

The equation for the cost compressor is expressed in (6.3)

$$CAPEX_{comp} = 6569\ k€ \tag{6.3}$$

This cost is proportional to the gap pressure level that in this case is from ambient pressure to 500 bar and to the mass flow equals to 400 kg/h.

At the end the cost for the fuel cell is calculated using the equation (6.4).

$$CAPEX_{fc} = 2000\ \left[\frac{€}{kW}\right] \tag{6.4}$$

For the fuel cell the efficiency is fixed to 55% as FCH (2017)'d document attests.

The results of this scenario are depicted in Figure 6.5 and 6.6 for different electricity prices.

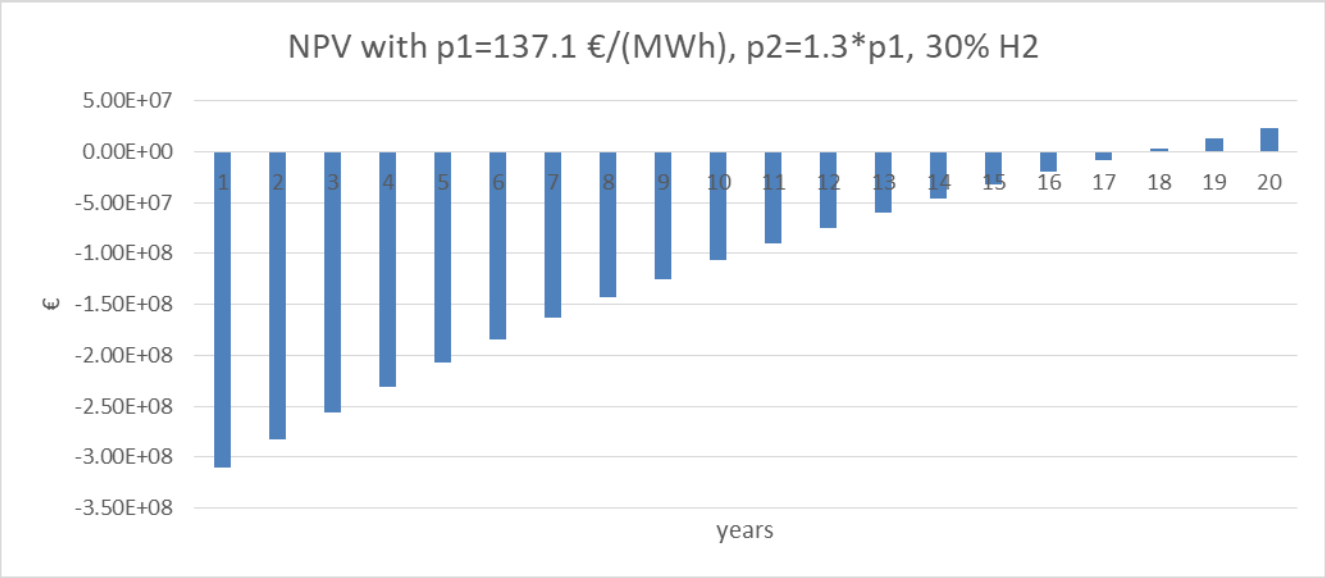

Figure 6.5 Daily H2 storage with re – electrification for a higher selling price; off peak price 137.1 €/(MWh) and peak price +30% than the off peak price.

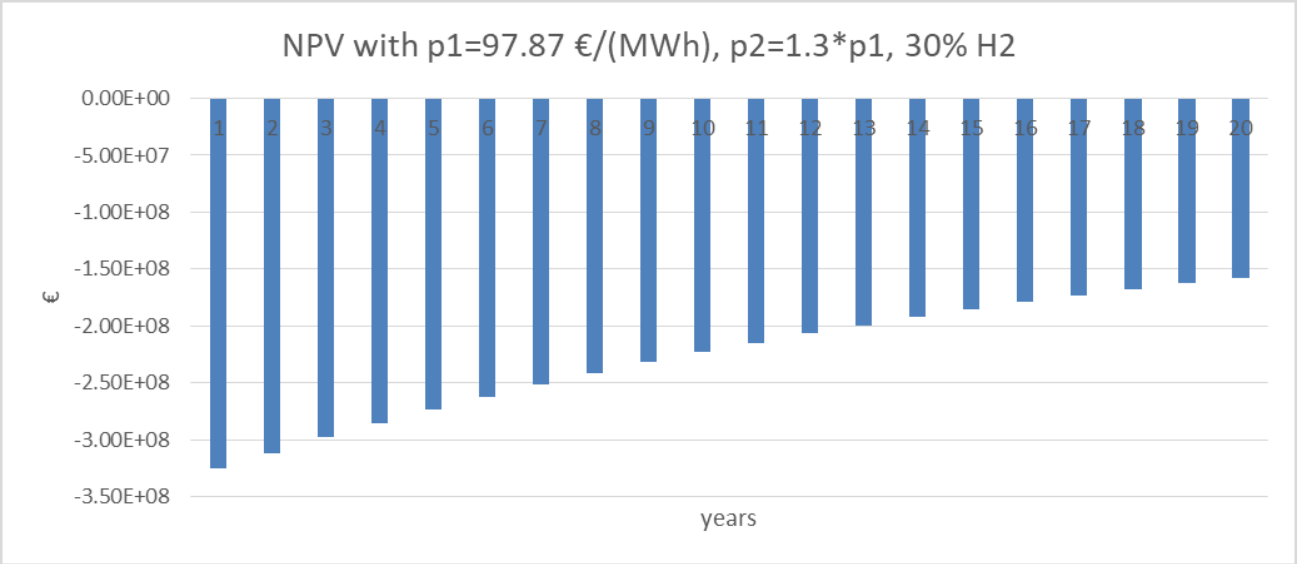

Figure 6.6 Daily H2 storage with re – electrification for a higher selling price; off peak price 97.87 €/(MWh) and peak price +30% than the off peak price

As it can be seen from Figure 6.5 and 6.6 the only possible solution is the one where the selling price is high, otherwise the investment is not able to make profit. This scenario is also more expensive respect Scenario 1 and Scenario 2 because there are more components and the efficiency of the re-electrification η_{re-el} is very low. The re-electrification efficiency can be calculated using equation (6.5).

$$\eta_{re-el} = \eta_{AEL} \cdot \eta_{stoc} \cdot \eta_{fc} = 0.82 \cdot 0.37 \cdot 0.55 = 16.69\ \% \tag{6.5}$$

Where η_{AEL} is the efficiency of the electrolyser, η_{stoc} is the efficiency of the storage and η_{fc} the efficiency of the fuel cell. The total efficiency of the re-electrification is equal to 16.69%, this value is very low and this does not permits to have an efficient system.

In order to analyse a possible favourable solution the price for the peak is increased to 90% than the off peak price. The results of the configurations are presented in Figure 6.7 and 6.8.

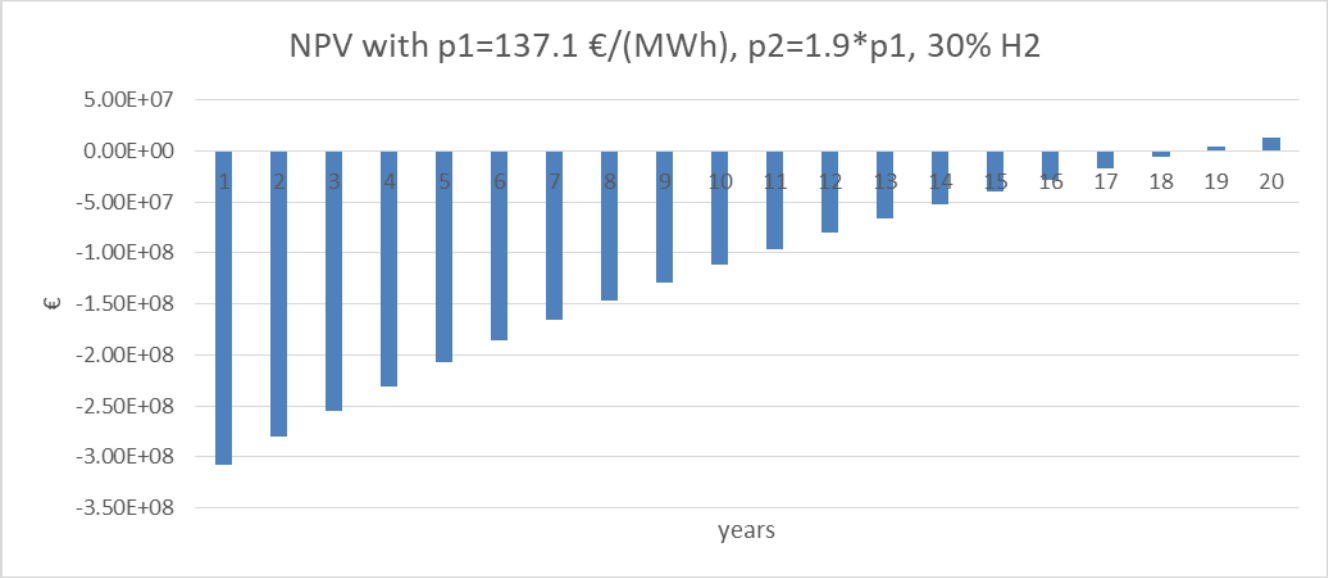

Figure 6.7 Daily H2 storage with re – electrification for a higher selling price; off peak price 137.1 €/(MWh) and peak price +90% than off peak price.

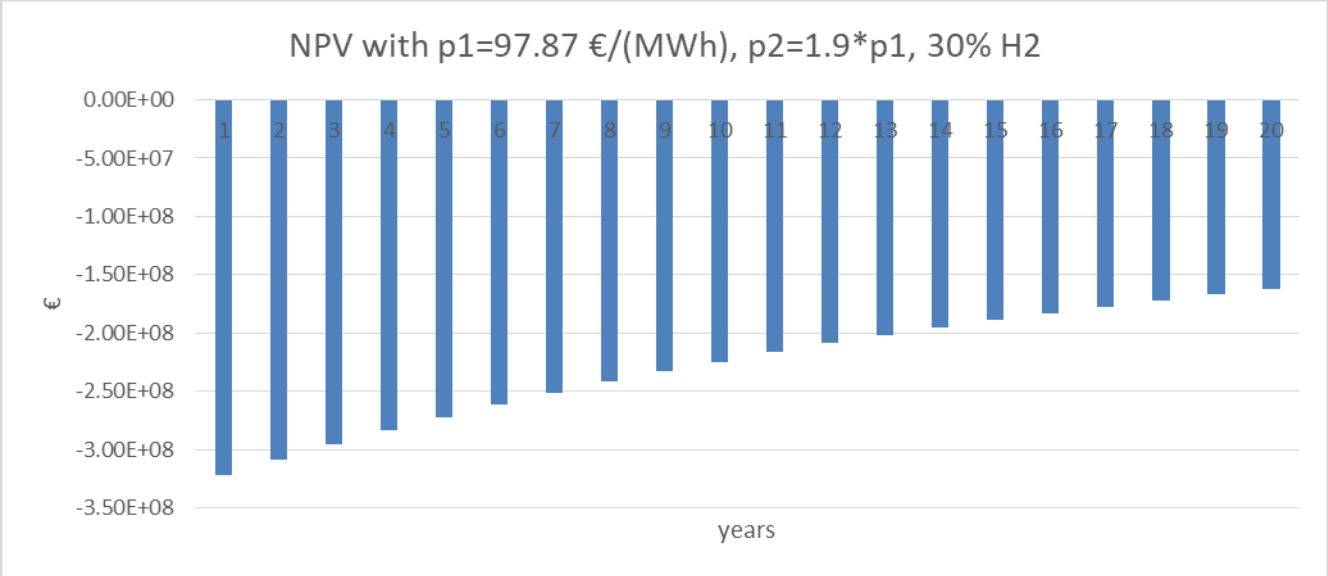

Figure 6.8 Daily H2 storage with re – electrification for a higher selling price; off peak price 97.87 €/(MWh) and peak price +90% than off peak price.

It can be seen how increasing the price of the 90% respect the off peak price is not enough to have a profitable investment and cover the increase of the costs for this scenario. In this case for having a reasonable DPB that is more convenient respect the traditional offshore plant it is necessary to have respectively a peak price that is 15, 16 times higher respect the 137.1 €/(MWh) and 97.87 €/(MWh) off peak prices. These results are depicted in Figure 6.9 and Figure 6.10.

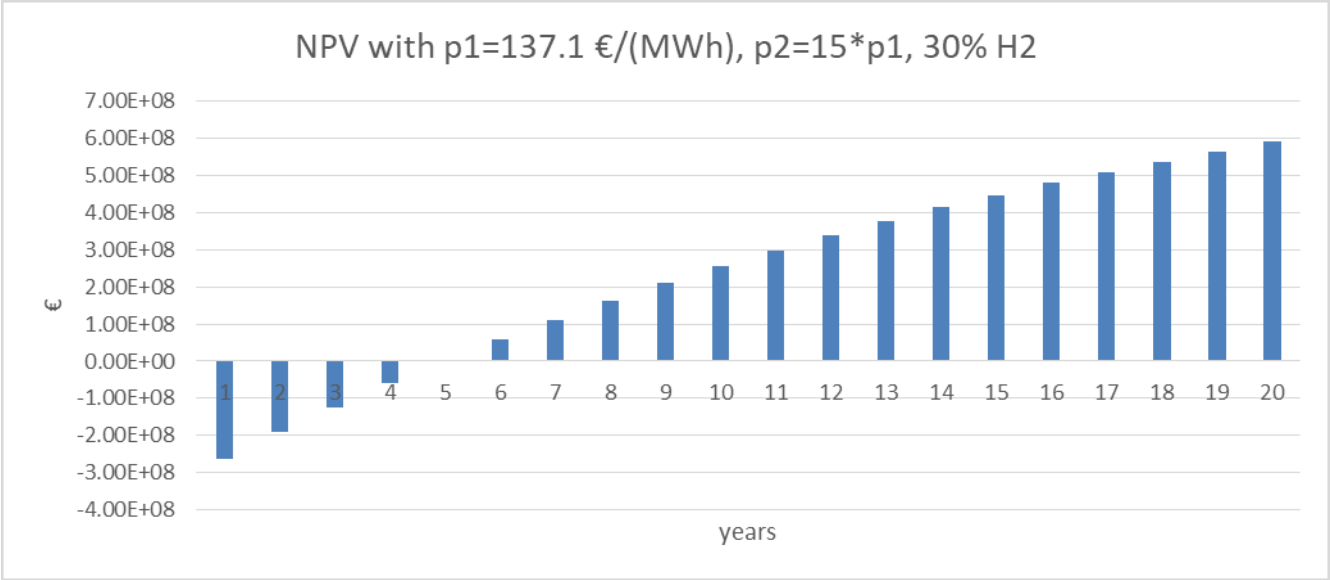

Figure 6.9 Daily H2 storage with re – electrification for a higher selling price; off peak price 137.1 €/(MWh) and peak price 15 times higher than off peak price.

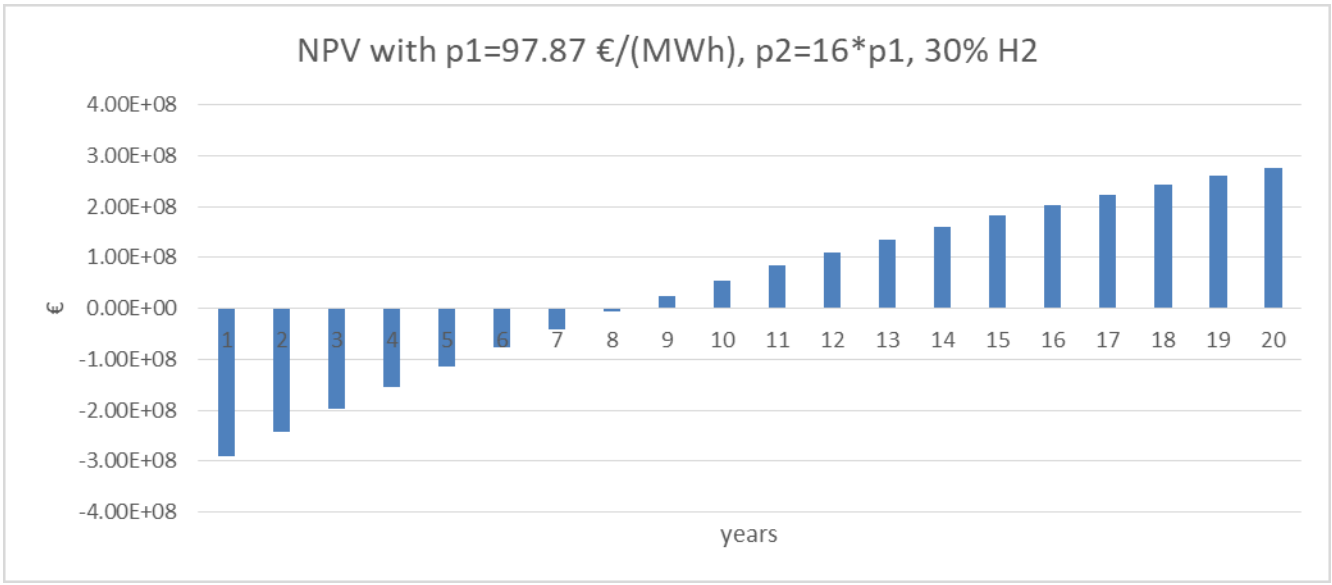

Figure 6.10 Daily H2 storage with re – electrification for a higher selling price; off peak price 97.87 €/(MWh) and peak price 16 times higher than off peak price.

It is important to notice that in Chapter §4.2 the DPB time for the traditional offshore wind farm with the selling electricity prices of 137.1 €/(MWh) and 97.87 €/(MWh) are respectively 6 and 10 years. Therefore, under these conditions the hybrid plant results to be more convenient than the traditional one and it can be consider to be installed.

6.4. – Future applications

From the previous scenario in Chapter §6.5 it has been seen that in the actual state of art of the market and technology the hybrid plant is not profitable if the peak electricity price is not enough high. Therefore, another interesting analysis is to study the future case where the prices for the components and the efficiency of the system are improved.

From the RSE (2021)'s document it is possible to obtain the future price in a long term (in more than 30 years) for the AEL electrolyser; the investment cost will be equal to 200 €/(kW). Using this new electrolyzer cost the results are presented in Figure 6.11 and 6.12.

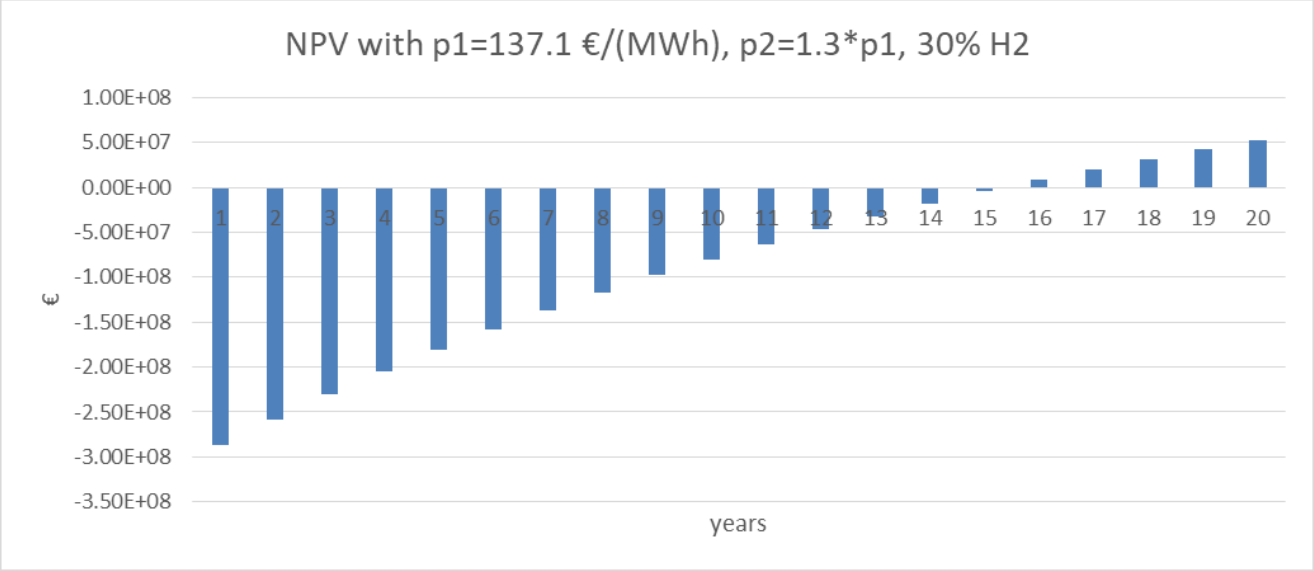

Figure 6.11 NPV trend with re-electrification, an off peak price 137.1 €/(MWh) and peak price +30% than the off peak price and reduction of the AEL's cost to 200 €/(kW)

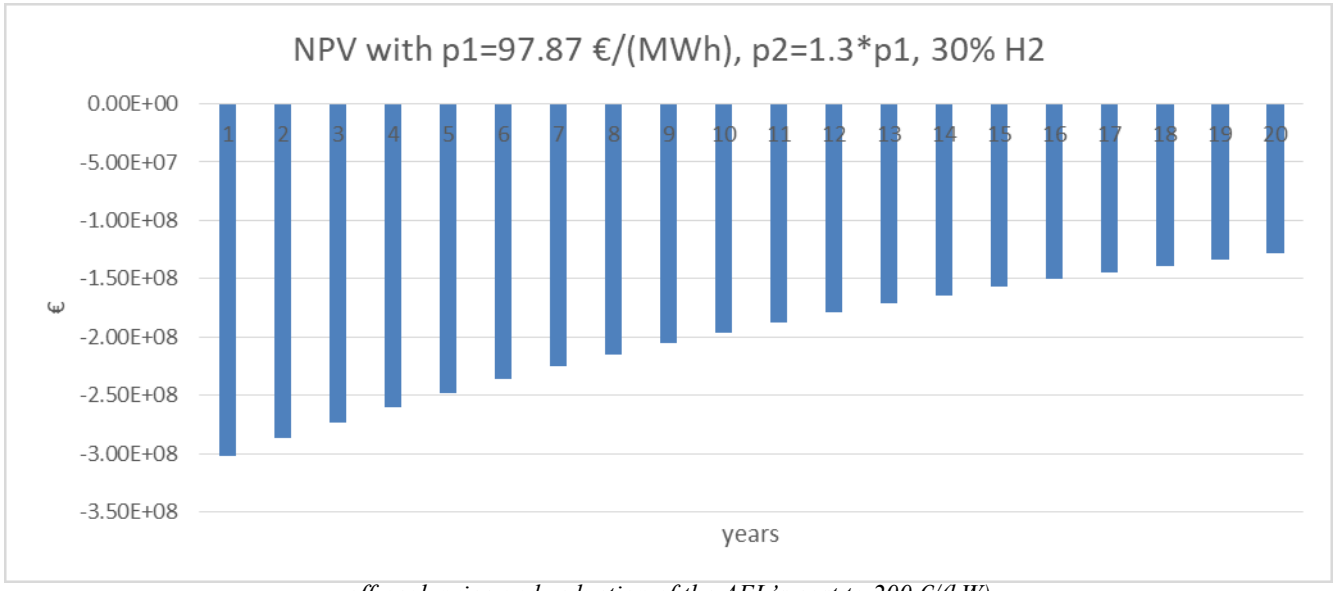

off peak price and reduction of the AEL's cost to 200 €/(kW)

As it can be seen in Figure 6.11 and 6.12 the reduction of the AEL electrolyser leads to a more favourable solution that it is more convenient for the solution with the selling electricity price equals to 137.1 €/(MWh). In this case the investment returns after the 15th years, that it is an acceptable value but it is still higher than the traditional offshore plant. Whereas, for the 97.87 €/(MWh) solution the investment never returns back in the lifetime of 20 years even if the cost for the electrolyser is reduced. In this case an important and effective solution would be the one to higher the selling price and this can be done using some incentives given by the State.

Another possible solution is to increase also the hydrogen re-electrification efficiency and decrease the price for the AEL elecrolyzer to 200 €/(kW). In this case it will be analyse the scenario with an off peak price of 97.87 €/(MWh) and a peak price90% higher than the off peak price. The results are depicted in Figure 6.13.

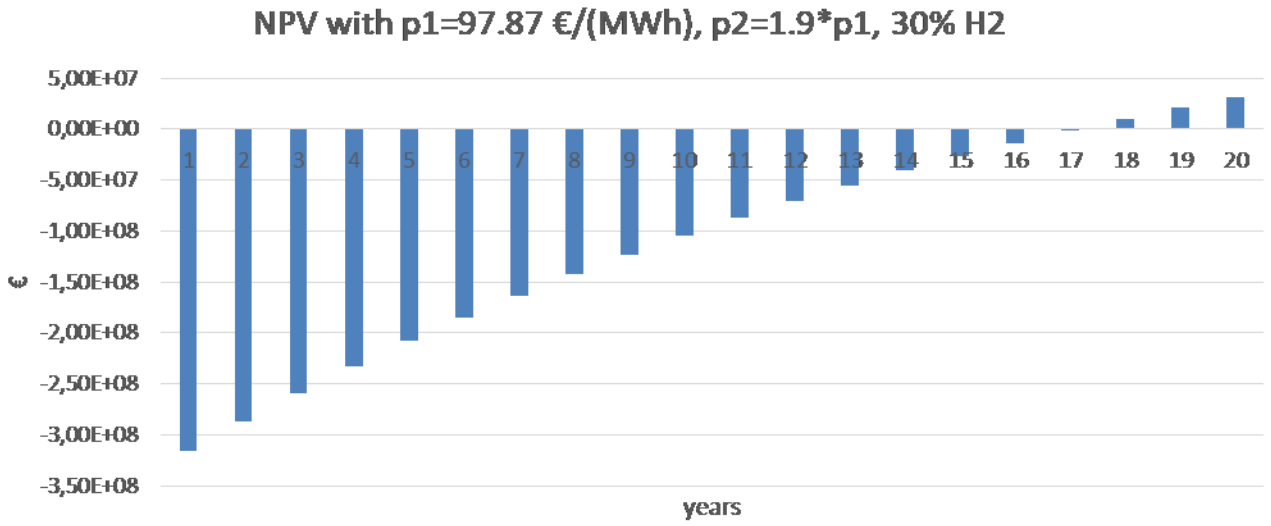

Figure 6.13 Daily H2 storage with re – electrification; off peak price 97.87 €/(MWh) and peak price +90% higher than off peak price, decreasing of the AEL's price and increasing of re-electrification efficiency.

The efficiency of storage and fuel cell instead of being equal to 0.20 is increased to 0.90. These modifications of the efficiency and the electrolyzer cost can be valid for a future configuration. Under these conditions it is possible to have a better investment respect the actual configuration. However, in order to have a solution that is competitive with the traditional offshore plants the peak price needs to be only 4 times higher respect the off peak price as it can be seen in Figure 6.14.

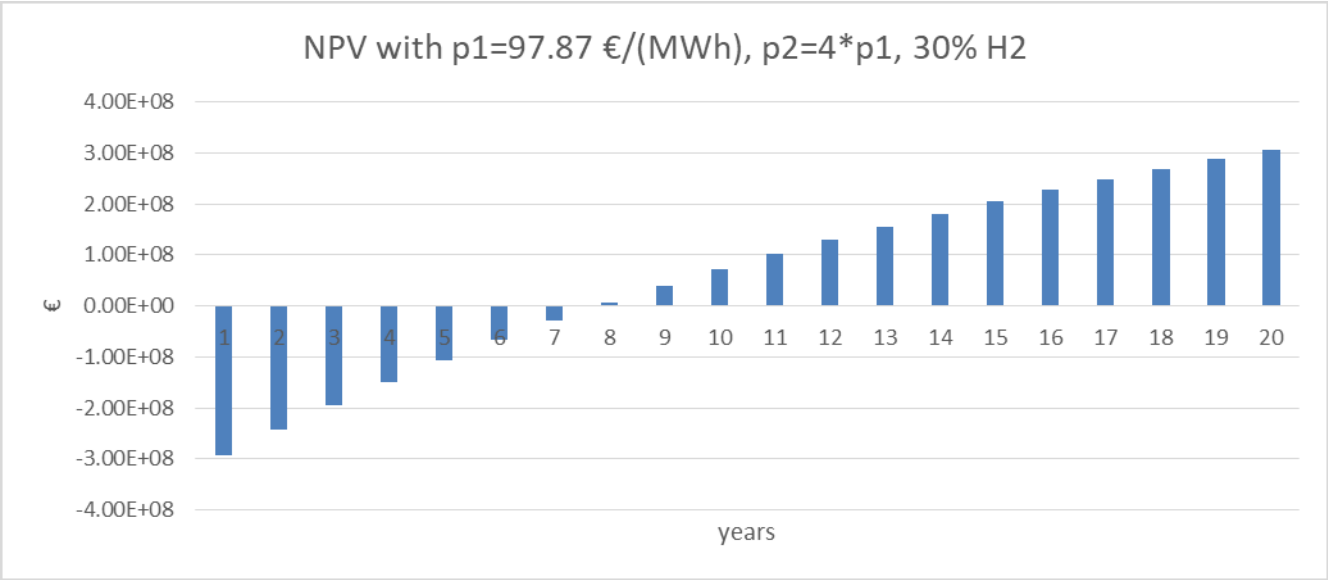

Figure 6.14 Daily H2 storage with re – electrification; off peak price 97.87 €/(MWh), peak price 4 times higher than off peak price and decreasing of the AEL's price and the increasing of re-electrification efficiency

In this case the investment is more convenient than the traditional one because the DPB time is lower than 10 years. Moreover the assumption of having a peak price higher 4 times than the off peak one is an acceptable assumption. This means that a fundamental aspect for this technology is to increase the research and trying to decrease the investment cost and to increase the efficiency of the system.

Conclusion

In Chapter §6 some possible scenarios were presented. All of them lead to the conclusion that for being a profitable investment the selling price for the electricity must be high to return faster the investment and the cost of the components should decrease along the years. The influence of setting the price is very important and it can vary along the lifetime of the plant by the effects of wars, economic crisis or high energy demand. However, in the normal state of art of the technologies and research it is not affordable to install this kind of hybrid offshore wind farm because the time for the return of the investment are higher respect the traditional offshore wind plants. The only exceptions are the cases with a high selling price for the electricity peak price or the one with a high hydrogen price. These assumptions can only be accepted for a short time because the electricity market presents a high variability however, is not precautionary to assume this price for the lifetime of the investment that is normally 20 years. It has been seen that the huge part of the investment cost is related to the traditional plant and that the contribution of the connection cost is not relevant respect the whole cost. For the hybrid plant the major part of the cost is due to the undeveloped technologies that they still present a higher cost such as the storage, the compressor and the fuel cells.

It is also important to notice that in the long future (in more than 30 years) the cost for the AEL electrolyser will decrease more than a half of the present value and this will permits to have a lower CAPEX. Moreover, with the future research even the total efficiency of conversion can be improved and this will lead to a more profitable solution. These two changes will lead the hybrid technology to a mature stage, like it happened in the past with the photovoltaic, and it will permit to have a convenience to install the hybrid plant instead of the traditional offshore wind plant as it was present with the DPB in Chapter §6.4.

The hydrogen plant presents the huge positive aspect that it is possible to implement only the hydrogen part of the plant in the existing offshore wind plant and to use the existing gas pipeline to blend and to inject hydrogen to the grid applying some modifications to the current devices. This aspect permits to lead some research without a high investment and to improve and to lead to a mature technology. Another important consideration to take in mind when a new technology is taken into exam is also related to the social acceptability of the citizens. In this case, the hybrid plants can be implemented where the traditional one are already installed where the state permissions and the social acceptability are already present. Moreover, the offshore plants are usually installed with a huge distance from the shore in order to avoid to damage the landscape. For all these reasons the social acceptability is not consider to be present for this kind of technology.

An important contribution for the spread of the hybrid wind technology is due to the State, in fact with right directives and incentives the high cost for the investment can be afforded. In order to fulfil the net zero emissions, the hybrid configurations for solar and wind will be a winning key because

the hydrogen storage permits to store the energy that is not requested and to inject it when it is needed. The match of the RES with hydrogen will be a good solution to store in a sustainable way the peak of produced energy that is not instantaneously needed. Moreover, the main RES's disadvantage is the huge variability in the energy production. In fact, in the near future penalties will be introduced for all the plants that are not able to inject in the grid a constant and predictable power, but the storage of hydrogen can help to solve this problem. The excess of energy can be used to produce and to store hydrogen that after can be reconverted into electricity.

The re-electrification needs an important research in the following years in order to increase the efficiency and being a more affordable solution for the investments. Therefore, the presence of wind and available space offshore around whole the island will be permit to develop and to lead Ireland to one of the main hydrogen producer around Europe. The presence of hybrid plants will also guide Ireland to be energetically independent from other countries and to do not be damaged by conflicts around the World that can importantly change the market price for electricity and gas. At the end, the strategic location of the island in the ocean will also permit to export hydrogen to England and France.

Appendices

Appendix A.1 - Simple Payback (SPB)

The simple payback (SPB) does not take into consideration the discount rate and it is defined by the equation (A.1).

$$SPB = \frac{C_O}{I_T - C_{T,O\&M}} \quad [year] \tag{A.1}$$

Where C_O is the capital cost that it is also called CAPEX, I_T is the yearly income and $C_{T,O\&M}$ is the OPEX that it is also called the total O&M expenditure in a year.

Appendix A.2 - Discounted Payback (DPB)

The discounted payback (DPB) takes into consideration the discount rate and it is defined by the equation (A.2).

$$DPB = \frac{\ln\left(\frac{1}{1 - i\frac{C_O}{R_{aa}}}\right)}{\ln\,(1+i)} \tag{A.2}$$

Where R_{aa} is the average annual revenue obtained as difference between the income I_T and the OPEX $C_{T,O\&M}$ and i is the discount rate. For this study the discount rate has been defined equals to 6% following the value suggested for the offshore sector by Grant Thornton's report (2018) for Ireland.

Appendix A.3 – Net Present Value (NPV)

The Net Present Value (NPV) is defined by the equation (A.3).

$$VAN = NPV = -C_o + \sum_{k=1}^{n} \frac{I_k - C_{k.O\&M}}{(1+i)^k} \tag{A.3}$$

Taking into consideration about all the components present in the hybrid plant it is calculated considering a lifetime of 20 years.

References

Bibliography

ABB (2011). *Quaderni di applicazione tecnica N. 13, impianti eolici*.

Argyle P. and Watson S. J. (2017). *Offshore turbine wake power losses: is turbine separation significant?* 14th Deep sea offshore wind R&D conference, EERA deeepwind 2017, Trondheim, Norway.

Benato R. (2018). *Esercizi di sistemi elettrici per l'energia*. Edizioni libreria progetto Padova. Pag.171

Bosch J., Staffell I., Hawkes A. D., (2019). Global levelised cost of electricity from offshore wind. https://www.sciencedirect.com/science/article/abs/pii/S0360544219320523

Calado G., Castro R. (2021). *Hydrogen production from offshore wind parks: current situation and future prespectives.* Article

Chainho P., Kiprakis A. E. (2017). *Electrical Components for marine renewable energy arrays: a techno-economic review.* Article

Christensen A. (2020). *Assessment of Hydrogen Production Costs from electrolysis: United States and Europe*. https://theicct.org/wp-content/uploads/2021/06/final_icct2020_assessment_of-_hydrogen_production_costs-v2.pdf

Collin A. J., Nambiar A. J., Bould D., Whitby B., Moonem M. A., Schenkman B., Atcitty S.,

CRU (Commission for Regulation of Utilities) (2018). National Preventive Action Plan Gas 2018-2022 Ireland.

Cummins, V. and Mc Keogh E. (2020). *Blueprint for offshore wind in Ireland 2020-2050: a research synthesis,* Report EirWind project, MaREI Ceter, ERI, University College Cork, Ireland.

Dhesi M. (2015). *Electricity Ten Year Statement 2015*, technical document, appendix E.

Eirgrid (2022). Renewable electricity support scheme 2, RESS 2 final auction results. https://www.eirgridgroup.com/site-files/library/EirGrid/RESS-2-Final-Auction-Results-(R2FAR).pdf

FCH (Fuel Cells and Hydrogen) (2017). *Study on early business cases for H2 in energy storage and more broadly power to H2 applications*.

Fernàndez-Guillamon, A., Kaushik, D., Cutuluis, N. A. and Molina-Garcia, A. (2019). *Offshore wind power integration into future power systems: overview and trends*. Article, Journal of Marine science and Engineering.

Gondal, I. A. (2019). *Offshore renewable energy resources and their potential in a green hydrogen supply chain trough power-to-gas,* Report, Royal Society of Chemistry. https://pubs.rsc.org/en/content/articlehtml/2019/se/c8se00544c?casa_token=cTLasTAtbkwAAAAA:GPb6fcZExotJ6TuMZEUt5a0rZYZqBU4_11tWoo6BkBpk23c8DXOecohj5PzLdWztudZVqUs4Yhbfs1I

Grant Thornton (2019). *Renewable energy discount rate survey results – 2018*. https://www.grantthornton.ie/globalassets/1.-member-firms/ireland/insights/publications/grant-thornton---renewable-energy.pdf

Hoyne S. (2007). ELREN European Leader and Renewable energy Network (2007) *Wind Energy*, **chapter 7.** Published by Carlow LEADER and Tipperary Institute ISBN: 978-0-9546561-2-6 (Ireland)

IEA (International Energy Agency) (2020). *G20 hydrogen report: the future of hydrogen, assumptions annex*. https://iea.blob.core.windows.net/assets/a02a0c80-77b2-462e-a9d5-1099e0e572ce/IEA-The-Future-of-Hydrogen-Assumptions-Annex.pdf

Leahy, P. (2021). *Vertical extrapolation of horizontal wind speeds*, Wind energy lecture notes, University College Cork, Ireland.

Lumbreras, S. and Ramos and A. (2013). *Offshore wind farm electrical design: a review*, Literature review, Institute for Research in Technology (IIT), Madrid, Spain.

Pavan F. (2010). *Sviluppo progettuale ed autorizzativo di un impianto eolico offshore in Italia, fattibilità tecnica ed economica*. Thesis, Università degli studi di Padova, Italy

RSE (Riflessioni Sull'Energia) (2021). *Idrogeno: un vettore energetico per la decarbonizzazione*.

Samorani M. (2013). *The wind farm layout optimization problem*.

Siemens Energy (2020). *Workshop PtG/PtL. Large scale PEM electrolysis and sector coupling 8th of March, 2021*.

Thyssen A. (2015). *Wind power plants internal distribution system and grid connection. A technical and economical comparison between a 33 kV and a 66 kV*. Technical University of Denmark DTU. https://www.powerandcables.com/wp-content/uploads/2019/03/33kV-v-66kV-A-Wind-Farm-Collection-Grid-Technical-Comparison.pdf

Timmers V., Egea- Àlvarez A., Gkountaras A., Li R., Xu L. (2022). All-DC offshore wind farms: when are they more cost-effective than AC designs?. IET (Institution of Engineering and Technology). https://ietresearch.onlinelibrary.wiley.com/doi/epdf/10.1049/rpg2.12550

Todesco P., Dinh V., Leahy P. (2021). *Techno-economic comparison of offshore hydrogen transmission via pipelines and tankers*.

Twidell, J. and Gaudiosi G. (2009). *Offshore wind power*, Emerlad Group, **chapter 6**.

Web sites

[1] https://www.europarl.europa.eu/news/en/headlines/society/20200618STO81513/green-deal-key-to-a-climate-neutral-and-sustainable-eu (last access: 29/04/2022)

[2] https://gwec.net/wp-content/uploads/2022/03/GWEC-GLOBAL-WIND-REPORT-2022.pdf

(last access: 29/04/2022)

[3] https://www.iea.org/reports/renewable-power (last access 12/07/2022)

[4] https://www.iea.org/reports/wind-power (last access 12/07/2022)

[5] https://theodora.com/pipelines/united_kingdom_and_ireland_pipelines.html

(last access 1/08/2022)

[6] https://gis.seai.ie/wind/ (last access 10/09/2022)

[7] https://www.vestas.com/en/products/offshore/V164-10-0-MW (last access 5/05/2022)

[8] https://www.iea.org/reports/offshore-wind-outlook-2019 (last access 10/09/2022)

[9] https://new.abb.com/docs/default-source/ewea-doc/xlpe-submarine-cable-systems-2gm5007.pdf

[10] https://www.seai.ie/data-and-insights/seai-statistics/key-statistics/prices/ (last access 5/09/2022)

[11] https://ucpcdn.thyssenkrupp.com/_legacy/UCPthyssenkruppBAISUhdeChlorineEngineers/assets.files/products/water_electrolysis/tk_19_0820_hydrogen_broschuere_2019_03.pdf

(last access 5/09/2022)

[12] https://www.heattofuel.eu/wp-content/uploads/2021/03/6_Ilona-Dickschas.pdf

(last access 5/09/2022)

[13] https://petrowiki.spe.org/Pipeline_design_consideration_and_standards#:~:text=The%20velocity%20in%20gas%20lines,sec%2C%20which%20minimizes%20liquid%20fallout. (last access 1/08/2022)

[14] https://www.piprocessinstrumentation.com/instrumentation/flowmeasurement/article/15554850/defining-maximum-gas-pipe-velocity (last access 1/08/2022)

[15] https://en.wikipedia.org/wiki/United_Kingdom%E2%80%93Ireland_natural_gas_interconnectors (last access 1/08/2022)

Acknowledgments

All this work is also due to the support and help of many people. Therefore I take the chance to publicly thank who helped me in these months.

I would like to thank Prof. Anna Stoppato, supervisor of this thesis, for your attention and the precious suggestions you gave me for writing this document.

I would also like to thank Prof. Paul Leahy, co-supervisor of the thesis, for being available to my curiosities and necessities. I thank you to let me feel part of the H-wind research group and for including me to the initiatives during my Erasmus at UCC in Ireland. I will always bring with me the experiences that I dealt with.

A special thanks goes to my H-wind colleagues: Hadi, Pedro and Quang for the useful advices and helps that you gave me for making this thesis. You will always be source of inspiration during my working career for your dedication and diligence in the research.

I would like also to thank my family, the moral and mental support of my study career. I can simply say that you are there since ever and for this reason you deserve for sure an honour thanksgiving. Mum and Dad I thank you for all the attention that you give me, you have never let me miss nothing. Eros, you are the best of the brother that I could ever have, you have always influence me with your passion for the science and the desire to know.

I continue thanking a unique and special person, Gabriele, that during the course of these months and of my university career never lose the chance to incite me and help me to the set of problems that I faced during all these years. I really thank you for all the affection that you have always show to me.

I conclude thanking relatives, friends and my new Irish family, you gifted me unique and unforgettable emotions. You are my source of energy and lightheartedness.

Ringraziamenti

Tutto questo lavoro è sicuramente dovuto anche grazie al sostegno e aiuto di tante persone. Pertanto colgo l'occasione di ringraziare pubblicamente coloro che mi hanno dato il loro aiuto in questi mesi.

Tengo in particolar modo a ringraziare la Prof.ssa Anna Stoppato, relatrice di questa tesi, per la sua attenzione e i preziosi suggerimenti che mi ha fornito per redigere questo elaborato.

Ringrazio anche il Prof. Paul Leahy, correlatore della tesi, per essere stato disponibile alle mie curiosità e necessità. Ringrazio di avermi fatto sentire parte del gruppo di ricerca H-wind e incluso nelle iniziative durante il mio Erasmus alla UCC in Irlanda. Porterò sempre con me il bagaglio di esperienze con cui ho avuto modo di cimentarmi.

In particolare un ringraziamento speciale va a Hadi, Pedro, Quang, colleghi del gruppo di ricerca H-wind, per gli utili consigli e aiuti che mi avete fornito per redigere questa tesi. Rimarrete sicuramente fonte di ispirazione durante la mia carriera lavorativa per la vostra dedizione e impegno che svolgete nella ricerca.

Tengo anche a ringraziare la mia famiglia, supporto morale e mentale del mio percorso di studi. Sicuramente posso semplicemente dire che ci siete da sempre e per questo meritate di certo un ringraziamento d'onore. Mamma e Papà vi ringrazio per tutte le attenzioni che mi dedicate, non mi avete mai fatto mancare nulla. Eros, sei il migliore dei fratelli che potessi mai avere, mi hai sempre influenzato con la tua passione verso la scienza e la voglia di conoscere.

Continuo con il ringraziare una persona unica e speciale, Gabriele, che nel corso di questi mesi e della mia carriera universitaria non ha mai perso l'occasione di incitarmi e di aiutarmi nelle problematiche che sono intercorse durante l'arco di questi anni. Ti ringrazio davvero per tutto l'affetto che mi hai sempre dimostrato.

Concludo con il ringraziare parenti, amici e la mia nuova famiglia irlandese, mi avete regalato emozioni uniche e indimenticabili. Siete la mia fonte di energia e spensieratezza.